

# 学位論文

## A Study of Degenerate Two-Body and Three-Body Coupled-Channels Scatterings -A New Formalism, Near-Thresholds Resonances and Its Implications For Exotic Hadrons

(縮退した2体-3体チャネル結合散乱の解析

-新たな定式化、閾値近傍での共鳴状態そしてエキゾチックハドロンとの関連について)

平成27年12月博士(理学)申請

東京大学大学院理学系研究科

物理学専攻

小西 篤業

# Abstract

Since the monumental discovery of the  $X(3872)$  in 2003 by the Belle collaboration group, a lot of candidates for the exotic hadron have been observed especially in the energy regions above the double open charm and bottom thresholds. Those observed resonances which nowadays aggregately called the  $X$  families are embedded in various hadronic scattering states coupling to it. Some of those candidates for the exotic hadron lie very close to hadronic two-body as well as three-body thresholds. For example, the mass of  $X(3872)$ ,  $3871.69 \pm 0.17$  MeV is very close to  $\bar{D}^{*0}D^0$  threshold  $\simeq 3871.8$  MeV and  $D^\pm \bar{D}^0 \pi^\mp$  threshold  $\simeq 3874.0$  MeV. Besides the  $X$  families that recently observed, possible exotic candidates such as the dibaryon resonances near  $\Delta N$  and  $\Lambda(1405)N$  thresholds and, though its existence has been denied, the pentaquark near  $\pi \bar{K} N$  threshold seem to lie in the energy regions where two-body and three-body hadronic thresholds reside close to each other. This feature indicates that two-body and three-body coupled-channels system whose thresholds are close might contain characteristic physics contributing to the existence of the exotic states.

In this thesis, motivated by such circumstances, we develop a general two-body and three-body coupled-channels scattering equations and analyze how poles of the  $S$ -matrix behave near the threshold mainly whose thresholds are degenerate. Due to some technical difficulties related to three-body scattering, we consider three-body elastic scattering equations in which the effects induced by the coupling to two-body channels are embedded as effective interactions in three-body channel which are constructed by leveraging the Feshbach projection method. Throughout this thesis, we denote three particles in the three-body channel as  $\phi_1\phi_2\phi_3$ . Assuming that  $\phi_1\phi_2$  couples to another particle  $\psi_3$ , the physical mass of  $\psi_3$  is shifted from the bare one. In quantum field theory, we often encounter such situation and we usually treat it by the mass and the field renormalization. Once the renormalization is done, it is necessary to add counterterms every time self-energies appear. Due to characteristic structure of the two-body and three-body coupled-channels scattering equations we develop, self-energies also appear when the scattering equations are *iterated*. However, we solve the scattering equation numerically, not iteratively. It is then necessary to find a way to incorporate those counterterms which should be added to the self-energies that appear when the scattering equations are iterated, into what we can give when we numerically solve the scattering equations. We have found a way to execute that task and discuss it in detail.

We analyze the  $S$ -matrix pole behavior near the thresholds in the degenerate two-body and three-body coupled-channels system by solving the two-body and three-body coupled-channels scattering equations we develop. The pole approaches the thresholds from the fourth quadrant of the unphysical energy sheet which might become a resonance if it lies close enough to the physical energy region. This is in contrast to a degenerate two-body coupled-channels system which contains two-body  $s$ -wave channel. In such a case, the  $S$ -matrix pole approaches the thresholds from the negative real axis in the unphysical sheet. It is therefore possible that resonances reside in the vicinity of hadronic two-body  $s$ -wave threshold if another hadronic three-body threshold lies nearby which might be realized in observed exotic states. We also

show that in the case of degenerate two-body and three-body coupled-channels system, the pole behaves universally near the threshold in the sense that they lie on an identical curve independent of the details of the system.

# Acknowledgment

First of all, I would like to sincerely express my special thanks of gratitude to my supervisor, Professor O. Morimatsu for suggesting me this subject and for his patience, continuous advices and discussions. I owe most of the studies in this thesis to him. My sincere thanks also goes to Dr. S. Yasui for suggesting me this subject and for his insightful comments and discussions.

Besides my advisor, I would like to thank my thesis committee Professor I. Tsutsui, Professor K. Ohtsuka, Professor T. Hatsuda, Professor K. Fukushima, Professor H. Sakurai for their insightful comments and also for the hard question which incited me to widen my research from various perspective.

I would also like to thank computational environments in high energy accelerator research organization (kek). Without their computational power, our research project would not have progressed as it has been.

Last but not least, I would like to sincerely thank my family, my parents, my grandmother and my sister for their continuous encouragement, advices and all kinds of helps. Without their help, I am quite sure that I could not have come so far, continued research activities and finished this thesis.

# Contents

<b>1</b>	<b>Introduction</b>	<b>8</b>
1.1	Exotics Near Hadronic Two- and Three-Body Thresholds . . . . .	8
1.2	Our Methods and Results . . . . .	9
1.3	Organization of Thesis . . . . .	11
<b>2</b>	<b>Prerequisites for Two-Body and Three-Body Coupled-Channels Approach</b>	<b>12</b>
2.1	Feshbach Projection Formalism . . . . .	12
2.1.1	The Feshbach Projection . . . . .	12
2.1.2	The Two-Body and Three-Body Coupled-Channels System and Effective Interactions in the Three-Body Channel . . . . .	14
2.2	The (Faddeev-)AGS Formalism . . . . .	15
2.2.1	Basic Notations and Concepts in Three-Body Physics . . . . .	15
2.2.2	The Faddeev Equations . . . . .	18
2.2.3	The AGS Equations . . . . .	21
2.3	Analytic Continuation of the $S$ -Matrix . . . . .	27
<b>3</b>	<b>The Effective AGS Approach and The Finite Mass Renormalization</b>	<b>30</b>
3.1	Notation . . . . .	30
3.2	The effective AGS equations . . . . .	34
3.3	The Unphysical Singularities Problem and Its Solution . . . . .	36
3.3.1	The Unphysical Singularities Problem . . . . .	37
3.3.2	A Problem of The Iteratively Appearing Self-Energies and Its Solutions . . . . .	38
<b>4</b>	<b>The Effective AGS Approach to The Near-Threshold <math>S</math>-Matrix Behavior</b>	<b>53</b>
4.1	The $S$ -Matrix Behavior for Single-Channel Two-Body and Three-Body System . . . . .	53
4.1.1	$\psi_3\phi_3$ Two-Body System . . . . .	53
4.1.2	$\phi_1\phi_2\phi_3$ Three-Body System . . . . .	55
4.2	Explicit Expressions of Matrix Elements in The effective AGS equations . . . . .	55
4.3	The $S$ -Matrix Pole Trajectories Near The Thresholds . . . . .	61
4.3.1	Analytic Continuation to The Unphysical Complex Energy Sheet . . . . .	62
4.3.2	Numerical Results and Discussion . . . . .	63
<b>5</b>	<b>Summary and Conclusion</b>	<b>67</b>
<b>A</b>	<b>Notations</b>	<b>70</b>
A.1	Channels . . . . .	70
A.2	Three-Body channel . . . . .	70
A.3	Two-Body Channel . . . . .	72
A.4	Two-Body and Three-Body Coupled-Channels . . . . .	72
A.5	The Effective Interactions in The Three-Body Channel . . . . .	73

<b>B</b>	<b>Some Algebras Related to the Feshbach Projection</b>	<b>75</b>
B.1	The Feshbach Projection . . . . .	75
B.2	Notes on the Induced Interaction . . . . .	78
<b>C</b>	<b>Two More Derivations of The (Faddeev-)AGS Equations</b>	<b>79</b>
C.1	Derivation By Considering Disconnected Processes . . . . .	79
C.2	Derivation Based on Reorganization of The Green Function . . . . .	80
<b>D</b>	<b>Reorganization Procedure with Detailed Calculations</b>	<b>82</b>
D.1	Detailed Calculation in section 3.3 . . . . .	82
D.2	Direct Derivation of the Modified Kernel . . . . .	86
D.3	Another Two-Body and Three-Body Coupled-Channels Equations . . . . .	90
D.4	In Case of $V_3 \neq 0$ . . . . .	91
<b>E</b>	<b>Formal Treatment of Two-Body Potential Scattering</b>	<b>96</b>
E.1	The Möller Operator and The Green Function . . . . .	96
E.2	Transition Amplitude . . . . .	97
E.3	Analytic Properties of The Green Function and The $T$ -Matrix . . . . .	98
<b>F</b>	<b>Analytical Approach to The Near-Threshold <math>S</math>-Matrix Pole Behavior</b>	<b>100</b>
F.1	Elastic Two-Body $T$ -Matrix In The $\phi_1\phi_2\phi_3 - \psi_3\phi_3$ Coupled-Channels System . .	100
F.2	The Dispersion Relation and The Optical Theorem . . . . .	102
F.2.1	The Dispersion Relation . . . . .	102
F.2.2	The Optical Theorem . . . . .	103
F.3	The Two-Body and Three-Body Coupled-Channels Optical Theorem . . . . .	105
F.4	The Leading Behavior of The Spectral Function and The $S$ -Matrix Near The Threshold . . . . .	108
F.5	Pole Behavior Near The Threshold . . . . .	110
F.6	Relation Between The Present Work and The Efimov States . . . . .	113

# List of Figures

2.1	A diagrammatic representation of the Lippmann-Schwinger Equation (2.10) . . .	14
2.2	A diagrammatic representation of the AGS equations without a three-body force	24
2.3	A diagrammatic representation of the AGS equations with a three-body force. . .	27
3.1	The elementary interactions . . . . .	34
3.2	A diagrammatic representation of the effective interactions . . . . .	34
3.3	A diagrammatic representation of the elements in The (Faddeev-)AGS Equations	35
3.4	A diagrammatic representation of The (Faddeev-)AGS Equations . . . . .	36
3.5	A diagrammatic representation of the dressed propagator of $\psi_3$ . . . . .	36
3.6	A diagrammatic representation of the fully-countertermed $t_3^{(3)}(E)$ . . . . .	40
3.7	A diagrammatic representation of the fully-countertermed $Z_4(E)$ . . . . .	41
3.8	A diagrammatic representation of the $X_3(E)$ . . . . .	44
3.9	A diagrammatic representation of the $W_4(E)$ . . . . .	45
3.10	A diagrammatic representation of the $\mathcal{G}(E)$ . . . . .	45
3.11	One of the diagrammatic representation of the $W_4(E)$ . . . . .	46
3.12	One of the diagrammatic representation of the $W_4(E)$ . . . . .	47
3.13	One of the diagrammatic representation of the $W_4(E)$ . . . . .	48
3.14	A diagrammatic representation of the countertermed dressed propagator of $\psi_3$ .	48
3.15	A diagrammatic representation of the $W_4(E)$ in terms of $Z_4(E)$ . . . . .	49
3.16	A diagrammatic representation of the modified driving term $Z_4(E)$ . . . . .	49
3.17	A diagrammatic representation of a relation between $Z_4(E)$ and $Z_4'(E)$ . . . . .	50
3.18	A diagrammatic representation of a set of self-energies . . . . .	51
3.19	A diagrammatic representation of the fully-modified driving term $Z_4(E)$ . . . . .	52
3.20	A diagrammatic representation of $X_3(E)$ . . . . .	52
4.1	The $S$ -matrix pole trajectory near the threshold; two-body $s$ -wave case. . . . .	54
4.2	The $S$ -matrix pole trajectory near the threshold; two-body higher-wave case. . .	54
4.3	The $S$ -matrix pole trajectories near the threshold . . . . .	64
D.1	A diagrammatic representation of another coupled-channels scattering equations	90
D.2	A diagrammatic representation of $t_3(E)$ . . . . .	91
D.3	A diagrammatic representation of $\Sigma(E) + \Delta$ . . . . .	92
D.4	A diagrammatic representation of equation (D.52) . . . . .	92
D.5	A diagrammatic representation of equation (D.52) . . . . .	93
D.6	A diagrammatic representation of the modified $Z_4(E)$ . . . . .	94
F.1	A diagrammatic representation of the single-channel optical theorem . . . . .	104
F.2	A diagrammatic representation of the two-channel optical theorem . . . . .	105
F.3	A diagrammatic representation of the coupled-channels optical theorem . . . . .	105
F.4	A diagrammatic representation of the coupled-channels optical theorem . . . . .	108

F.5	A graphical expression of the equation (F.68).	111
F.6	A graphical expression of the equation (F.71)	112
F.7	The $S$ -matrix pole trajectories characterized by (F.74)	113



# Chapter 1

## Introduction

In this introduction, we review current status of the exotic hadron studies and discuss its relation with hadronic two-body and three-body channels lying nearby to motivate our research objective, an analysis of two-body and three-body coupled-channels system. We then briefly present methods we adopt to analyze the two-body and three-body coupled-channels systems. The Feshbach projection formalism, a method that effects induced by coupling to other channels are embedded into effective interactions in the channel we focus on, and the (Faddeev-)AGS equations which three-body transition amplitudes satisfy. We outline an organization of thesis at the end.

### 1.1 Exotics Near Hadronic Two- and Three-Body Thresholds

In this section, we review current status of the exotic hadron spectroscopy focusing on those lying in the energy regions where two-body and three-body hadronic thresholds lie close to each other. We then discuss a relation between those exotic candidates and hadronic two-body and three-body coupled-channels systems.

It is pointed out that possible dibaryon state lies near  $N\Delta$  threshold both experimentally [1] and theoretically [2, 3, 4, 5, 6, 7, 8, 9, 10, 11, 12, 13]. Since  $\Delta$  strongly couples to  $\pi N$  two-body state, it is obvious that we need to consider  $\pi NN - \Delta N$  two-body and three-body coupled-channels system. We also note that the  $\Delta N$  two-body threshold lies close to  $\pi NN$  three-body and  $\pi\pi NN$  four-body thresholds.

$$m_N + m_\Delta \simeq 2172 \text{ [MeV]} \quad (1.1)$$

$$2m_\pi + 2m_N \simeq 2156 \text{ [MeV]} \quad (1.2)$$

$$m_\pi + 2m_N \simeq 2017 \text{ [MeV]} \quad (1.3)$$

In 2003, the Belle collaboration observed a narrow excess in the invariant mass of  $J/\psi\pi^+\pi^-$  around the energy of 3870 MeV [14] which is confirmed by the following experiments [15, 16, 17, 18, 19, 20, 21, 22, 23, 24, 25] and the state is nowadays called the  $X(3872)$ . Since the discovery of the  $X(3872)$ , a lot of charmonium- and bottomonium-like states have been observed especially in the energy regions above the double open charm and bottom thresholds. See [26, 27, 28] for recent reviews for heavy quarkonium spectroscopy. In the following, we list some of them that are most likely the exotic states.

One of candidates for the exotic hadron is the  $X(3872)$ . Its PDG average mass is,  $3871.68 \pm 0.17$  MeV and the upper limit of its width is  $< 1.2$  MeV [14]. Its quantum number is also determined to be  $J^{PC} = 1^{++}$ . It is known that the  $X(3872)$  strongly violates the isospin symmetry [16]. The  $X(3872)$  therefore cannot be a simple charmonium. We also note that the

dominant decay mode is  $\pi D\bar{D}$  whose  $\pi D$  are decay products of  $D^*$  which motivates us to regard it to be hadronic molecule composed of  $\pi D\bar{D}$  and  $D\bar{D}^*$ .

Another candidate for the exotic hadron is the  $X^+(4430)$  which was once referred to as  $Z^+(4430)$ . It is found as a decay product of  $Z^+(4430) \rightarrow \pi^+\psi(2S)$  [29] in 2008 and later confirmed by other groups [30, 31, 32, 33]. It is obviously the exotic state since it is charged and cannot be a simple charmonium. Other candidates for the exotics are reviewed in [26, 27].

It is experimentally [34] indicated that strange dibaryon exists near  $\bar{K}NN - \pi\Sigma N$  threshold and there have been an extensive theoretical studies based on variational approach [35, 36, 37, 38, 39, 40] and on coupled-channels AGS approach [41, 42, 43, 44, 45, 46, 47]. Though there are studies that  $\Lambda(1405)$  is dynamically generated through hadronic interactions in  $\bar{K}N - \pi\Sigma$  coupled-channels system [48, 49], we can also formulate it as two-body and three-body coupled-channels system regarding  $\Lambda(1405)$  as an elementary degree of freedom.

Comparing various hadronic thresholds and masses of those exotic candidates we can see that some of them lie in the energy regions where hadronic two-body and three-body thresholds lie close to each other. For example, the mass of the  $X(3872)$ ,  $3871.69 \pm 0.17$  MeV is very close to  $\bar{D}^{*0}D^0$  two-body threshold  $\simeq 3871.8$  MeV and it is also very close to  $D^\pm\bar{D}^0\pi^\mp$  *three-body* threshold  $\simeq 3874.0$  MeV. It is then natural to ask that a two-body and three-body coupled-channels system whose thresholds lie close to each other might contains interesting physics not studied yet.

This feature that various hadronic thresholds whose number of mesons differ lie close to each other is characteristic in QCD. This originates from the fact that the typical QCD scale  $\simeq 200$  [MeV] is comparable to light mesons, especially pion whose mass is  $\simeq 140$  [MeV]. This is in contrast to other interactions such as electromagnetic one. In electromagnetic interaction, differences in the discrete energy levels is of order  $\sim 1$  [eV] while the lightest particles that interact electromagnetically is electron whose mass is  $\sim 1$  [MeV] which is far heavy compared to differences in the discrete energy levels.

## 1.2 Our Methods and Results

Motivated by such circumstances discussed above, we consider two-body and three-body coupled-channels system, focusing mainly whose thresholds are degenerate.

There are several related works that focus on hadronic two-body and three-body coupled-channels perspective, to name a few, [50, 51, 52]. As far as we know, those calculations are more or less perturbative one. This might be due to some technical cumbersomeness related to three-body scattering. A two-body scattering can be examined with the Lippmann-Schwinger equation while the corresponding three-body scattering equations are the so-called (Faddeev) AGS equations which might not be so popular. Our objective in this thesis is to establish the general two-body and three-body coupled-channels formalism. To be more specific, we focus on constructing the general two-body and three-body coupled-channels scattering equations in which all assumed interactions are summed.

In order to perform analysis for two-body and three-body coupled-channels system, we employ the Feshbach projection formalism [53, 54], a method that effects induced by coupling to other channels, often referred to as  $Q$ -channel, are taken into account as effective interactions in a channel we focus on, which is often referred to as  $P$ -channel (in case of two-channels system). In the case we are interested in, we consider the three-body channel as  $P$ -channel and coupling to the two-body channels,  $Q$ -channels, are taken into account as the effective interactions in the three-body channel. We formulate the problem in that way because of subtle cumbersomeness we encounter when we deal with the full Green function in three-body channel. We will see that even in the absence of elementary three-body interactions in the three-body channel, the cou-

pling to the two-body channel generates effective three-body interactions. Here by elementary interaction, we mean interaction that still remain even after the channels decouple.

Once we reformulate the two-body and three-body coupled-channels problem as an effective three-body problem, we then solve the three-body scattering equations which is known as the (Faddeev-)AGS equations [55, 56] which enable us to calculate physical quantities such as scattering cross sections, phase shifts and poles of the  $S$ -matrix.

Throughout this thesis, we denote three particles in the three-body channel as  $\phi_1\phi_2\phi_3$ . Assuming that  $\phi_1\phi_2$  couple to another particle  $\psi_3$ , the two-body channel is then  $\psi_3\phi_3$  and the physical mass of  $\psi_3$  shifts from the bare one. This causes subtle problems when we perform numerical calculations. To be more specific, a singularity originating from the bare mass of  $\psi_3$  appears if we naively write down the (Faddeev-)AGS equations which makes the numerical calculations doubtful. In quantum field theory [57], we often encounter such situations, and we deal with the problems by the mass and the field renormalization. Although we do not consider in a framework of quantum field theory, we proceed in a similar manner. We decompose the mass term of  $\psi_3$  into the physical one and the counterterm. It is then however necessary to add counterterms every time the self-energies appear. The problem is, that due to characteristic structure of the scattering equations we develop, the self-energies appear when the scattering equations are *iterated* in addition to those appearing in the kernel of the scattering equations. However, we solve the scattering equations *numerically, not iteratively*. We therefore need to find a way to incorporate those counterterms to be added to self-energies which appear when the scattering equations are iterated, into what we can feed to the scattering equations, namely the driving term and the kernel of the (Faddeev-)AGS equations. We somehow invented a method to execute that task, and discuss it in detail in chapter 3.

In chapter 4, by numerically solving the effective AGS equation, we discuss the  $S$ -matrix pole trajectories close to thresholds for degenerate two-body and three-body coupled-channels system since the exotic candidates tend to lie in the energy regions where hadronic two-body and three-body thresholds lie close to each other. Numerical results show that the  $S$ -matrix pole approaches the threshold from fourth quadrant of the unphysical energy sheet which might become resonance if they lie close to the physical energy region. This is in contrast to degenerate multi-channel two-body systems which contain a two-body  $s$ -wave state. In such coupled-channels system, the  $S$ -matrix pole approaches the threshold from the negative real axis on the unphysical energy sheet no matter how the interaction in the two-body  $s$ -wave channel is weak, that is, the two-body  $s$ -wave behavior dominates in the low energy region. We also show that poles behave universally near the threshold in a sense that pole trajectories do not depend on details of the system such as coupling constants. The result indicates that there might be resonances near hadronic two-body  $s$ -wave thresholds if another hadronic three-body threshold lies near by which might be realized in the exotic hadron spectroscopy.

The question everyone asks when we discuss candidates for the exotic hadron is, “Are they two-body (or three-body) hadronic molecule or something like we can refer to as tetraquark, pentaquark, dibaryon, glueball or hybrid?”. In reality, if the quantum numbers are the same, the state is superposition of those and the problem is how to determine which component dominates or how they are mixed. Such bare-hadron-molecule mixing has been discussed in relation with not-well understood states such as scalar mesons and axial-vector mesons. See, for example, [58, 59].

One of possible applications of our two-body and three-body coupled-channels approach is, given a bound state or resonance of the system, to estimate how much two-body and three-body components it has respectively, the analogue of bare-hadron and hadronic two-body molecule mixing. We will discuss it in a more quantitative fashion in chapter 5.

### 1.3 Organization of Thesis

In chapter 2, we present prerequisites we need to discuss the two-body and three-body coupled-channels system, namely the Feshbach projection formalism, the (Faddeev-)AGS formalism. After that in chapter 3, we write down the effective AGS equations in which effects due to coupling to two-body channel is taken into account as effective interactions. We then discuss the unphysical singularities problem and present the method which cure these unphysical singularities disease in detail. In chapter 4, we perform close analysis of degenerate two-body and three-body coupled-channels problem by performing numerical calculations on the effective AGS equations. In chapter 5, we summarize our research results and conclusion is given. The relation between the present work and the Efimov physics is also briefly discussed.

## Chapter 2

# Prerequisites for Two-Body and Three-Body Coupled-Channels Approach

In this chapter, we review methods we adopt to develop the two-body and three-body coupled-channels scattering equations namely, the Feshbach projection formalism and the (Faddeev-)AGS formalism.

### 2.1 Feshbach Projection Formalism

Our objective is to develop a two-body and three-body coupled-channels scattering equations. To achieve that, we employ the Feshbach projection formalism developed by Feshbach [53, 54]. The Feshbach projection embed effects due to coupling to other channels into interactions of the channel we focus on. In our case, we consider three-body elastic scattering in which the effects due to two-body channels are embedded as effective interactions in three-body channels. In this section, we introduce the Feshbach projection procedure in detail and see how effects due to couplings to two-body channel are embedded as effective interactions in the three-body channel.

#### 2.1.1 The Feshbach Projection

We start from the general perspective not limited to two-body and three-body coupled-channels system. To simplify the argument, we consider a system in which two two-body channels are coupled. Let  $H$  be a full Hamiltonian of the system.  $H$  is composed of the kinetic and interaction terms.

$$H = H_0 + V \quad (2.1)$$

where  $V$  contains interactions which couple two channels in addition to interactions within each channel. The  $T$ -matrix, from which we can extract scattering quantities such as scattering cross sections, phase shifts and decay width can be formally expressed as (see appendix E for a brief review of formal treatment of scattering theory).

$$T(E) = V + VG(E)V \quad (2.2)$$

where  $G(E)$  is the full Green function whose explicit expression is given as below

$$G(E) = \frac{1}{E - H_0 - V} \quad (2.3)$$

With the aid of an identity for operators

$$\frac{1}{A-B} = \frac{1}{A} + \frac{1}{A} B \frac{1}{A-B} \quad (2.4)$$

we can show that  $G(E)$  satisfies the Dyson-Schwinger equation

$$G(E) = G_0(E) + G_0(E) V G(E) \quad (2.5)$$

This equation leads to the Lippmann-Schwinger equation which the  $T$ -matrix satisfies.

$$T(E) = V + V G_0(E) T(E) \quad (2.6)$$

$E$  is a total energy of the system. The expression above is valid for analytically continued off-shell  $T$ -matrix while if we are interested in physical energy regions, we need to introduce the infinitesimal quantity  $\epsilon$  and replace the argument  $E$  by  $E + i\epsilon$ .

We next define the projection operators which project any state into each channels.

$$P = |ch.1\rangle\langle ch.1| \quad (2.7)$$

$$Q = |ch.2\rangle\langle ch.2| \quad (2.8)$$

where  $P$  and  $Q$  satisfies the relation

$$P + Q = 1 \quad (2.9)$$

In the remaining part of this section, we refer each channel as  $P$ -channel and  $Q$ -channel which is a often-used terminology. The elastic  $P$ -channel scattering  $T$ -matrix is obtained by multiplying the projection operator  $P$  from both of left and right

$$\begin{aligned} PT(E)P &= PVP + PV \frac{1}{E-H} VP \\ \Rightarrow T_{PP}(E) &= U_{PP}(E) + U_{PP}(E) \frac{P}{E-H_0^P - U_{PP}(E)} U_{PP}(E) \end{aligned} \quad (2.10)$$

the second equality is referred to as the Feshbach projection and  $U_{PP}(E)$  is the effective interaction in the  $P$ -channel whose explicit expression is

$$U_{PP}(E) = PVP + PVQ \frac{Q}{E-QHQ} QVP =: V_{PP} + V_{PQ} G_Q(E) V_{QP} \quad (2.11)$$

See the appendix B for a derivation.  $G_Q(E)$  in the second term is  $Q$ -channel Green function whose interaction is  $V_{QQ}$  and satisfies the Dyson-Schwinger equation

$$G_Q(E) = G_0^Q(E) + G_0^Q(E) V_{QQ}(E) G_Q(E) \quad (2.12)$$

It can also be represented with the  $Q$ -channel  $T$ -matrix as below

$$G_Q(E) = G_0^Q(E) + G_0^Q(E) T_Q(E) G_0^Q(E) \quad (2.13)$$

where  $T_Q(E)$  is the  $T$ -matrix in the  $Q$ -channel which satisfies the Lippmann-Schwinger equation

$$T_Q(E) = V_{QQ} + V_{QQ} G_0^Q(E) T_Q(E) \quad (2.14)$$

We can see that the effective interaction in the  $P$ -channel  $U_{PP}(E)$  consists of two parts. The first term is the bare interactions in the  $P$ -channel while the other is an effective interaction which is *induced* due to the coupling to the  $Q$ -channel. The second term is a sum of interactions which contain transition to  $Q$ -channel *once*. That is, a  $P$ -channel state makes a transition to  $Q$ -channel, then particles in the  $Q$ -channel fully propagate with the interactions in the  $Q$ -channel which we denote  $V_{QQ}$  and make transition back to  $P$ -channel. Processes that contain more than once transition between the  $P$ -channel and the  $Q$ -channel appears when the scattering equation (2.10) is *iterated*. We present a diagrammatic representation of the Lippmann-Schwinger equation (2.10) which  $T_{PP}(E)$  satisfies in figure 2.1.

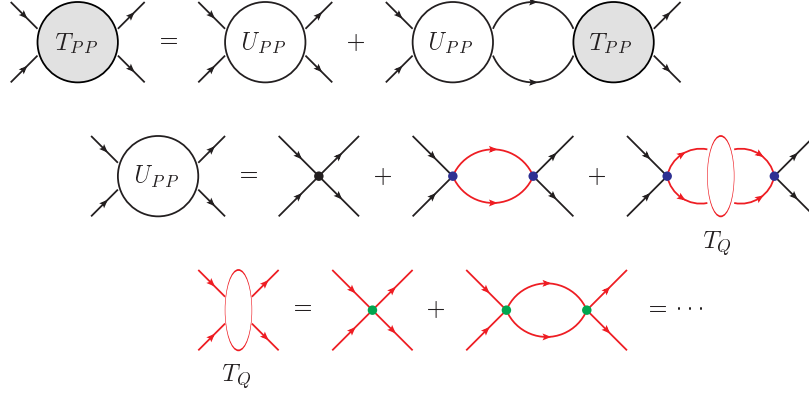


Figure 2.1: A diagrammatic representation of the Lippmann-Schwinger Equation (2.10)

$P$ -channel	$Q$ -channel
$\phi_1\phi_2\phi_3$	$\psi_3\phi_3$

Table 2.1:  $P$ - and  $Q$ -channel

### 2.1.2 The Two-Body and Three-Body Coupled-Channels System and Effective Interactions in the Three-Body Channel

Having introduced the Feshbach projection formalism, we focus on our interest, that is, we apply the Feshbach projection method to the two-body and three-body coupled-channels system.

We denote three particles in the three-body channel as  $\phi_1\phi_2\phi_3$  and assume that  $\phi_1\phi_2$  couple to another particle  $\psi_3$ . The two-body state is therefore consists of  $\psi_3\phi_3$ . Let  $P$  and  $Q$  be projection operators which project any state into three-body and two-body state respectively. An elastic two-body scattering  $T$ -matrix  $T_{QQ}(E)$  is formally represented as

$$T_{QQ}(E) = U_{QQ}(E) + U_{QQ}(E) \frac{Q}{E - H_0^Q - U_{QQ}(E)} U_{QQ}(E) \quad (2.15)$$

where the effective two-body interaction  $U_{QQ}(E)$  is

$$U_{QQ}(E) = V_{QQ} + V_{QP}G_P(E)V_{PQ} \quad (2.16)$$

where  $G_P(E)$  is full three-body Green function which satisfies

$$G_P(E) = G_0^P(E) + G_0^P(E)V_{PP}G_P(E) \quad (2.17)$$

It is however, known that calculating the full three-body propagator is technically cumbersome. We therefore consider *elastic three-body* scattering instead throughout this thesis.

An explicit form of an elastic three-body  $T$ -matrix is simply

$$T_{PP}(E) = U_{PP}(E) + U_{PP}(E) \frac{P}{E - H_0^P - U_{PP}(E)} U_{PP}(E) \quad (2.18)$$

where  $U_{PP}(E)$  is the effective three-body interaction whose explicit form is,

$$U_{PP}(E) = V_{PP} + V_{PQ}G_Q(E)V_{QP} \quad (2.19)$$

$G_Q(E)$  is a full Green function in the two-body channel which can be expressed as

$$G_Q(E) = G_0^Q(E) + G_0^Q(E) T_{QQ}(E) G_0^Q(E) \quad (2.20)$$

The effective three-body interactions are therefore expressed as

$$U_{PP}(E) = V_{PP} + V_{PQ} G_0^Q(E) V_{QP} + V_{PQ} G_0^Q(E) T_Q(E) G_0^Q(E) V_{QP} \quad (2.21)$$

where  $T_Q(E)$  is a two-body  $T$ -matrix whose interaction is bare two-body interaction  $V_{QQ}$  which satisfies the Lippmann-Schwinger equation

$$T_Q(E) = V_{QQ} + V_{QQ} G_0^Q(E) T_Q(E) \quad (2.22)$$

It is diagrammatically obvious that the first and the second term in  $U_{PP}(E)$  are effective two-body interactions while the last term is effective *three-body interaction*. Though we do not assume bare three-body interaction, coupling to the two-body channel induces an effective three-body interaction.

We now have reformulated the two-body and three-body coupled-channels scattering problem as an effective three-body scattering problem whose interactions are replaced by the effective one. Our next task is to solve this effective three-body scattering equation which is known as the (Faddeev-)AGS equations. We explore the (Faddeev-)AGS equations in detail in the next section.

## 2.2 The (Faddeev-)AGS Formalism

When we deal with a two-body scattering problem, we can solve the Lippmann-Schwinger equation to obtain physical quantities such as scattering cross section or phase shift. However, in case of more than two particles are considered, the Lippmann-Schwinger equation is no longer well-defined and it is necessary to introduce the so-called (Faddeev-)AGS equations [55, 56]. It was Alt-Grassberger-Sandhas who figured out that in case of separable potentials are considered for two-body interactions, the scattering equations which three-body transition amplitudes satisfy reduces formally to that of the multi-channel Lippmann-Schwinger equation and is tractable in practical calculation. In this section, we review the Faddeev-AGS formalism in detail.

### 2.2.1 Basic Notations and Concepts in Three-Body Physics

In this subsection, we present basic notations and concepts common in three-body physics. After introducing the Jacobi coordinates and momenta in three-body channel, we explore the energy eigenstates of a part of the Hamiltonian which is called the channel states.

#### The Jacobi Coordinates and Momenta

Throughout this thesis, we denote three particles as  $\phi_1\phi_2\phi_3$  as shown in table 2.2. In the following,  $i, j, k$  are assumed to be a cyclic permutation of 1, 2, 3. We introduce the Jacobi coordinates and momenta which will be used throughout the following part of this thesis. The notation we use in this thesis are also summarized in the appendix C.

We denote the masses of  $\phi_1$ ,  $\phi_2$  and  $\phi_3$  as  $m_1$ ,  $m_2$  and  $m_3$  respectively. In three-body problems, we often introduce the Jacobi coordinates defined as below. Let  $\mathbf{x}_1$ ,  $\mathbf{x}_2$  and  $\mathbf{x}_3$  be



Three-body channel
$\phi_1\phi_2\phi_3$

Table 2.2: Three Particles in Three-Body Channel

position vectors in the Cartesian coordinate. The Jacobi coordinates are then defined as

$$\mathbf{R} = \frac{\sum_i m_i \mathbf{x}_i}{\sum_i m_i} \quad (2.23)$$

$$\mathbf{R}_i = \mathbf{x}_i - \frac{m_j \mathbf{x}_j + m_k \mathbf{x}_k}{m_j + m_k} \quad (2.24)$$

$$\mathbf{r}_i = \mathbf{x}_j - \mathbf{x}_k \quad (2.25)$$

$\mathbf{R}$ ,  $\mathbf{R}_i$  and  $\mathbf{r}_i$  are center of mass, relative coordinate between  $\phi_i$  and the pair of  $\phi_j\phi_k$  and relative coordinate between  $\phi_j$  and  $\phi_k$  respectively.  $i, j$  and  $k$  are cyclic permutation of 1, 2, 3.

Let  $\mathbf{k}_1$ ,  $\mathbf{k}_2$  and  $\mathbf{k}_3$  be momenta in Cartesian coordinate. The Jacobi momenta are then,

$$\mathbf{P} = \sum_i \mathbf{k}_i \quad (2.26)$$

$$\mathbf{q}_i = \frac{(m_j + m_k) \mathbf{k}_i - m_i (\mathbf{k}_j + \mathbf{k}_k)}{\sum_i m_i} \quad (2.27)$$

$$\mathbf{p}_i = \frac{m_j \mathbf{k}_j - m_k \mathbf{k}_k}{m_j + m_k} \quad (2.28)$$

where  $\mathbf{P}$  is the center of mass momentum,  $\mathbf{q}_i$  are the relative momenta between  $\phi_i$  and the pair of  $\phi_j\phi_k$  and  $\mathbf{p}_i$  are relative momenta between  $\phi_j$  and  $\phi_k$ .

We consider the problem in the three-body center-of-mass frame in which  $\mathbf{P} = \mathbf{0}$ . The kinetic energy in the three-body system which we denote as  $H_0^{(3)}$  then is

$$H_0^{(3)} = \sum_{i=1}^3 \frac{k_i^2}{2m_i} = \frac{P^2}{2M} + \frac{q_i^2}{2M_i} + \frac{p_i^2}{2\mu_i} = \frac{q_i^2}{2M_i} + \frac{p_i^2}{2\mu_i} \quad (2.29)$$

where,  $M$ ,  $M_i$  and  $\mu_i$  are defined as below

$$M = m_1 + m_2 + m_3 \quad (2.30)$$

$$M_i^{-1} = m_i^{-1} + (m_j + m_k)^{-1} \quad (2.31)$$

$$\mu_i^{-1} = m_j^{-1} + m_k^{-1} \quad (2.32)$$

$M$  is the total mass,  $M_i$  is the reduced mass between  $\phi_i$  and the pair of  $\phi_j$  and  $\phi_k$  while  $\mu_i$  is the reduced mass between  $\phi_j$  and  $\phi_k$ .

The three-body plane-wave state is an eigenstate of the free Hamiltonian

$$H_0^{(3)} |\mathbf{k}_1 \mathbf{k}_2 \mathbf{k}_3\rangle = \sum_i \frac{k_i^2}{2m_i} |\mathbf{k}_1 \mathbf{k}_2 \mathbf{k}_3\rangle \quad (2.33)$$

The three-body plane-wave states  $|\mathbf{k}_1 \mathbf{k}_2 \mathbf{k}_3\rangle$  therefore span the three-body Hilbert space, that is, they form the complete set of basis whose normalization conditions are

$$\int d\mathbf{k}_1 d\mathbf{k}_2 d\mathbf{k}_3 |\mathbf{k}_1 \mathbf{k}_2 \mathbf{k}_3\rangle \langle \mathbf{k}_1 \mathbf{k}_2 \mathbf{k}_3| = 1 \quad (2.34)$$

$$\langle \mathbf{k}_1 \mathbf{k}_2 \mathbf{k}_3 | \mathbf{k}'_1 \mathbf{k}'_2 \mathbf{k}'_3 \rangle = \delta(\mathbf{k}_1 - \mathbf{k}'_1) \delta(\mathbf{k}_2 - \mathbf{k}'_2) \delta(\mathbf{k}_3 - \mathbf{k}'_3) \quad (2.35)$$

A similar expression holds for the Jacobi momenta

$$H_0^{(3)} |\mathbf{P}_i \mathbf{q}_i \mathbf{p}_i\rangle = \left( \frac{P_i^2}{2M} + \frac{q_i^2}{2M_i} + \frac{p_i^2}{2\mu_i} \right) |\mathbf{P}_i \mathbf{q}_i \mathbf{p}_i\rangle \quad (2.36)$$

$$\int d\mathbf{P} d\mathbf{q}_i d\mathbf{p}_i |\mathbf{P} \mathbf{q}_i \mathbf{p}_i\rangle \langle \mathbf{P} \mathbf{q}_i \mathbf{p}_i| = 1 \quad (2.37)$$

$$\langle \mathbf{P} \mathbf{q}_i \mathbf{p}_i | \mathbf{P}' \mathbf{q}'_i \mathbf{p}'_i \rangle = \delta(\mathbf{P} - \mathbf{P}') \delta(\mathbf{q}_i - \mathbf{q}'_i) \delta(\mathbf{p}_i - \mathbf{p}'_i) \quad (2.38)$$

Since the three-body center-of-mass momentum  $\mathbf{P}$  conserves, we consider the three-body center-of-mass frame, that is, we set  $\mathbf{P} = \mathbf{0}$  in the following part of this thesis. Then the total kinetic energy reduces to

$$H_0^{(3)} = \frac{q_i^2}{2M_i} + \frac{p_i^2}{2\mu_i}, \quad i = 1, 2, 3 \quad (2.39)$$

The completeness relation and the normalization of Jacobi momenta states are

$$\int d\mathbf{q}_i d\mathbf{p}_i |\mathbf{q}_i \mathbf{p}_i\rangle \langle \mathbf{q}_i \mathbf{p}_i| = 1 \quad (2.40)$$

$$\langle \mathbf{q}_i \mathbf{p}_i | \mathbf{q}'_i \mathbf{p}'_i \rangle = \delta(\mathbf{q}_i - \mathbf{q}'_i) \delta(\mathbf{p}_i - \mathbf{p}'_i) \quad (2.41)$$

## Interactions and Channel States

Three two-body pairwise interactions in a three-body system are commonly expressed as

$$V_i = V_{jk} \quad (2.42)$$

that is, a two-body interaction between particles  $j$  and  $k$  is labeled by the index of the spectator particle  $i$ . Three pairwise interactions are denoted as  $V_1, V_2, V_3$  and therefore, three-body interactions are naturally expressed as  $V_4$ . As a matter of convention, we also define superscripted interactions  $V^i$  as a sum of pairwise interactions without  $V_i$

$$V^i = V_j + V_k + V_4 \quad (2.43)$$

The full Hamiltonian can then be written as

$$H = H_0^{(3)} + V_i + V^i = H_i + V^i \quad (2.44)$$

where we have defined the channel Hamiltonian  $H_i$

$$H_i = H_0^{(3)} + V_i \quad (2.45)$$

It is convenient to define the above expression also for  $i = 0$ , that is,

$$V_0 = 0 \quad (2.46)$$

$$V^0 = V_1 + V_2 + V_3 + V_4 \quad (2.47)$$

the equation (2.44) is then satisfied for  $i = 0, 1, 2, 3, 4$

When  $\phi_i$  is far from the rest of the two, interaction between  $\phi_i$  and the pair  $\phi_j \phi_k$  can be ignored while  $\phi_j \phi_k$  interact with each other. We call such a channel a *fragmentation channel*. If the interaction between  $\phi_j \phi_k$  is strong enough, the pair form a bound state and we denote

it  $|\varphi_i\rangle$ . The state of the fragmentation channel then is denoted as  $|\varphi_i\rangle|\mathbf{q}_i\rangle = |\phi_i\rangle$  and in the following, we call this state a *channel state*.

$$H_i|\phi_i\rangle = \left(\frac{q_i^2}{2M_i} - \epsilon_i\right)|\phi_i\rangle \quad H_i = H_0 + V_i \quad (2.48)$$

where  $\epsilon_i$  is the binding energy of the pair  $\phi_j\phi_k$ . Note that the channel Hamiltonian has a three-body scattering states besides the channel state as eigenstates.

$$H_i|\phi_i\rangle^{(+)} = \left(\frac{q_i^2}{2M_i} + \frac{p_i^2}{2\mu_i}\right)|\phi_i\rangle^{(+)} \quad (2.49)$$

where we defined a three-body scattering state  $|\phi_i\rangle^{(+)}$  as

$$|\phi_i\rangle^{(+)} = |\mathbf{q}_i\rangle|\mathbf{p}_i\rangle^{(+)} \quad (2.50)$$

the completeness relation which the eigenstates of the channel Hamiltonian satisfies is

$$\int d\mathbf{q}_i |\phi_i\rangle\langle\phi_i| + \int d\mathbf{q}_i d\mathbf{p}_i |\phi_i\rangle^{(+)}\langle\phi_i|^{(+)} = 1 \quad (2.51)$$

There are three possible fragmentation channels which are obviously denoted as

$$1; 2, 3 \quad 2; 3, 1 \quad 3; 1, 2 \quad (2.52)$$

If we scatter a particle with bounded two-particle pair, the final state possibly be three particles. We call such a state a break-up channel.

### 2.2.2 The Faddeev Equations

In this subsection, we present basic notations and concepts common in three-body physics and the Faddeev equation which three-body states satisfy. After introducing basic notations and concepts, we derive the fundamental set of Lippmann-Schwinger equations by considering the boundary conditions three-body scattering states satisfies. We then present the Faddeev equations first derived by Faddeev [55] but in a different manner from the Faddeev's original paper. Two more derivations of the Faddeev equations are presented in the appendix ( ref appendix ). In this subsection, we consider only three pairwise interactions and ignore three-body interactions. We incorporate three-body interactions after we derived the (Faddeev-)AGS equations which three-body transition amplitudes satisfy in the next subsection. Following discussions relies largely on the book written by Glöckle [60].

#### The Fundamental Set of Lippmann-Schwinger Equations

Channel States obey the following time-dependent Schroedinger equations

$$i\frac{d}{dt}|\phi_i\rangle = H_i|\phi_i\rangle \quad (2.53)$$

$$i\frac{d}{dt}|\phi_i\rangle^{(+)} = H_i|\phi_i\rangle^{(+)} \quad (i = 0, 1, 2, 3) \quad (2.54)$$

which has the formal solutions

$$|\phi_i(t)\rangle = e^{-iH_it}|\phi_i(0)\rangle \quad (2.55)$$

the channel states develop to four different states which are the solutions of the full time-dependent Schroedinger equation

$$i \frac{d}{dt} |\Psi_i\rangle^{(+)} = (H_i + V^i) |\Psi_i\rangle^{(+)} \quad (2.56)$$

which can be formally solved as

$$|\Psi_i(t)\rangle^{(+)} = e^{-iHt} |\Psi_i(0)\rangle^{(+)} \quad (2.57)$$

Requiring that the norm  $\| |\Psi_i\rangle^{(+)} - |\phi_i\rangle \|$  vanishes at the infinite past, we find that the two states can be related by the channel Möller operators  $\Omega_i^{(+)}$

$$|\Psi_i(0)\rangle^{(+)} = \lim_{t \rightarrow -\infty} e^{iHt} e^{-iH_i t} |\phi_i(0)\rangle =: \Omega_i^{(+)} |\phi_i(0)\rangle \quad (2.58)$$

we have simpler, practical expression of the Möller operator

$$|\Psi_i\rangle^{(+)} = \lim_{\epsilon \rightarrow 0} i\epsilon G(E_i + i\epsilon) |\phi_i\rangle \quad (2.59)$$

where we have defined the full Green function  $G(E)$

$$G(E) = \frac{1}{E - H} \quad H = H_i + V^i \quad (2.60)$$

In the following, we do not explicitly write  $\lim_{\epsilon \rightarrow 0}$  and assume this limit is taken whenever  $\epsilon$  appears.

Now we set up the scattering equation that the scattering state  $|\Psi_i\rangle^{(+)}$  satisfies. In case of two-body scattering problems, Lippmann-Schwinger equation is derived by considering the resolvent identity

$$\frac{1}{E - H_0 - V} = \frac{1}{E - H_0} + \frac{1}{E - H_0} V \frac{1}{E - H_0 - V} \quad (2.61)$$

Let us proceed in the same manner in case of three-body problem. To that end, we define the channel Green function

$$G_i(E) = \frac{1}{E - H_i} \quad (2.62)$$

It is easy to show that the full and the channel resolvent operators satisfy the identity

$$G(E) = G_i(E) + G_i(E) V^i G(E) \quad (2.63)$$

which leads to the Lippmann-Schwinger equations

$$\begin{aligned} |\Psi_i\rangle^{(+)} &= i\epsilon G(E_i + i\epsilon) |\phi_i\rangle \\ &= i\epsilon G_i(E_i + i\epsilon) |\phi_i\rangle + G_i(E_i + i\epsilon) V^i |\Psi_i\rangle^{(+)} \\ &= |\phi_i\rangle + G_i(E_i + i\epsilon) V^i |\Psi_i\rangle^{(+)} \end{aligned} \quad (2.64)$$

where the second equality follows from

$$\frac{i\epsilon}{E_i + i\epsilon - H_0 - V_i} |\phi_i\rangle = |\phi_i\rangle \quad (2.65)$$

It seems that we have obtained the equation which governs the three-body scattering problem. However, what will happen if we insert the resolvent identity for  $j \neq i$ .

$$|\Psi_i\rangle^{(+)} = i\epsilon (G_j(E) + G_j(E) V^j G(E)) |\phi_i\rangle \quad (2.66)$$

the first term vanishes since  $|\phi_i\rangle$  is not an eigenstate of  $H_j$

$$\frac{i\epsilon}{E_i + i\epsilon - H_j} |\phi_i\rangle = 0 \quad (\text{Lippman's identity}) \quad (2.67)$$

which leads to

$$|\Psi_j\rangle^{(+)} = G_i (E_j + i\epsilon) V^i |\Psi_j\rangle^{(+)} \quad j \neq i \quad (2.68)$$

that is,  $|\Psi_j\rangle^{(+)}$  also satisfies the homogeneous Lippmann-Schwinger equations. Therefore, the inhomogeneous Lippmann-Schwinger equation (2.64) do not uniquely define  $|\Psi_i\rangle^{(+)}$ , but allows  $|\Psi_j\rangle^{(+)}$  to mix with it. We discuss this problem in the next paragraph.

We consider the spectral representation of  $G_i$

$$G_i (E_i + i\epsilon) = \int d\mathbf{q}_i \frac{|\phi_i\rangle\langle\phi_i|}{E_i + i\epsilon - \frac{q_i^2}{2M_i} - \epsilon_i} + \int d\mathbf{q}_i d\mathbf{p}_i \frac{|\mathbf{q}_i\rangle|\mathbf{p}_i\rangle^{(+)} \langle\mathbf{p}_i|\langle\mathbf{q}_i|}{E_i + i\epsilon - \frac{q_i^2}{2M_i} - \frac{p_i^2}{2\mu_i}} \quad (2.69)$$

the first term is responsible for free propagation of the particle  $i$  with respect to the bound pair and allow only *outgoing* waves. However, since  $|\Psi_j\rangle^{(+)}$  are also eigenstates of  $G_i V^i$  (2.68) and do contain *incoming* waves in channel  $j$ . The Lippmann-Schwinger equation (2.64) therefore does not fully specify the *boundary conditions* the scattering states must satisfy. It is the part  $G_0 V_j$  in  $G_i V^i = G_i (V_j + V_k)$  which let the incoming waves in channel  $j$  through. Indeed,

$$(H_0 + V_j) |\phi_j\rangle = E |\phi_j\rangle \Leftrightarrow V_j |\phi_j\rangle = (E - H_0) |\phi_j\rangle \Leftrightarrow G_0 (E) V_j |\phi_j\rangle = |\phi_j\rangle \quad (2.70)$$

Therefore, in addition to the Lippmann-Schwinger equation (2.64), we need equations which specify the appropriate boundary condition that the initial state contains only the incoming waves. Recall that the  $|\Psi_i\rangle^{(+)}$  also satisfy the homogeneous equations

$$|\Psi_i\rangle^{(+)} = G_j (E_i + i\epsilon) V^j |\Psi_i\rangle^{(+)} \quad (2.71)$$

which actually indicates that  $|\Psi_i\rangle^{(+)}$  does not contain incoming waves in channels  $j$  and  $k$ . It is thus natural to require the above equations as well as the Lippmann-Schwinger equation (2.64) and we arrive at the fundamental set of Lippmann-Schwinger equations.

$$|\Psi_i\rangle^{(+)} = |\phi_i\rangle + G_i (E) V^i |\Psi_i\rangle^{(+)} \quad (2.72)$$

$$|\Psi_i\rangle^{(+)} = G_j (E) V^j |\Psi_i\rangle^{(+)} \quad (2.73)$$

$$|\Psi_i\rangle^{(+)} = G_k (E) V^k |\Psi_i\rangle^{(+)} \quad (2.74)$$

We next consider  $|\Psi_0\rangle^{(+)}$ , the three-body break-up channel state. We first note that the state satisfies the usual Lippmann-Schwinger equation

$$|\Psi_0\rangle^{(+)} = |\phi_0\rangle + G_0 (E) V |\Psi_0\rangle \quad (2.75)$$

Inserting the resolvent identity  $G = G_0 + G_0 V^i G$ , we obtain another Lippmann-Schwinger equations

$$|\Psi_0\rangle^{(+)} = i\epsilon G_i (E) |\phi_0\rangle + G_i (E) V^i |\Psi_0\rangle^{(+)} \quad (2.76)$$

where the first term is transformed as

$$i\epsilon G_i (E_0 + i\epsilon) |\phi_0\rangle = \frac{i\epsilon}{E_0 + i\epsilon - H_0 - V_i} |\mathbf{q}_i \mathbf{p}_i\rangle = |\mathbf{q}_i\rangle |\mathbf{p}_i\rangle^{(+)} \quad (2.77)$$

thus, we have

$$|\Psi_0\rangle^{(+)} = |\mathbf{q}_i\rangle |\mathbf{p}_i\rangle^{(+)} + G_i (E) V^i |\Psi_0\rangle^{(+)} \quad (i = 1, 2, 3) \quad (2.78)$$

That is,  $|\Psi_0\rangle^{(+)}$  satisfies the inhomogeneous Lippmann-Schwinger equation in the sense the equation (2.78).  $|\Psi_0\rangle$  therefore does not mix with  $|\Psi_i\rangle$  and the above three equations are necessary and sufficient to uniquely determine  $|\Psi_0\rangle$ .

## The Faddeev Equations

In the previous subsection, we derived the fundamental set of Lippmann-Schwinger equations which three channel states satisfy. In this subsection, we derive the Faddeev equations by applying the so-called Faddeev decomposition to the fundamental set of Lippmann-Schwinger equations.

Recalling the definitions of  $|\Psi_i\rangle^{(+)}$  lead us to the following identity

$$|\Psi_i\rangle^{(+)} = i\epsilon G(E_i + i\epsilon) |\phi_i\rangle = i\epsilon G_0(E) |\phi_i\rangle + G_0(E) V |\Psi_i\rangle^{(+)} = G_0(E) V |\Psi_i\rangle^{(+)} \quad (2.79)$$

the first term vanishes because  $|\phi_i\rangle$  are not eigenstates of the free-Hamiltonian  $H_0$ . We thus obtain the following decomposition

$$|\Psi_i\rangle^{(+)} = G_0(E) V |\Psi_i\rangle^{(+)} = G_0(E) \sum_{j=1}^3 V_j |\Psi_i\rangle^{(+)} =: \sum_{j=1}^3 |\psi_{i,j}\rangle \quad (2.80)$$

which is called the Faddeev decomposition. We now multiply  $G_0 V_i$  to the fundamental set of Lippmann-Schwinger equations

$$G_0(E) V_i |\Psi_i\rangle^{(+)} = G_0(E) V_i |\phi_i\rangle + G_0(E) V_i G_i(E) V^i |\Psi_i\rangle^{(+)} \quad (2.81)$$

$$G_0(E) V_j |\Psi_i\rangle^{(+)} = G_0(E) V_j G_j(E) V^j |\Psi_i\rangle^{(+)} \quad (2.82)$$

$$G_0(E) V_k |\Psi_i\rangle^{(+)} = G_0(E) V_k G_k(E) V^k |\Psi_i\rangle^{(+)} \quad (2.83)$$

and noting that  $G_0 V_i G_i = G_i V_i G_0$  and  $G_0 V_i |\phi_i\rangle = |\phi_i\rangle$ , we obtain the following set of three coupled equations

$$\begin{aligned} |\psi_{i,i}\rangle &= |\phi_i\rangle + G_i(E) V_i (|\psi_{i,j}\rangle + |\psi_{i,k}\rangle) \\ |\psi_{i,j}\rangle &= G_j(E) V_j (|\psi_{i,k}\rangle + |\psi_{i,i}\rangle) \\ |\psi_{i,k}\rangle &= G_k(E) V_k (|\psi_{i,i}\rangle + |\psi_{i,j}\rangle) \end{aligned}$$

they are the Faddeev equations first derived by Faddeev [55] whose solutions  $|\psi_{i,j}\rangle$  sum up to give  $|\Psi_i\rangle^{(+)} = \sum_j |\psi_{i,j}\rangle$ .

### 2.2.3 The AGS Equations

In the previous section, we derived the Faddeev equations which the three-body channel states satisfy. In practical calculations, we often estimate quantities related with scattering experiments such as cross sections, phase shifts and poles of the scattering amplitudes. In this section, we derive the scattering equations which the three-body channel scattering amplitudes satisfy known as the AGS equations first derived by Alt-Grassberger-Sandhas [56]. After motivating the expression for the scattering amplitudes, we derive the AGS equations from the Faddeev equations. We then show the AGS equations reduce to that are formally equivalent form to the multi-channel Lippmann-Schwinger equation in case separable interactions are assumed for the two-body interactions. The relation between the AGS amplitudes and the physical scattering amplitudes and partial-wave representation form of the AGS equations is noted in the last.

### Three-Body Scattering Amplitudes

In the previous subsection, we introduced  $|\Psi_i\rangle^{(+)}$  which is the solution of the full Schroedinger equation and coincides with the channel state  $|\phi_i\rangle$  in the infinite past. Similarly, we can introduce

another solution of the full Schroedinger equation which coincides with the  $|\phi_i\rangle$  in the infinite future which we obviously denote as  $|\Psi_i\rangle^{(-)}$  and the corresponding Möller operator as  $\Omega^{(-)}$

$$|\Psi_i\rangle^{(\pm)} = \Omega^{(\pm)}|\phi_i\rangle \quad (2.84)$$

The  $S$ -matrix is defined as an overlap between the above states

$$S_{ij} = {}^{(-)}\langle\Psi_i|\Psi_j\rangle^{(+)} \quad (2.85)$$

The explicit expressions for the Möller operator ( ref equation ) and the resolvent identity leads to the formal solution of  $|\Psi_i\rangle^{(\pm)}$  as below

$$|\Psi_i\rangle^{(\pm)} = |\phi_i\rangle + \frac{1}{E_i \pm i\epsilon - H} V^i |\phi_i\rangle \quad (2.86)$$

and recalling that

$$\frac{1}{z \pm i\epsilon} = \mathcal{P} \frac{1}{z} \mp i\pi\delta(z) \quad (2.87)$$

we obtain the relation between  $|\Psi_i\rangle^{(\pm)}$

$$|\Psi_i\rangle^{(-)} - |\Psi_i\rangle^{(+)} = 2i\pi\delta(E_i - H) V^i |\phi_i\rangle \quad (2.88)$$

which leads to the following expression for the  $S$ -matrix

$$\begin{aligned} S_{ij} &= {}^{(+)}\langle\Psi_i|\Psi_j\rangle^{(+)} - 2i\pi\delta(E_i - E_j) \langle\phi_i|V^i|\Psi_j\rangle^{(+)} \\ &= \delta_{ij}\delta(\mathbf{q}_i - \mathbf{q}_j) - 2i\pi\delta(E_i - E_j) \langle\phi_i|V^i|\Psi_j\rangle^{(+)} \end{aligned} \quad (2.89)$$

We can see that the three-body scattering amplitudes  $U_{ij}$  where  $i$  and  $j$  denotes the indices of the initial and final channel states is obviously defined as

$$U_{ij} = \langle\phi_i|V^i|\Psi_j\rangle^{(+)} \quad (2.90)$$

The equations which the above scattering amplitudes satisfy are known as the AGS equations. We shall derive that equations in the next subsection

## Derivation

We now derive the AGS equations which three-body scattering amplitudes satisfy from the fundamental set of Lippmann-Schwinger equations or equivalently, the Faddeev equations.

We first rewrite the Faddeev equations by noting the definition of the scattering amplitude (2.90) as follows

$$\begin{aligned} V_i|\Psi_i\rangle^{(+)} &= G_0^{-1}(E)|\phi_i\rangle + V_i G_i(E)(V_j + V_k)|\Psi_i\rangle^{(+)} \\ &= G_0^{-1}(E)|\phi_i\rangle + V_i G_i(E)(E) V^i |\Psi_i\rangle^{(+)} \\ &= G_0^{-1}(E)(E)|\phi_i\rangle + V_i G_i(E)(E) U_{ii} |\phi_i\rangle \end{aligned} \quad (2.91)$$

$$V_j|\Psi_i\rangle^{(+)} = V_j G_j(E)(V_k + V_i)|\Psi_i\rangle^{(+)} = V_j G_j(E) V^j |\Psi_i\rangle^{(+)} = V_j G_j(E) U_{ji} |\phi_i\rangle \quad (2.92)$$

$$V_k|\Psi_i\rangle^{(+)} = V_k G_k(E)(V_i + V_j)|\Psi_i\rangle^{(+)} = V_k G_k(E) V^k |\Psi_i\rangle^{(+)} = V_k G_k(E) U_{ki} |\phi_i\rangle \quad (2.93)$$

(2.92) + (2.93), (2.93) + (2.91) and (2.91) + (2.92) gives

$$U_{ii}(E)|\phi_i\rangle = V_j G_j(E) U_{ji}(E)|\phi_i\rangle + V_k G_k(E) U_{ki}(E)|\phi_i\rangle \quad (2.94)$$

$$U_{ji}(E)|\phi_i\rangle = G_0^{-1}(E)|\phi_i\rangle + V_k G_k(E) U_{ki}(E)|\phi_i\rangle + V_i G_i(E) U_{ii}(E)|\phi_i\rangle \quad (2.95)$$

$$U_{ki}(E)|\phi_i\rangle = G_0^{-1}(E)|\phi_i\rangle + V_i G_i(E) U_{ii}(E)|\phi_i\rangle + V_j G_j(E) U_{ji}(E)|\phi_i\rangle \quad (2.96)$$

We can now omit  $|\phi_i\rangle$  and these set of equations can be written in a compact form

$$U_{ij}(E) = \bar{\delta}_{ij} G_0^{-1}(E) + \sum_{k=1}^3 \bar{\delta}_{ik} V_k G_k(E) U_{kj}(E) \quad (2.97)$$

Two-body scattering amplitude in the three-body channel is defined as follows

$$V_k G_k(E) = t_k G_0(E) \quad (2.98)$$

It can be easily shown that  $t_k$  defined above satisfies the usual Lippmann-Schwinger equation

$$t_k(E) = V_k(E) + V_k G_0(E) t_k(E) \quad (2.99)$$

The AGS equation is then written as

$$U_{ij}(E) = \bar{\delta}_{ij} G_0^{-1}(E) + \sum_{k=1}^3 \bar{\delta}_{ik} t_k(E) G_0(E) U_{kj}(E) \quad (2.100)$$

In the next subsection, we will discuss how to extract physical informations from these equations in practical calculations.

### Reduction of the AGS Equations into Multi-Channel Lippmann-Schwinger Equation

Alt-Grassberger-Sandhas [56] showed that if the two-body interaction takes the separable form, the AGS equations are reduced to that is formally equivalent to multi-channel Lippmann-Schwinger equation which can be easily solved in a standard numerical procedure.

Let us remind that the AGS equations in operator form are written as

$$U_{ij}(E) = \bar{\delta}_{ij} G_0^{-1}(E) + \sum_k \bar{\delta}_{ik} t_k(E) G_0(E) U_{kj}(E) \quad (2.101)$$

sandwiching with  $G_0$  from both sides, we obtain

$$X_{ij}(E) = Z_{ij}(E) + \sum_k Z_{ik}(E) t_k(E) X_{kj}(E) \quad (2.102)$$

where  $X_{ij}$  and  $Z_{ij}$  are defined as

$$X_{ij}(E) = G_0(E) U_{ij}(E) G_0(E) \quad \text{and} \quad Z_{ij}(E) = \bar{\delta}_{ij} G_0(E) \quad (2.103)$$

It is convenient to consider the equation in a  $3 \times 3$  matrix

$$X(E) = Z(E) + Z(E) T(E) X(E) \quad (2.104)$$

where  $X(E)$ ,  $Z(E)$  and  $T(E)$  are all  $3 \times 3$  matrices. Each components of the driving term  $Z(E)$  is, written explicitly,

$$(Z(E))_{ij} = \bar{\delta}_{ij} G_0(E) \quad (2.105)$$

$T(E)$  is  $3 \times 3$  diagonal matrix whose matrix elements are

$$(T(E))_{ij} = \delta_{ij} t_i(E) \quad (2.106)$$

$t_k(E)$  are re-summed  $V_k$

$$t_k(E) = V_k + V_k G_0(E) V_k + \cdots = V_k \frac{1}{1 - G_0(E) V_k} \quad (2.107)$$



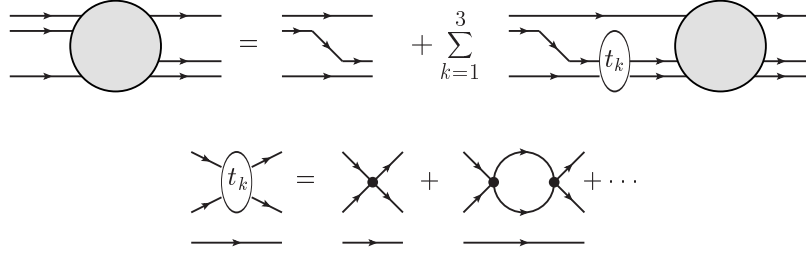


Figure 2.2: A diagrammatic representation of the AGS equations without a three-body force

If the two-body interactions are described by the separable potential of the form

$$V_i = \int d\mathbf{q}_i |\mathbf{q}_i g\rangle \lambda_i \langle \mathbf{q}_i g| \quad (2.108)$$

It can be easily shown that the  $V_i$  is indeed two-body separable interaction by considering the matrix element

$$\langle \mathbf{q}_i \mathbf{p}_i | V_i | \mathbf{q}'_i \mathbf{p}'_i \rangle = \delta(\mathbf{q}_i - \mathbf{q}'_i) \langle \mathbf{p}_i | g \rangle \lambda_i \langle g | \mathbf{p}'_i \rangle \quad (2.109)$$

The two-body scattering amplitudes  $t_i$  which are sums of the interaction  $V_i$  and satisfies the Lippmann-Schwinger equation

$$t_i(E) = V_i + V_i G_0(E) t_i(E) \quad (2.110)$$

can then be analytically solvable to give also the separable two-body scattering amplitude as follows

$$t_i(E) = \int d\mathbf{q}_i |\mathbf{q}_i g\rangle \tau_i(E) \langle \mathbf{q}_i g| \quad \text{where} \quad \tau_i(E) = \frac{\lambda_i}{1 - \lambda_i \langle g | G_0(E) | g \rangle} \quad (2.111)$$

substituting the above expressions gives the following integral equation

$$X_{ij}(E \mathbf{q}_i \mathbf{q}_j) = Z_{ij}(E \mathbf{q}_i \mathbf{q}_j) + \sum_{k=1}^3 \int d\mathbf{q}_k Z_{ij} E(\mathbf{q}_i \mathbf{q}_k) \tau_k \left( E - \frac{q_k^2}{2\mu_k} \right) X_{kj} E(\mathbf{q}_k \mathbf{q}_j) \quad (2.112)$$

where,

$$X_{ij}(E \mathbf{q}_i \mathbf{q}_j) = \langle \mathbf{q}_i g | X_{ij}(E) | \mathbf{q}_j g \rangle, \quad Z_{ij}(E \mathbf{q}_i \mathbf{q}_j) = \langle \mathbf{q}_i g | Z_{ij}(E) | \mathbf{q}_j g \rangle \quad (2.113)$$

which is formally equivalent to multi-channel Lippmann-Schwinger equation. This type of integral equation is well-known and numerically solvable by the standard procedure.

The AGS equation above is diagrammatically represented as Fig 2.2. Diagrammatic representation of the AGS equations reveals the simple interpretation of the equations. That is, two-body interactions are summed up respectively beforehand to give the three amplitudes  $t_i$  and then sum the amplitudes up mixing with each other while intermediate propagations are mediated by the free three-body Green function  $G_0$ .

If we are interested in analytical properties of the  $X_{ij}$  that is, pole positions of the scattering amplitudes, one can solve an eigenvalue equation for the kernel of the AGS equations instead of solving (2.104)

$$Z(E) T(E) |n\rangle = \eta_n |n\rangle \quad (2.114)$$

According to the Fredholm theory [61], the integral equation can be formally solved and represented with the eigenvalues and eigenvectors to give  $X$  as follows

$$X(E) = \frac{1}{1 - Z(E) T(E)} Z(E) = \sum_n \frac{|n\rangle \langle n| Z(E)}{1 - \eta_n(E)} \quad (2.115)$$

whose pole energy  $E_{\text{pole}}$  obviously satisfies

$$\eta_n(E_{\text{pole}}) = 1 \quad (2.116)$$

We will mainly focus on the equation (2.114) in the following part of this thesis. For the sake of completeness, we present the integral form of the equation

$$\sum_j \int d\mathbf{q}_j Z_{ij}(E\mathbf{q}_i\mathbf{q}_j) \tau_j \left( E - \frac{q_j^2}{2\mu_j} \right) \phi_n(\mathbf{q}_j) = \eta_n(E) \phi_n(\mathbf{q}_i) \quad (2.117)$$

### Relation between The Matrix Element and The Physical Scattering Amplitude

Now we have the integral equation which the  $X_{ij}$  satisfies. However,  $X$  itself is not identical to the scattering amplitude which is obvious from the definition (2.103). The question is, how is the  $X$  related to the physical scattering amplitude? To that end, we follow the argument in the original article by Alt-Grassberger-Sandhas [56].

The Hamiltonian for the two-body subsystem in a three-body system, namely, particle  $j$  and  $k$  is

$$\frac{p_i^2}{2\mu_i} + V_i \quad (2.118)$$

eigenstates of this Hamiltonian includes scattering states  $|\mathbf{p}_i\rangle^{(+)}$  and if the interaction is attractive enough, bound states  $|b\rangle$ . Thus, the spectral representation of the two-body amplitude  $t_i$  is

$$t_i(E) = V_i + \sum_b \frac{V_i|b\rangle\langle b|V_i}{E - E_b} + \int d\mathbf{p}_i \frac{V_i|\mathbf{p}_i\rangle^{(+)}\langle^{+}|\mathbf{p}_i|V_i}{E - E_{p_i}} \quad (2.119)$$

in the limit  $E \rightarrow E_b$ ,  $T_i$  is dominated by the pole term

$$t_i(E) \rightarrow \frac{V_i|b\rangle\langle b|V_i}{E - E_b} \quad (E \rightarrow E_b) \quad (2.120)$$

comparing this expression with that of the separable one equation (2.111), we have the following correspondence

$$|g\rangle \leftrightarrow V_i|b\rangle \quad \tau(E) \leftrightarrow \frac{1}{E - E_b} \quad (2.121)$$

Therefore, in the limit  $E \rightarrow \frac{q_i^2}{2M_i} + E_b$  the solutions of the integral equation (2.112) become

$$\langle \mathbf{q}_i g | X_{ij}(E) | \mathbf{q}_i g \rangle = \langle \mathbf{q}_i g | \bar{\delta}_{ij} G_0(E) | \mathbf{q}_i g \rangle \rightarrow \langle \mathbf{q}_i \varphi_i | V_i G_0(E) U_{ij}(E) G_0(E) V_i | \mathbf{q}_j \varphi_j \rangle \quad (2.122)$$

Recalling that

$$G_0(E) V_i | \mathbf{q}_i \varphi_i \rangle = | \mathbf{q}_i \varphi_i \rangle = | \phi_i \rangle \quad \left( E \rightarrow \frac{q_i^2}{2M_i} + E_b \right) \quad (2.123)$$

Thus, when the energy is on-shell, in a sense of channel state, the matrix element ( ref equation ) is identical to the physical scattering amplitude for channel state to channel state scattering.

$$\langle \mathbf{q}_i g | X_{ij}(E) | \mathbf{q}_i g \rangle \rightarrow \langle \phi_i | U_{ij}(E) | \phi_j \rangle \quad \left( E \rightarrow \frac{q_i^2}{2M_i} + E_b \right) \quad (2.124)$$

Since the on-shell matrix element (2.124) is identical to the physical scattering amplitude, even its off-shell matrix element has the same analytic properties that the physical scattering amplitude has. We will therefore discuss pole positions of the matrix element (2.124) even if non of three pairs in three particles form bound state in order to analyze energy of bound states or resonances.

## Partial-Wave Representations of The AGS Equations

In a practical calculation, we frequently consider the problem in a partial-wave basis. We therefore present explicit expressions of the AGS equations for completeness in this subsection.

We consider the two-body separable interactions which in a partial-wave basis are represented as follows

$$V_i = \sum_{JM} \sum_{\alpha_i \alpha'_i} \int q_i^2 dq_i |q_i g \alpha_i JM\rangle \lambda_{\alpha_i \alpha'_i} \langle q_i g \alpha'_i JM| \quad (2.125)$$

where  $J, M$  are the total angular momentum and its  $z$  component,  $\alpha_i$  are the rest of quantum numbers such as relative angular momenta or spins and  $g$  is the partial-wave form factor. Then, as in the plane-wave basis case, the two-body partial-wave scattering amplitudes can be solved analytically and are represented as

$$t_i(E) = \sum_{JM} \sum_{\alpha_i \alpha'_i} \int q_i^2 dq_i |q_i g \alpha_i JM\rangle \tau_{\alpha_i \alpha'_i}(E) \langle q_i g \alpha'_i JM| \quad (2.126)$$

The explicit expression of  $\tau_{\alpha_i \alpha'_i}$  is

$$\tau_{\alpha_i \alpha'_i}(E) = \frac{\lambda_{\alpha_i \alpha'_i}}{1 - \lambda_{\alpha_i \alpha'_i} \langle g \alpha_i | G_0(E) | g \alpha'_i \rangle} \quad (2.127)$$

Substituting these expressions to the AGS equations (2.104) leads to the AGS equations in a partial-wave basis

$$X_{\alpha_i \alpha_j}(Eq_i q_j) = Z_{\alpha_i \alpha_j}(Eq_i q_j) + \sum_{k, \alpha_k} \int_0^\infty q_k^2 dq_k Z_{\alpha_i \alpha_k}(Eq_i q_k) \tau_{\alpha_k} \left( E - \frac{q_k^2}{2\mu_k} \right) X_{\alpha_k \alpha_j}(Eq_k q_j) \quad (2.128)$$

and its corresponding eigenvalue equations are

$$\sum_{k, \alpha_k} \int_0^\infty q_k^2 dq_k Z_{\alpha_i \alpha_k}(Eq_i q_k) \tau_{\alpha_k} \left( E - \frac{q_k^2}{2\mu_k} \right) \phi_{k, \alpha_k}(q_k) = \eta_n(E) \phi_{i, \alpha_i}(q_i) \quad (2.129)$$

The explicit expression for  $Z_{\alpha_i \alpha_k}(Eq_i q_k)$  is given in the appendix.

## The AGS Equations with a Three-Body Force

So far in this section, we have been considering only two-body interactions. However, as we saw in previous section, a coupling to two-body channels induces the effective *three-body forces*. It is therefore necessary to modify the AGS equations so that it can treat three-body forces in addition to two-body forces. We present the method developed by Glöckle [62] in this section.

$$U_{ij}(E) = (\bar{\delta}_{ij} + t_4(E) G_0(E)) G_0^{-1}(E) + \sum_k (\bar{\delta}_{ik} + t_4(E) G_0(E)) T_k(E) U_{kj}(E) \quad (2.130)$$

Applying the  $G_0(E)$  from both of left and right, we obtain

$$X_{ij}(E) = Z_{ij}(E) + \sum_k Z_{ik}(E) T_k(E) X_{kj}(E) \quad (2.131)$$

where we have defined

$$X_{ij}(E) = G_0(E) U_{ij}(E) G_0(E) \quad (2.132)$$

$$Z_{ij}(E) = \bar{\delta}_{ij} G_0(E) + G_0(E) t_4(E) G_0(E) 1_{ij} =: (Z_0(E))_{ij} + (Z_4(E))_{ij} \quad (2.133)$$

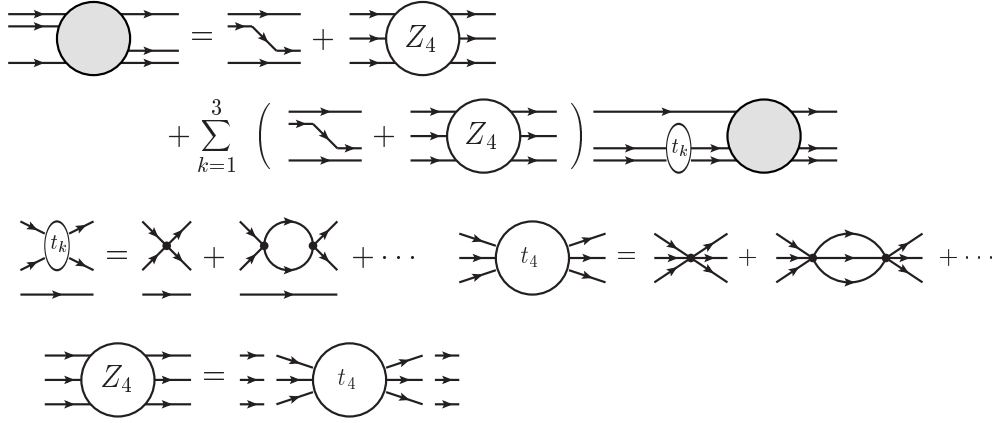


Figure 2.3: A diagrammatic representation of the AGS equations with a three-body force.

This ensures that the same two-body  $T$ -matrix does not appear in a row. The second term is re-summed effective three-body interaction multiplied by the free Green function from both of left and right sides

$$\begin{aligned} Z_4(E) &= G_0(E) (V_4 + V_4 G_0(E) V_4 + \dots) G_0(E) \\ &= G_0(E) V_4 \frac{1}{1 - G_0(E) V_4} G_0(E) \end{aligned} \quad (2.134)$$

in contrast to the exchange operator,  $Z_4(E)$  has all  $3 \times 3$  components. Written explicitly,

$$(Z_4(E))_{ij} = G_0(E) V_4 \frac{1}{1 - G_0(E) V_4} G_0(E) 1_{ij} \quad (2.135)$$

Diagrammatic representation of the AGS equations in figure 2.3 with a three-body force leads to the following intuitive interpretation. That is, we sum up two-body forces *and* three-body forces respectively beforehand to give scattering amplitudes for two-body and three-body forces, then sum the amplitudes up mixing with each other where the intermediate propagation is mediated by the three-body free Green function  $G_0(E)$ .

## 2.3 Analytic Continuation of the $S$ -Matrix

Bound states and resonances are poles of the analytically continued  $S$ -matrix in the complex energy plane. Bound states lie on a real axis below thresholds while resonances lie in the forth quadrant of the unphysical complex energy plane near the branch cut corresponding to scattering states. The  $T$ -matrix can be obtained by solving the Lippmann-Schwinger equation in case of two-body scattering or (Faddeev-)AGS equations in case of three-body scattering. However, the  $T$ -matrix and transition amplitudes we obtain by solving those scattering equations usually have branch cut starting from threshold along the positive real axis and if we want to investigate resonances and virtual states, analytic continuation to the unphysical energy sheet is necessary. We adopted the so-called contour rotation method [63, 64] to reveal the unphysical sheet and we briefly review the method in this subsection.

Since the  $S$ -matrix and the  $T$ -matrix have the same analyticities and that the  $T$ -matrix is directly related to physical scattering quantities such as scattering cross sections and phase shifts, we consider the  $T$ -matrix instead of the  $S$ -matrix in the following. We focus on single-channel two-body system whose particles have spin zero and in  $s$ -wave in order to simplify the

argument. The  $T$ -matrix has poles on the real axis below the two-body threshold corresponding to bound states of the system and there is a branch cut along the real axis starting from the two-body threshold which corresponds to two-body scattering state. The analyticities of the  $T$ -matrix is most manifestly represented in the form of the spectral representation

$$T(E) = V + \sum_b \frac{V|b\rangle\langle b|V}{E - E_b} + \int_0^\infty p^2 dp \frac{V|p\rangle^{(+)(+)}\langle p|V}{E - \frac{p^2}{2\mu}} \quad (2.136)$$

the pole behaviors at energies corresponding to bound states and discontinuities at scattering energies can be seen as below

$$T(E + i\epsilon) - T^\dagger(E - i\epsilon) = \sum_b V|b\rangle\langle b|V(-2\pi i\delta(E - E_b)) + V|p\rangle^{(+)(+)}\langle p|V(-2\pi i\mu k\Theta(k)) \quad (2.137)$$

where  $k$  is defined as

$$E = \frac{k^2}{2\mu} \quad (2.138)$$

with  $\mu$  is the reduced mass of the two particles. We can see that the  $T$ -matrix has poles at energies corresponding to the bound states and discontinuity for  $k > 0$ , that is, in the physical energy region.

If we perform the change of variables  $p \rightarrow e^{-i\theta}p$ , the spectral representation of the  $T$ -matrix becomes

$$T(E) = V + \sum_b \frac{V|b\rangle\langle b|V}{E - E_b} + \int_0^{\infty e^{i\theta}} e^{-2i\theta} p^2 e^{-i\theta} dp \frac{V|p\rangle^{(+)(+)}\langle p|V}{E - e^{-2i\theta} \frac{p^2}{2\mu}} \quad (2.139)$$

If there are no singularities between the rotated integration path and the real-axis, we can deform the integration contour to lie on a real axis.

$$T(E) = V + \sum_b \frac{V|b\rangle\langle b|V}{E - E_b} + \int_0^\infty e^{-2i\theta} p^2 e^{-i\theta} dp \frac{V|p\rangle^{(+)(+)}\langle p|V}{E - e^{-2i\theta} \frac{p^2}{2\mu}} \quad (2.140)$$

The branch cut of the  $T$ -matrix which corresponds to two-body scattering state obviously shifted from the real-axis to rotated line whose amount of rotation is  $-2\theta$  counter clockwise. We have therefore performed analytic continuation of the  $T$ -matrix to the unphysical sheet where resonances lie.

In practice, we solve, in case of two-body scattering problems, the Lippmann-Schwinger equation shown below

$$T(Epp') = V(pp') + \int_0^\infty p''^2 dp'' \frac{V(pp'')T(Ep''p')}{E - \frac{p''^2}{2\mu}} \quad (2.141)$$

However, the philosophy is the same as we just discussed for the formal  $T$ -matrix. Assuming the interaction  $V(pp')$  does not have any singularity in the forth quadrant of complex  $p$ -plane, the integration contour can be rotated by an amount  $\theta$  clock-wise.

$$T(Epp') = V(pp') + \int_0^{\infty e^{-i\theta}} p''^2 dp'' \frac{V(pp'')T(Ep''p')}{E - \frac{p''^2}{2\mu}} \quad (2.142)$$

We then perform variable transformation to obtain

$$T(Epp') = V(pp') + \int_0^\infty e^{-3i\theta} p''^2 dp'' \frac{V(pe^{-i\theta}p'')T(Ee^{-i\theta}p''p')}{E - e^{-2i\theta} \frac{p''^2}{2\mu}} \quad (2.143)$$

The branch cut once lying on the real axis is now rotated by an amount of  $2\theta$  clock-wise.

As long as the integration contour does not cross singularities originated from the interaction  $V(pp')$ , we can deform the integration path. In case of practical calculations, the form of the interaction restricts the complex energy region we can perform analytic continuation as we will see in the case of the Yamaguchi-type interaction. If we consider the following Yamaguchi-type interaction,

$$V(pp') = g(p) \lambda g(p'), \quad g(p) = \frac{\Lambda^2}{p^2 + \Lambda^2} \quad (2.144)$$

$V(pp')$  has poles at  $p = \pm i\Lambda$  and it is therefore not possible to perform contour rotation for  $\theta \geq \frac{\pi}{2}$ . If we want to search poles lying on, for example, negative real axis on the unphysical sheet such as virtual state, we need to adopt another method such as contour deformation [65, 66].

## Chapter 3

# The Effective AGS Approach and The Finite Mass Renormalization

In the previous chapter, we have explored the methods we employ to analyze the two-body and three-body coupled channels system, namely the Feshbach projection formalism, the (Faddeev-)AGS formalism and the dispersion theory with the optical theorem. In this chapter, we combine these to build our two-body and three-body coupled-channels (Faddeev-)AGS scattering equations.

We then discuss the problem of unphysical singularities which we encounter when we perform numerical calculation. We discuss how those problematic unphysical singularities appear and how it can be cured by an appropriate reorganization of those terms that appear in the effective AGS equations.

### 3.1 Notation

In this section, we introduce and summarize our notation we use in the following part of the thesis. We present notation in three-body as well as two-body channels because we slightly change notation in the three-body.

#### Channels

We consider a two-body and a three-body systems which couple with each other. We denote the three particles in the three-body channel as  $\phi_1\phi_2\phi_3$ . We assume  $\phi_1\phi_2$  couple to another particle  $\psi_3$ . The two-body channel is therefore consists of two particles  $\psi_3\phi_3$ . The channels are summarized in the table 3.1 below.

Three-body channel	Two-body channel
$\phi_1\phi_2\phi_3$	$\psi_3\phi_3$

Table 3.1: The two-body and three-body channels

### Three-Body channel

We denote the masses of  $\phi_1\phi_2\phi_3$  as  $m_1$ ,  $m_2$  and  $m_3$  respectively. In three-body problems, we often introduce the Jacobi coordinates. Let  $\mathbf{x}_1$ ,  $\mathbf{x}_2$  and  $\mathbf{x}_3$  be position vectors in the Cartesian coordinate. The Jacobi coordinates are then defined as

$$\mathbf{R} = \frac{\sum_i m_i \mathbf{x}_i}{\sum_i m_i} \quad (3.1)$$

$$\mathbf{R}_i = \mathbf{x}_i - \frac{m_j \mathbf{x}_j + m_k \mathbf{x}_k}{m_j + m_k} \quad (3.2)$$

$$\mathbf{r}_i = \mathbf{x}_j - \mathbf{x}_k \quad (3.3)$$

$\mathbf{R}$ ,  $\mathbf{R}_i$  and  $\mathbf{r}_i$  are center of mass, relative coordinate between  $\phi_i$  and the pair of  $\phi_j\phi_k$  and relative coordinate between  $\phi_j$  and  $\phi_k$  respectively.  $i$ ,  $j$  and  $k$  are cyclic permutation of 1, 2, 3.

Let  $\mathbf{k}_1$ ,  $\mathbf{k}_2$  and  $\mathbf{k}_3$  be momenta in Cartesian coordinate. The Jacobi momenta are then,

$$\mathbf{P} = \sum_i \mathbf{k}_i \quad (3.4)$$

$$\mathbf{q}_i = \frac{(m_j + m_k) \mathbf{k}_i - m_i (\mathbf{k}_j + \mathbf{k}_k)}{\sum_i m_i} \quad (3.5)$$

$$\mathbf{p}_i = \frac{m_j \mathbf{k}_j - m_k \mathbf{k}_k}{m_j + m_k} \quad (3.6)$$

where  $\mathbf{P}$  is the center of mass momentum,  $\mathbf{q}_i$  are the relative momenta between  $\phi_i$  and the pair of  $\phi_j\phi_k$  and  $\mathbf{p}_i$  are relative momenta between  $\phi_j$  and  $\phi_k$ .

We consider the problem in the three-body center-of-mass frame in which  $\mathbf{P} = \mathbf{0}$ . The kinetic energy in the three-body system which we denote as  $H_0^{(3)}$  then is

$$H_0^{(3)} = \sum_{i=1}^3 \frac{k_i^2}{2m_i} = \frac{P^2}{2M} + \frac{q_i^2}{2M_i} + \frac{p_i^2}{2\mu_i} = \frac{q_i^2}{2M_i} + \frac{p_i^2}{2\mu_i} \quad (3.7)$$

where,  $M$ ,  $M_i$  and  $\mu_i$  are defined as below

$$M = m_1 + m_2 + m_3 \quad (3.8)$$

$$M_i^{-1} = m_i^{-1} + (m_j + m_k)^{-1} \quad (3.9)$$

$$\mu_i^{-1} = m_j^{-1} + m_k^{-1} \quad (3.10)$$

$M$  is the total mass,  $M_i$  is the reduced mass between  $\phi_i$  and the pair of  $\phi_j$  and  $\phi_k$  while  $\mu_i$  is the reduced mass between  $\phi_j$  and  $\phi_k$ .

We next present notations for interactions and related quantities. We denote bare two-body interactions between  $\phi_j\phi_k$  as  $V_i^{(3)}$ .

$$V_i^{(3)} = V_{jk}^{(3)} = V_{\phi_j\phi_k}^{(3)}, \quad i = 1, 2, 3 \quad (3.11)$$

The (Faddeev-)AGS equation contains three two-body  $T$ -matrices which are sums of each interactions  $V_i$  and we denote them as  $t_i^{(3)}(E)$  which satisfy the Lippmann-Schwinger equations

$$t_i^{(3)}(E) = V_i^{(3)} + V_i^{(3)} G_0^{(3)}(E) t_i^{(3)}(E), \quad i = 1, 2, 3 \quad (3.12)$$

where we have introduced the three-body free Green function  $G_0^{(3)}(E)$  defined as below

$$G_0^{(3)}(E) = \frac{1}{E - H_0^{(3)}} \quad (3.13)$$



An explicit expression in the momentum space is,

$$\begin{aligned}\langle \mathbf{q}_i \mathbf{p}_i | G_0^{(3)}(E) | \mathbf{q}_i' \mathbf{p}_i' \rangle &= \frac{1}{E - \frac{q_i^2}{2M_i} - \frac{p_i^2}{2\mu_i}} \delta(\mathbf{q}_i - \mathbf{q}_i') \delta(\mathbf{p}_i - \mathbf{p}_i') \\ &= G_0^{(3)}(E q_i p_i) \delta(\mathbf{q}_i - \mathbf{q}_i') \delta(\mathbf{p}_i - \mathbf{p}_i')\end{aligned}\quad (3.14)$$

### Two-Body Channel

The two particles in the two-body channel are  $\psi_3$  and  $\phi_3$ . We denote their masses  $\eta_3$  and  $m_3$  and their position vectors in the Cartesian coordinate as  $\mathbf{X}_3$  and  $\mathbf{x}_3$  respectively. The center-of-mass and relative coordinates are,

$$\mathbf{R} = \frac{\mathcal{M}_3 \mathbf{X}_3 + m_3 \mathbf{x}_3}{\mathcal{M}_3 + m_3} \quad (3.15)$$

$$\mathbf{r}_3 = \mathbf{X}_3 - \mathbf{x}_3 \quad (3.16)$$

The center-of-mass momentum and the relative momentum are

$$\mathcal{P} = \mathbf{K}_3 + \mathbf{k}_3 \quad (3.17)$$

$$\mathbf{Q}_3 = \frac{m_3 \mathbf{K}_3 - \mathcal{M}_3 \mathbf{k}_3}{\mathcal{M}_3 + m_3} \quad (3.18)$$

In the two-body center-of-mass system, the center-of-mass momentum is zero  $\mathcal{P} = 0$  and therefore the kinetic energy which we denote as  $H_0^{(2)}$  becomes

$$H_0^{(2)} = \frac{\mathbf{K}_3^2}{2\mathcal{M}_3} + \frac{\mathbf{k}_3^2}{2m_3} = \frac{\mathcal{P}^2}{2\mathcal{M}} + \frac{\mathbf{Q}_3^2}{2\nu_3} = \frac{\mathbf{Q}_3^2}{2\nu_3} \quad (3.19)$$

where  $\mathcal{M}$  and  $\nu_3$  are the total mass and the reduced mass of  $\psi_3$  and  $\phi_3$  respectively.

$$\mathcal{M} = \mathcal{M}_3 + m_3 \quad (3.20)$$

$$\nu_3^{-1} = \mathcal{M}_3^{-1} + m_3^{-1} \quad (3.21)$$

We denote the bare two-body interaction between  $\psi_3\phi_3$  as  $V^{(2)}$ .

$$V^{(2)} = V_{\psi_3\phi_3} \quad (3.22)$$

The  $T$ -matrix in which  $V^{(2)}$  is summed is then expressed as  $t^{(2)}(E)$

$$t^{(2)}(E) = V^{(2)} + V^{(2)} G_0^{(2)}(E) t^{(2)}(E) \quad (3.23)$$

with the non-interacting  $\psi_3\phi_3$  two-body Green function defined as below

$$G_0^{(2)}(E) = \frac{1}{E - H_0^{(2)}} \quad (3.24)$$

An explicit representation in the momentum space is,

$$\langle \mathbf{Q} | G_0^{(2)}(E) | \mathbf{Q}' \rangle = \frac{1}{E - \frac{Q^2}{2\nu_3}} \delta(\mathbf{Q} - \mathbf{Q}') = G_0^{(2)}(EQ) \delta(\mathbf{Q} - \mathbf{Q}') \quad (3.25)$$

## Two-Body and Three-Body Coupled-Channels

The coupling between  $\phi_1\phi_2$  and  $\psi_3$  comes from the off-diagonal interaction which we denote  $V^{(23)}$

$$V^{(23)} = V_{\phi_1\phi_2\phi_3 \rightarrow \psi_3\phi_3} \quad \text{and} \quad V^{(32)} = V_{\phi_1\phi_2\phi_3 \rightarrow \psi_3\phi_3} \quad (3.26)$$

The matrix element of this interaction is diagonal with respect to momentum of  $\phi_3$ , that is, the momentum of  $\phi_3$  conserves because  $\phi_3$  does not interact with other particles

$$\langle \mathbf{k}_1 \mathbf{k}_2 \mathbf{k}_3 | V^{(32)} | \mathbf{K}_3 \mathbf{k}'_3 \rangle \propto \delta(\mathbf{k}_3 - \mathbf{k}'_3) \quad (3.27)$$

where  $\mathbf{k}_i$  are three Cartesian momenta of  $\phi_i$  in the three-body system while  $\mathbf{K}_3$  is Cartesian momentum of  $\psi_3$ .

In case the three-body and two-body thresholds are degenerated, that is,

$$\mathcal{M}_3 = m_1 + m_2 \quad (3.28)$$

the reduced mass in two-body  $\psi_3\phi_3$  channel denoted as  $\nu_3$  is equal to reduced mass between  $\phi_3$  and the pair of  $\phi_1\phi_2$  which we denote  $M_3$

$$\begin{aligned} \nu_3 &= \frac{\mathcal{M}_3 m_3}{\mathcal{M}_3 + m_3} \\ &= \frac{(m_1 + m_2) m_3}{m_1 + m_2 + m_3} = M_3 \end{aligned} \quad (3.29)$$

We also note that if the two thresholds are degenerated, the momentum of  $\psi_3$  which we denote  $\mathbf{K}_3$  is equal to the sum of momenta of  $\phi_1$  and  $\phi_2$

$$\mathbf{K}_3 = \mathbf{k}_1 + \mathbf{k}_2 \quad (3.30)$$

The matrix element of  $V^{(32)}$  is then proportional also to  $\delta(\mathbf{K}_3 - \mathbf{k}_1 - \mathbf{k}_2)$

$$\langle \mathbf{k}_1 \mathbf{k}_2 \mathbf{k}_3 | V^{(32)} | \mathbf{K}_3 \mathbf{k}'_3 \rangle \propto \delta(\mathbf{K}_3 - \mathbf{k}_1 - \mathbf{k}_2) \delta(\mathbf{k}_3 - \mathbf{k}'_3) = \delta(\mathbf{P} - \mathcal{P}) \delta(\mathbf{k}_3 - \mathbf{k}'_3) \quad (3.31)$$

The last equality indicates that the center-of-mass momentum in both of the two-body and the three-body channel are equal

$$\mathbf{P} = \mathcal{P} \quad (3.32)$$

If we consider in the two-body as well as the three-body center-of-mass coordinate, that is,  $\mathbf{P} = \mathcal{P} = \mathbf{0}$ , the relative momentum between  $\psi_3$  and  $\phi_3$  which we denote  $\mathbf{Q}_3$  is equal to ( up to sign ) the relative momentum between  $\phi_3$  and the pair of  $\phi_1\phi_2$

$$\begin{aligned} \mathbf{Q}_3 &= \frac{m_3 \mathbf{K}_3 - \mathcal{M}_3 \mathbf{k}_3}{\mathcal{M}_3 + m_3} \\ &= \frac{m_3 (\mathbf{k}_1 + \mathbf{k}_2) - (m_1 + m_2) \mathbf{k}_3}{m_1 + m_2 + m_3} \\ &= -\mathbf{q}_3 \end{aligned} \quad (3.33)$$

The elementary interactions are therefore diagrammatically represented as in figure 3.1.

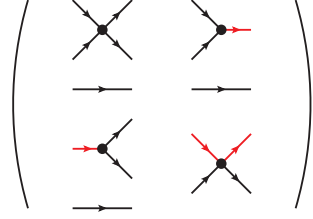


Figure 3.1: The elementary interactions

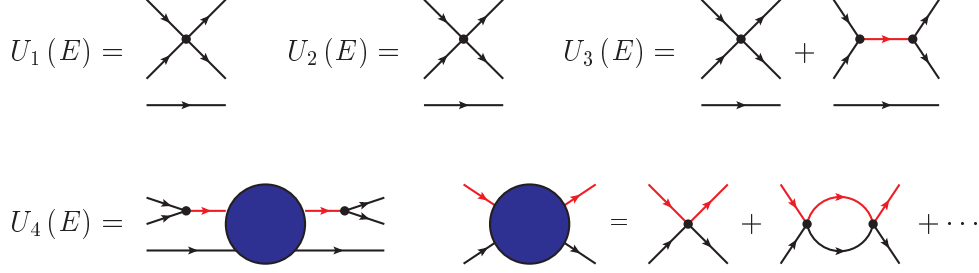


Figure 3.2: A diagrammatic representation of the effective interactions

### 3.2 The effective AGS equations

We concentrate on the elastic  $\phi_1\phi_2\phi_3$  three-body scattering and we embed effects due to coupling to the  $\psi_3\phi_3$  two-body channels into interactions utilizing the Feshbach projection method. We regard the three-body channel as  $P$ -channel and the two-body channel as  $Q$ -channel. The effective interactions in the three-body channel is therefore (see section 2.1 for the Feshbach projection procedure),

$$\begin{aligned}
 U(E) &= \sum_{i=1}^3 V_i^{(3)} + V^{(32)} G^{(2)}(E) V^{(23)} \\
 &= \sum_{i=1}^3 V_i^{(3)} + V^{(32)} G_0^{(2)}(E) V^{(23)} + V^{(32)} \left( G^{(2)}(E) - G_0^{(2)}(E) \right) V^{(23)} \\
 &= \sum_{i=1}^3 V_i + V^{(32)} G_0^{(2)}(E) V^{(23)} + V^{(32)} G_0^{(2)}(E) t^{(2)}(E) G_0^{(2)}(E) V^{(23)} \quad (3.34)
 \end{aligned}$$

where we have introduced the full Green function in two-body channel which satisfies the Dyson-Schwinger equation

$$G^{(2)}(E) = G_0^{(2)}(E) + G_0^{(2)}(E) V^{(2)} G^{(2)}(E) \quad (3.35)$$

and used the fact that it has the following formal solution

$$G^{(2)}(E) = G_0^{(2)}(E) + G_0^{(2)}(E) t^{(2)}(E) G_0^{(2)}(E) \quad (3.36)$$

where  $t^{(2)}(E)$  is the  $T$ -matrix in two-body channel we presented in the previous subsection. The three effective two-body interaction in the three-body channel are therefore

$$U_1(E) = V_1^{(3)} \quad (3.37)$$

$$U_2(E) = V_2^{(3)} \quad (3.38)$$

$$U_3(E) = V_3^{(3)} + V^{(32)} G_0^{(2)}(E) V^{(23)} \quad (3.39)$$

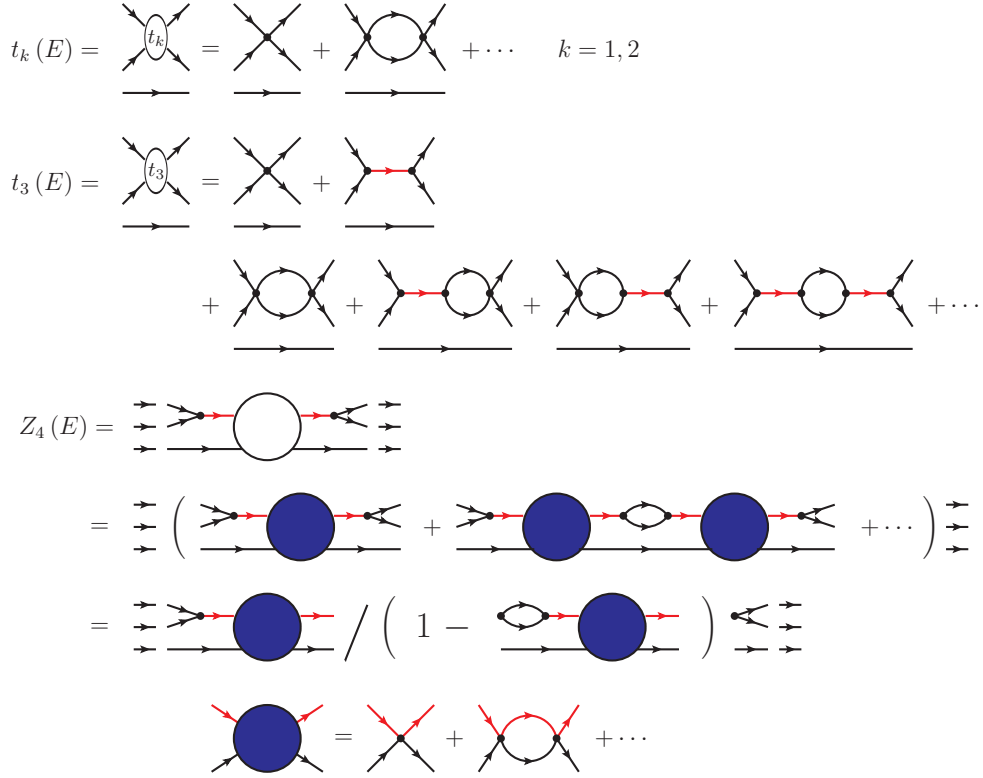


Figure 3.3: A diagrammatic representation of the elements in The (Faddeev-)AGS Equations

while the effective three-body interaction is given as

$$U_4(E) = V^{(32)} G_0^{(2)}(E) t^{(2)}(E) G_0^{(2)}(E) V^{(23)} \quad (3.40)$$

By performing the Feshbach projection procedure above, we now have reformulated the two-body and three-body coupled-channels problem as an effective three-body problem whose effects due to coupling to the two-body channels are embedded into the effective interactions in three-body channels. Diagrammatic representation of the effective interactions are given in figure 3.2.

The elements in the (Faddeev-)AGS equations are modified accordingly. Specifically, three two-body  $T$ -matrices which we denote  $t_k^{(2)}(E)$   $k = 1, 2, 3$  and the three-body  $T$ -matrix sandwiched by  $G_0^{(3)}(E)$  which we denote as  $Z_4(E)$  are modified as shown in figure 3.3.

$$t_i^{(3)}(E) = U_i(E) + U_i(E) G_0^{(3)}(E) t_i^{(3)}(E) \quad i = 1, 2, 3, 4 \quad (3.41)$$

$$Z_4(E) = G_0^{(3)} t_4^{(3)}(E) G_0^{(3)}(E) \quad (3.42)$$

The effective AGS equations are therefore represented as shown in figure 3.4.

The energies  $E$  which have appeared so far does not necessarily be the  $q_i^2/2M_i - \epsilon_i$  in case of the fragmentation scattering or  $q_i^2/2M_i + p_i^2/2\mu_i$  in case of free three-body scattering. When the energy is those we mentioned, we need to replace  $E$  with  $E + i\epsilon$  which ensures that the transition amplitudes are actually the physical one.

### Self-Energy Correction to the Mass of $\psi_3$ and The Unphysical Singularities Problem

A one of particle in the two-body channel  $\psi_3$  couples to  $\phi_1\phi_2$  in the three-body channel and the physical mass of  $\psi_3$  which appears in  $G_0^{(2)}(E)$ ,  $G^{(2)}(E)$  and  $t^{(2)}(E)$  in the above equations

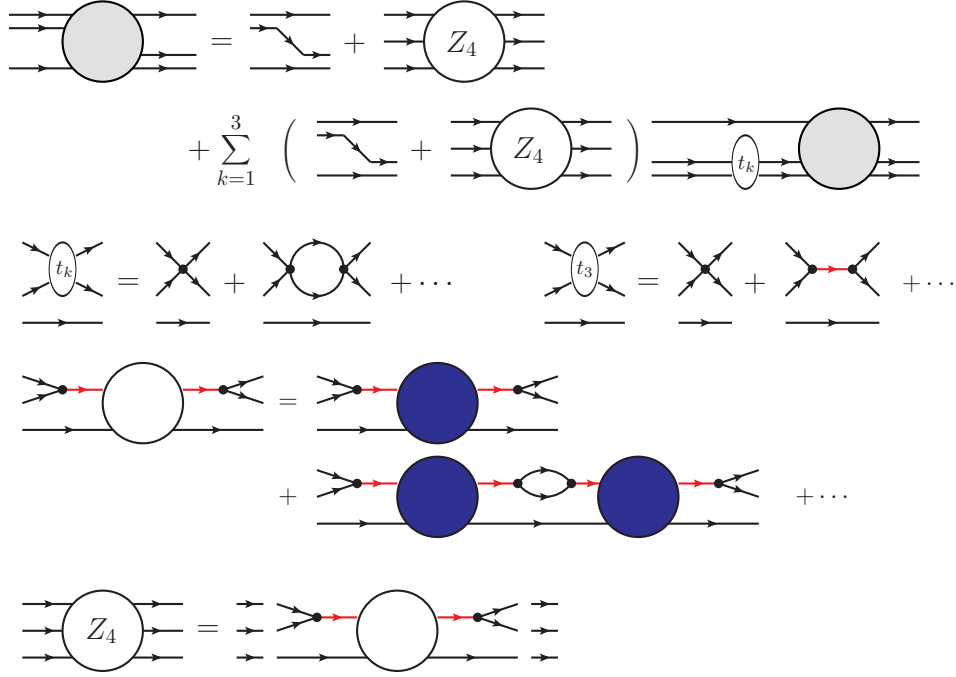


Figure 3.4: A diagrammatic representation of The (Faddeev-)AGS Equations

$$\Rightarrow = \rightarrow + \rightarrow \text{ (loop) } \rightarrow + \dots$$

Figure 3.5: A diagrammatic representation of the dressed propagator of  $\psi_3$

is shifted from the bare one due to self-energy correction to the propagator of  $\psi_3$  (see fig 3.5). This fact, combined with analytical properties of the kernel of the (Faddeev-)AGS equations, causes subtle problem when we perform numerical calculations. We will discuss this problem in detail in the next section in which we explicitly write down the effective AGS equations.

In the previous chapter, we have reformulated the two-body and three-body coupled-channels problem as an effective three-body problem and written down the effective AGS equations. Since  $\psi_3$  couples to  $\phi_1\phi_2$ , the physical mass of  $\psi_3$  shifts from the bare one. Two-body quantities such as  $G_0^{(2)}(E)$  therefore have *unphysical* singularities. This causes subtle problem when we perform numerical calculations. In this chapter, we closely discuss how those unphysical singularities appear and how it can be cured by the reorganization of the scattering equations.

### 3.3 The Unphysical Singularities Problem and Its Solution

As we mentioned at the end of the last section, the physical mass of  $\psi_3$  shifts from the bare one due to coupling to  $\phi_1\phi_2$ . If we exactly solve the effective AGS equations, those unphysical singularities do not appear. However, we solve the eigenvalue equation of the kernel of the scattering equation instead of solving the equation itself. Though the full transition amplitudes do not have unphysical singularities, the kernel of the scattering equation does. We then face the problem of the *unphysical singularities*.

We deal with this problem by the renormalization of mass and field of  $\psi_3$ . We divide the bare mass term into the physical one and the counterterm. It is then necessary to add counterterms every time the self-energies appear. The self-energies appear in terms which appear

when scattering equations are *iterated* in addition to those in kernels. We therefore need to find a way to incorporate those counterterms to be added to iteratively appearing self-energies into what we can give to the eigenvalue equation, namely kernel of the equation.

In the following, we show how these unphysical singularities appear and how it can be cured by an appropriate reorganization of the scattering equations.

### 3.3.1 The Unphysical Singularities Problem

Since we are primarily interested in pole trajectories near the thresholds, we solve eigenvalue equation of the kernel of the (Faddeev-)AGS equations instead of the equation itself. The eigenvalue equation of the kernel of the (Faddeev-)AGS equation is,

$$Z(E) T(E) |n\rangle = \eta_n(E) |n\rangle \quad (3.43)$$

where  $|n\rangle$  and  $\eta_n(E)$  are eigenvectors and eigenvalues respectively. The (Faddeev-)AGS equations

$$X(E) = Z(E) + Z(E) T(E) X(E) \quad (3.44)$$

have the formal solution

$$X(E) = \frac{1}{1 - Z(E) T(E)} Z(E) \quad (3.45)$$

As we saw in section 2.2.3, it can be expressed with the eigenvectors and eigenvalues as

$$X(E) = \sum_n \frac{|n\rangle\langle n|}{1 - \eta_n(E)} Z(E) \quad (3.46)$$

The above equation obviously shows that the poles of the amplitudes  $E_p$  satisfies

$$\eta_n(E_p) = 1 \quad (3.47)$$

We often consider the Fredholm determinant defined as

$$\prod_n (1 - \eta_n(E)) \quad (3.48)$$

which becomes zero at energies which correspond to the poles of the  $S$ -matrix. In practice, we numerically solve the eigenvalue equation (3.43) and calculate the Fredholm determinant and search energies where it becomes zero corresponding to poles of the  $S$ -matrix.

As we mentioned earlier, the physical mass of  $\psi_3$  is different from the bare one due to the coupling to  $\phi_1\phi_2$  two-body state. However, the mass of  $\psi_3$  which appear in  $G_0^{(2)}(E)$ ,  $G_2(E)$  and  $t^{(2)}(E)$  in the above equations are bare one. The Fredholm determinant therefore has *unphysical singularities* originating from the bare mass of  $\psi_3$ .

The problem we are facing occurs even in the following simple example. We consider a particle whose bare mass is  $m_b$  with the constant interaction  $\delta m$ . The Hamiltonian in the rest frame is simply

$$H = m_b + \delta m \quad (3.49)$$

The physical mass  $m_p$  is obviously

$$m_p = m_b + \delta m \quad (3.50)$$

The Green function of the particle whose mass is the physical one satisfies the Dyson-Schwinger equation

$$G_p(E) = G_b(E) + G_b(E) \delta m G_p(E) \quad (3.51)$$

where the physical and the bare Green functions are defined as

$$G_p(E) = \frac{1}{E - m_p}, \quad G_b(E) = \frac{1}{E - m_b} \quad (3.52)$$

The corresponding eigenvalue equation, the eigenvalue equation of the kernel of the Dyson-Schwinger equation is

$$G_b(E) \delta m \phi = \eta(E) \phi \quad (3.53)$$

whose eigenvalue is obviously

$$\eta(E) = \frac{\delta m}{E - m_b} \quad (3.54)$$

It has a pole at  $E = m_b$ , that is, it has an *unphysical singularity*. However, the eigenvalue equation gives a correct eigenenergy. As we discussed in the previous paragraph, the pole of the physical Green function  $G_p(E)$  is obtained as a solution of the equation

$$\eta(E) = 1 \quad (3.55)$$

which gives a pole  $E_p = m_p$ , the physical mass. The unphysical singularity is therefore a superficial one. It is however, still desirable not to present the bare or unphysical quantities as we usually do not in, such as, quantum field theory.

### 3.3.2 A Problem of The Iteratively Appearing Self-Energies and Its Solutions

In order to cure this unphysical singularity disease, we split the original mass term of  $\psi_3$  into the physical one and the counterterm as we usually do in quantum field theory. It is then, as a result, necessary to add counterterm every time the self-energy appears. It is however, not straightforward to implement it due to characteristic structure of the effective AGS equations we presented in the previous subsection and we need a trick to actually do it. We discuss the problems we face and the trick we invented in detail in this subsection.

We denote bare mass of  $\psi_3$  as  $\mathcal{M}_3^B$ . The bare free Green function of  $\psi_3$  is then written as,

$$G_0^B(E) = \frac{1}{E - \mathcal{M}_3^B} \quad (3.56)$$

The dressed propagator which we denote  $G_\Sigma^{(2)}(E)$  is,

$$G_\Sigma^{(2)}(E) = G_0^B(E) + G_0^B(E) \Sigma(E) G_0^B(E) + \dots = \frac{1}{(G_0^B(E))^{-1} - \Sigma(E)} \sim \frac{1}{E - \mathcal{M}_3^P} \quad (3.57)$$

where,  $\Sigma(E)$  is the self-energy which is induced due to the coupling to  $\phi_1\phi_2$  two-body state and  $\mathcal{M}_3^P$  is the physical mass. In quantum field theory, we often encounter such situations and we usually treat those by mass and field renormalization. In our case, we decompose the bare mass term into the physical mass term and the other into the counterterm

$$\mathcal{M}_3^B + \frac{K_3^2}{2\mathcal{M}_3^B} = \mathcal{M}_3^P + \frac{K_3^2}{2\mathcal{M}_3^P} + \Delta \quad (3.58)$$

It is then necessary to add counterterms every time the self-energies appear

$$\Sigma(E) \rightarrow \Sigma(E) + \Delta \quad (3.59)$$

The counterterm is determined by the renormalization condition on  $G_\Sigma^{(2)}(E)$ . In equation (ref equation), the renormalization condition we imposed is

$$\left(G_\Sigma^{(2)}(E)\right)^{-1} \sim 0 \quad \text{as} \quad E \sim \mathcal{M}_3^P \quad (3.60)$$

It is worth noted that if we decompose the mass term in such a way, the mass in the free Green function of  $\psi_3$  is the physical one and not the bare one

$$G_0(E) = \frac{1}{E - \mathcal{M}_3^P} \quad (3.61)$$

Having decomposed the Hamiltonian in that way, the quantities related to the two-body channel such as  $G_0^{(2)}$ ,  $G^{(2)}(E)$  and  $t^{(2)}(E)$  which had problematic unphysical singularities do not have those singularities any more and so does not the eigenvalue of the kernel of the (Faddeev-)AGS equation.

Once the decomposition is done, the eigenvalue of the kernel of the (Faddeev-)AGS equations does not have unphysical singularities. However, it is necessary to add counterterms every time the self-energies appear and this forces us to reorganize the original effective AGS equations. We will discuss the reorganization step by step in the following.

### Counterterms in $\phi_1\phi_2$ Two-Body $T$ -Matrix $t_3^{(3)}(E)$

The self-energies appear in three ways. One is in the two-body  $T$ -matrix of  $\phi_1\phi_2$  which we denote as  $t_3^{(3)}(E)$ . It satisfies the Lippmann-Schwinger equation

$$t_3^{(3)}(E) = U_3(E) + U_3(E) G_0^{(3)}(E) t_3^{(3)}(E) \quad (3.62)$$

where,  $U_3(E)$  is the effective two-body interactions between  $\phi_1\phi_2$

$$U_3(E) = V_3^{(3)} + V^{(32)} G_0^{(2)}(E) V^{(23)} \quad (3.63)$$

In order to simplify the argument, we temporarily neglect the bare interaction between  $\phi_1\phi_2$  which we denoted as  $V_3^{(3)}$  in the above equation. It is then easy to add counterterms to the self-energies which appear in the  $t_3^{(3)}(E)$  as shown below

$$\begin{aligned} t_3^{(3)}(E) &= U_3(E) + U_3(E) G_0^{(3)}(E) U_3(E) + \dots \\ &= V^{(32)} \left( G_0^{(2)}(E) + G_0^{(2)}(E) \Sigma(E) G_0^{(2)}(E) \right) V^{(23)} + \dots \\ &= V^{(32)} G_0^{(2)}(E) \frac{1}{1 - \Sigma(E) G_0^{(2)}(E)} V^{(23)} \end{aligned} \quad (3.64)$$

where we have defined the self-energy  $\Sigma(E)$  as

$$\Sigma(E) = V^{(23)} G_0^{(3)}(E) V^{(32)} \quad (3.65)$$

It is easy to add counterterms to  $t_3^{(3)}(E)$ . We just replace the self-energy with the countertermed one as below

$$t_3^{(3)}(E) \rightarrow V^{(32)} G_0^{(2)}(E) \frac{1}{1 - (\Sigma(E) + \Delta) G_0^{(2)}(E)} V^{(23)} =: V^{(32)} G_\Sigma^{(2)}(E) V^{(23)} \quad (3.66)$$



$$\begin{aligned}
t_3(E) &= \text{diagram of } t_3 \\
&= \text{diagram of } t_3 + \text{diagram of } t_3 \text{ with loop} + \text{diagram of } t_3 \text{ with cross} + \dots \\
&= \text{diagram of } t_3 \frac{1}{1 - \text{diagram of } t_3 \text{ with loop}} =: \text{diagram of } t_3 \text{ with cross}
\end{aligned}$$

Figure 3.6: A diagrammatic representation of the fully-countertermed  $t_3^{(3)}(E)$

where we have defined the fully-countertermed dressed propagator of  $\psi_3\phi_3$  two-body propagator  $G_\Sigma^{(2)}(E)$  as

$$G_\Sigma^{(2)}(E) = G_0^{(2)}(E) \frac{1}{1 - (\Sigma(E) + \Delta) G_0^{(2)}(E)} \quad (3.67)$$

It satisfies the Dyson-Schwinger equation

$$G_\Sigma^{(2)}(E) = G_0^{(2)}(E) + G_0^{(2)}(E) (\Sigma(E) + \Delta) G_\Sigma^{(2)}(E) \quad (3.68)$$

Diagrammatic representation of the fully-countertermed  $t_3^{(3)}(E)$  is given in figure 3.6.

### Counterterms in one of the Driving Term $Z_4(E)$

The other way the self-energies appear is in  $Z_4(E)$ , one of the driving terms in the effective AGS equations

$$Z_4(E) = G_0^{(3)}(E) \left( U_4(E) + U_4(E) G_0^{(3)}(E) U_4(E) + \dots \right) G_0^{(3)}(E) \quad (3.69)$$

where  $U_4(E)$  is the effective three-body interaction which is induced due to the coupling to the two-body channel whose definition is

$$U_4(E) = V^{(32)} G_0^{(2)}(E) t^{(2)}(E) G_0^{(2)}(E) V^{(23)} \quad (3.70)$$

$t_4(E)$  is the two-body  $t$ -matrix of  $\psi_3\phi_3$  which satisfies the Lippmann-Schwinger equation

$$t^{(2)}(E) = V^{(2)} + V^{(2)} G_0^{(2)}(E) t^{(2)}(E) \quad (3.71)$$

Let  $G^{(2)}(E)$  be the full  $\psi_3\phi_3$  two-body Green function which satisfies the following Dyson-Schwinger equation

$$G^{(2)}(E) = G_0^{(2)}(E) + G_0^{(2)}(E) V^{(2)} G^{(2)}(E) \quad (3.72)$$

Then,  $t^{(2)}(E)$  and  $G^{(2)}(E)$  are related to each other by the identity

$$G^{(2)}(E) = G_0^{(2)}(E) + G_0^{(2)}(E) t^{(2)}(E) G_0^{(2)}(E) \quad (3.73)$$

The second term in the right-hand side of the above equation is the very factor which appear in equation (3.70), and we name it  $\bar{G}^{(2)}(E)$  just for notational simplicity

$$\bar{G}^{(2)}(E) := G^{(2)}(E) - G_0^{(2)}(E) = G_0^{(2)}(E) t^{(2)}(E) G_0^{(2)}(E) \quad (3.74)$$

$$Z_4(E) = \frac{\text{Diagram 1} + \text{Diagram 2} + \dots}{1 - \text{Diagram 3}}$$

Figure 3.7: A diagrammatic representation of the fully-countertermed  $Z_4(E)$

$U_4(E)$  is then expressed as

$$U_4(E) = V^{(32)} \bar{G}^{(2)}(E) V^{(23)} \quad (3.75)$$

With these notations we have defined, the second term of  $Z_4(E)$  in equation (3.69) for example, contains the self-energy shown below (see also diagrammatic representation of  $Z_4(E)$  in figure 3.6)

$$U_4(E) G_0^{(3)}(E) U_4(E) = V^{(32)} \bar{G}^{(2)}(E) \Sigma(E) \bar{G}^{(2)}(E) V^{(23)} \quad (3.76)$$

It is also easy to add counterterms to it. We simply replace the self-energy with the countertermed one

$$U_4(E) G_0^{(3)}(E) U_4(E) \rightarrow V^{(32)} \bar{G}^{(2)}(E) (\Sigma(E) + \Delta) \bar{G}^{(2)}(E) V^{(23)} \quad (3.77)$$

The driving term  $Z_4(E)$  is therefore modified as right hand side of the last equation below

$$\begin{aligned}
Z_4(E) &= G_0^{(3)}(E) \left( V^{(32)} \bar{G}^{(2)}(E) V^{(23)} + V^{(32)} \bar{G}^{(2)}(E) \Sigma(E) \bar{G}^{(2)}(E) V^{(23)} + \dots \right) G_0^{(3)}(E) \\
&= G_0^{(3)}(E) V^{(32)} \bar{G}^{(2)}(E) \frac{1}{1 - \Sigma(E) \bar{G}^{(2)}(E)} V^{(23)} G_0^{(3)}(E) \\
&\rightarrow G_0^{(3)}(E) V^{(32)} \bar{G}^{(2)}(E) \frac{1}{1 - (\Sigma(E) + \Delta) \bar{G}^{(2)}(E)} V^{(23)} G_0^{(3)}(E) \quad (3.78)
\end{aligned}$$

Substituting the definition of  $\bar{G}^{(2)}(E)$  in equation (3.74), we obtain the following expression for the counterterm  $Z_4(E)$

$$Z_4(E) = G_0^{(3)}(E) V^{(32)} G_0^{(2)}(E) t^{(2)}(E) G_0^{(2)}(E) \\ \times \frac{1}{1 - (\Sigma(E) + \Delta) G_0^{(2)}(E) t^{(2)}(E) G_0^{(2)}(E)} V^{(23)} G_0^{(3)}(E)$$

We can see that  $Z_4(E)$  can be interpreted as a sum of processes that the three-body state propagates freely and makes transition to two-body state, then  $\psi_3\phi_3$  two-body  $T$ -matrix  $t^{(2)}(E)$  is summed up inserting the self-energy plus counterterm *once* between them (see figure 3.7).

### Counterterms in cross terms between $t_3^{(3)}(E)$ and $Z_4(E)$

We need to add counterterms to the every self-energies that appear in the (Faddeev-)AGS equations and saw that the self-energies which appear in  $t_3^{(3)}(E)$  and  $Z_4(E)$  can be fully countertermed by modifying  $t_3^{(3)}(E)$  and  $Z_4(E)$ . The remaining and the most problematic way in which the self-energies appear is the ones in the cross terms among  $Z_4(E)$  and  $t_3^{(3)}(E)$  such as

$$Z_0(E) t_3^{(3)}(E) Z_4(E) \quad \text{or} \quad Z_4(E) t_3^{(3)}(E) Z_4(E) \quad (3.79)$$

In the following, we will see why these self-energies are that problematic. We first recall the two-body and three-body coupled-channels (Faddeev-)AGS equation

$$X(E) = Z(E) + Z(E)T(E)X(E) \quad (3.80)$$

where  $X(E)$ ,  $Z(E)$  and  $T(E)$  are all  $3 \times 3$  matrices whose components represent three channels. The driving term  $Z(E)$  consists of two terms

$$Z(E) = Z_0(E) + Z_4(E) \quad (3.81)$$

As we saw in chapter 2,  $Z_0(E)$  is an intrinsic operator in three-body physics and it ensures that the same two-body  $T$ -matrices do not appear in a row.  $Z_0(E)$  has therefore only off-diagonal components as below

$$(Z_0(E))_{ij} = \bar{\delta}_{ij} G_0^{(3)}(E) \quad (3.82)$$

where  $\bar{\delta}_{ij}$  is

$$\bar{\delta}_{ij} = 1 - \delta_{ij} = \begin{cases} 1 & i \neq j \\ 0 & i = j \end{cases} \quad (3.83)$$

or written explicitly in a matrix form

$$Z_0(E) = \begin{pmatrix} 0 & G_0(E) & G_0(E) \\ G_0(E) & 0 & G_0(E) \\ G_0(E) & G_0(E) & 0 \end{pmatrix} \quad (3.84)$$

Another term in  $Z(E)$ ,  $Z_4(E)$  on the other hand, has all  $3 \times 3$  components

$$(Z_4(E))_{ij} = Z_4(E) 1_{ij} \quad (3.85)$$

written explicitly in a matrix form,

$$Z_4(E) = \begin{pmatrix} Z_4(E) & Z_4(E) & Z_4(E) \\ Z_4(E) & Z_4(E) & Z_4(E) \\ Z_4(E) & Z_4(E) & Z_4(E) \end{pmatrix} \quad (3.86)$$

$T(E)$  is a diagonal matrix whose components are two-body  $T$ -matrices in three-body channel

$$(T(E))_{ij} = \delta_{ij} t_j^{(3)}(E) \quad i, j = 1, 2, 3 \quad (3.87)$$

or in a matrix form,

$$T(E) = \begin{pmatrix} t_1^{(3)}(E) & 0 & 0 \\ 0 & t_2^{(3)}(E) & 0 \\ 0 & 0 & t_3^{(3)}(E) \end{pmatrix} \quad (3.88)$$

This diagonal nature of the two-body  $T$ -matrix, combined with the property of one of the driving term  $Z_0(E)$  that it has only off-diagonal components, ensure that the same two-body  $T$ -matrices do not appear in a row.

We solve the above (Faddeev-)AGS equation numerically and what we can give to it are the driving term  $Z(E)$  and the two-body  $T$ -matrix  $T(E)$ . The problematic self-energies however, appear when the (Faddeev-)AGS equations are *iterated*, such as those contained in the second term of the equation below

$$\begin{aligned} X(E) &= Z(E) + Z(E) T Z(E) + \dots \\ &= Z_0(E) + Z_4(E) + (Z_0(E) + Z_4(E)) T (Z_0(E) + Z_4(E)) + \dots \end{aligned}$$

The second term contains the self-energies such as

$$\begin{aligned} Z_0(E) t_3^{(3)}(E) Z_4(E) &= Z_0(E) \times V^{(32)} G_\Sigma^{(2)}(E) V^{(23)} \times G_0^{(3)}(E) V^{(32)} \bar{G}^{(2)}(E) V^{(23)} \\ &= Z_0(E) V^{(32)} G_\Sigma^{(2)}(E) \Sigma(E) \bar{G}^{(2)}(E) V^{(23)} \end{aligned} \quad (3.89)$$

and those shown below

$$\begin{aligned} Z_4(E) t_3^{(3)}(E) Z_4(E) &= G_0^{(3)}(E) V^{(32)} \bar{G}_2^{(2)}(E) V^{(23)} G_0^{(3)}(E) \times V^{(32)} G_\Sigma^{(2)}(E) V^{(23)} \\ &\times G_0^{(3)}(E) V^{(32)} \bar{G}^{(2)}(E) V^{(23)} G_0^{(3)}(E) \\ &= G_0^{(3)}(E) V^{(32)} \bar{G}^{(2)}(E) \Sigma(E) G_\Sigma^{(2)}(E) \Sigma(E) \bar{G}^{(2)}(E) V^{(23)} G_0^{(3)}(E) \end{aligned}$$

We need to add counter terms to those self-energies as well

$$\begin{aligned} &Z_0(E) t_3^{(3)}(E) Z_4(E) \\ \rightarrow &Z_0(E) V^{(32)} G_\Sigma^{(2)}(E) (\Sigma(E) + \Delta) \bar{G}^{(2)}(E) V^{(23)} \end{aligned} \quad (3.90)$$

$$\begin{aligned} &Z_4(E) t_3^{(3)}(E) Z_4(E) \\ \rightarrow &G_0^{(3)}(E) V^{(32)} \bar{G}^{(2)}(E) (\Sigma(E) + \Delta) G_\Sigma^{(2)}(E) (\Sigma(E) + \Delta) \bar{G}^{(2)}(E) V^{(23)} G_0^{(3)}(E) \end{aligned} \quad (3.91)$$

However, as we mentioned, we solve the (Faddeev-)AGS equation numerically, not iteratively. Therefore, a strategy that we add counterterms when the self-energies appear as we usually do in perturbative calculation does not work in our case. We rather need to find a way to incorporate those counterterms, counterterms which need to be added to the self-energies that appear when (Faddeev-)AGS equations are *iterated*, into what we can feed to the equations, namely the driving term  $Z(E)$  and the two-body  $T$ -matrix  $T(E)$ . In fact, we have invented a method to accomplish the task and are going to explain in detail in the following. Our method is, roughly speaking, that we reorganize each terms so as to keep the structure of the (Faddeev-)AGS equations the same while the counterterms to be added to the iteratively appearing self-energies are fully incorporated.

We start from the formal solution of the (Faddeev-)AGS equations.

$$Z(E) = Z(E) \frac{1}{1 - T(E) Z(E)} \quad (3.92)$$

The problematic self-energies appear when  $Z_4(E)$  is multiplied by  $t_3^{(3)}(E)$ . We therefore sum a part of terms up which contain the  $\phi_1\phi_2$  two-body  $T$ -matrix denoted as  $t_3^{(3)}(E)$ . We denote that partially-summed terms as  $X_3(E)$  which is defined as below

$$X_3(E) = Z(E) \frac{1}{1 - T_3(E) Z(E)} \quad (3.93)$$

where we have defined  $T_3(E)$  as a  $3 \times 3$  matrix which contains only  $t_3^{(3)}(E)$

$$T_3(E) = \begin{pmatrix} 0 & 0 & 0 \\ 0 & 0 & 0 \\ 0 & 0 & t_3^{(3)}(E) \end{pmatrix} \quad (3.94)$$

In the following discussion, we often use the following identity. Let  $A$ ,  $B$  and  $C$  be any operators and sum  $A$  inserting  $B + C$  between as below

$$\begin{aligned} A + A(B + C)A + \dots &= A \frac{1}{1 - (B + C)A} \\ &= A \frac{1}{1 - BA} \frac{1}{1 - CA \frac{1}{1 - BA}} \end{aligned} \quad (3.95)$$

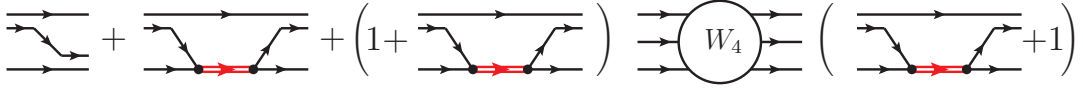


Figure 3.8: A diagrammatic representation of the  $X_3(E)$

Its meaning is that in the first equation, we sum  $A$  up inserting  $B + C$  between it while in the second equation, we first sum  $A$  up inserting  $B$  in between, we then sum that partially summed terms up inserting  $C$  between it.

The formal solution of the (Faddeev-)AGS equations can be written with  $X_3(E)$  using the above identity as shown below

$$\begin{aligned}
X(E) &= Z(E) \frac{1}{1 - T(E) Z(E)} \\
&= Z(E) \frac{1}{1 - (\bar{T}_3(E) + T_3(E)) Z(E)} \\
&= Z(E) \frac{1}{1 - T_3(E) Z(E)} \frac{1}{1 - \bar{T}_3(E) Z(E)} \frac{1}{1 - \bar{T}_3(E) Z(E)} \\
&= X_3(E) \frac{1}{1 - \bar{T}_3(E) X_3(E)} \\
&= X_3(E) + X_3(E) \bar{T}_3(E) X_3(E) + \dots
\end{aligned} \tag{3.96}$$

where we have defined  $\bar{T}_3(E)$  as

$$\bar{T}_3(E) = T(E) - T_3(E) = \begin{pmatrix} t_1^{(3)}(E) & 0 & 0 \\ 0 & t_2^{(3)}(E) & 0 \\ 0 & 0 & 0 \end{pmatrix} \tag{3.97}$$

Recalling the fact that the additional self-energies appear when  $Z_4(E)$  and  $t_3^{(3)}(E)$  are multiplied, we see that all of the additional self-energies are put into  $X_3(E)$  and the new self-energies do not appear when  $X_3(E)$  and  $\bar{T}_3(E)$  are multiplied.

Since the  $Z_0(E)$  has only off-diagonal component with respect to channels, the  $X_3(E)$  can be simplified as follows

$$X_3(E) = Z_0(E) + Z_0(E) T_3(E) Z_0(E) + (1 + Z_0(E) T_3(E)) W_4(E) (T_3(E) Z_0(E) + 1) \tag{3.98}$$

where, we have defined  $W_4(E)$  as

$$W_4(E) = Z_4(E) + Z_4(E) T_3(E) Z_4(E) + \dots \tag{3.99}$$

An intuitive meaning of the equation (3.98) is obvious. The first and the second terms are free propagation and propagation with interaction only between  $\phi_1\phi_2$  respectively. The third term is a sum of diagrams which consists of sum of effective three-body interaction  $Z_4(E)$  and two-body  $T$ -matrix of  $\phi_1\phi_2$  which we denote  $t_3^{(3)}(E)$ . The third term in equation (3.98) contains all of the additional self-energies and we can see that they always appear as a set

$$(1 + Z_0(E) T_3(E)) W_4(E) (T_3(E) Z_0(E) + 1) \tag{3.100}$$

It is therefore sufficient if we can show that it is possible to add counterterms to the every

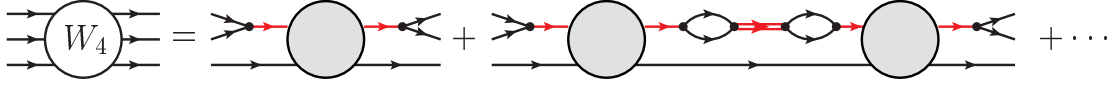


Figure 3.9: A diagrammatic representation of the  $W_4(E)$

$$\begin{aligned} \mathcal{G}(E) &= \text{circle with 4 external lines} := \text{blue circle with 4 external lines} + \text{blue circle with 4 external lines} \left( \text{loop with red line} + \text{loop with red line and cross} \right) \text{blue circle with 4 external lines} + \dots \\ &= \text{blue circle with 4 external lines} / \left( 1 - \left( \text{loop with red line} + \text{loop with red line and cross} \right) \text{blue circle with 4 external lines} \right) \end{aligned}$$

Figure 3.10: A diagrammatic representation of the  $\mathcal{G}(E)$

self-energies in the above equation by modifying the driving term  $Z_4(E)$ . Diagrammatic representation of the equation (3.99) is given in figure 3.9. Note that quantities appeared so far are all  $3 \times 3$  matrices. However, the fact that matrix structures of  $Z_4(E)$  and  $T_3(E)$  are

$$Z_4(E) \sim \begin{pmatrix} 1 & 1 & 1 \\ 1 & 1 & 1 \\ 1 & 1 & 1 \end{pmatrix} \quad T_3(E) \sim \begin{pmatrix} 0 & 0 & 0 \\ 0 & 0 & 0 \\ 0 & 0 & 1 \end{pmatrix} \quad (3.101)$$

ensures their products are also proportional to  $1_{ij}$

$$Z_4(E) + Z_4(E) T_3(E) Z_4(E) + \dots \sim \begin{pmatrix} 1 & 1 & 1 \\ 1 & 1 & 1 \\ 1 & 1 & 1 \end{pmatrix} \quad (3.102)$$

We therefore proceed the following discussion as if they are not matrices. We however must also be noticed that they are all proportional to  $1_{ij}$ .

We first consider adding counterterms to the self-energies in  $W_4(E)$ . Since only the left and rightmost structures of  $Z_4(E)$  are important, we rewrite  $Z_4(E)$  as follows just for notational simplicity

$$\begin{aligned} Z_4(E) &= G_0^{(3)}(E) V^{(32)} \bar{G}^{(2)}(E) \frac{1}{1 - (\Sigma(E) + \Delta) \bar{G}^{(2)}(E)} V^{(23)} G_0^{(3)}(E) \\ &=: G_0^{(3)}(E) V^{(32)} \mathcal{G}(E) V^{(23)} G_0^{(3)}(E) \end{aligned} \quad (3.103)$$

we have defined  $\mathcal{G}(E)$  as

$$\begin{aligned} \mathcal{G}(E) &= \bar{G}^{(2)}(E) \frac{1}{1 - (\Sigma(E) + \Delta) \bar{G}^{(2)}(E)} \\ &= G_0^{(2)}(E) t^{(2)}(E) \frac{1}{1 - G_0^{(2)}(E) (\Sigma(E) + \Delta) G_0^{(2)}(E) t^{(2)}(E)} G_0^{(2)}(E) \end{aligned} \quad (3.104)$$

We can see from the second equation, that  $\mathcal{G}(E)$  is a sum of  $\psi_3 \phi_3$  two-body  $T$ -matrix which we denote  $t^{(2)}(E)$  inserting the self-energy plus counterterm *once* between it and multiplied by two-body free propagator  $G_0^{(2)}(E)$  from both of left- and right-sides. With these notations,  $W_4(E)$  is then expressed as

$$\begin{aligned} W_4(E) &= Z_4(E) + Z_4(E) T_3(E) Z_4(E) + \dots \\ &= G_0^{(3)}(E) V^{(32)} \mathcal{G}(E) \frac{1}{1 - \Sigma(E) G_\Sigma^{(2)}(E) \Sigma(E) \mathcal{G}(E)} V^{(23)} G_0^{(3)}(E) \end{aligned} \quad (3.105)$$

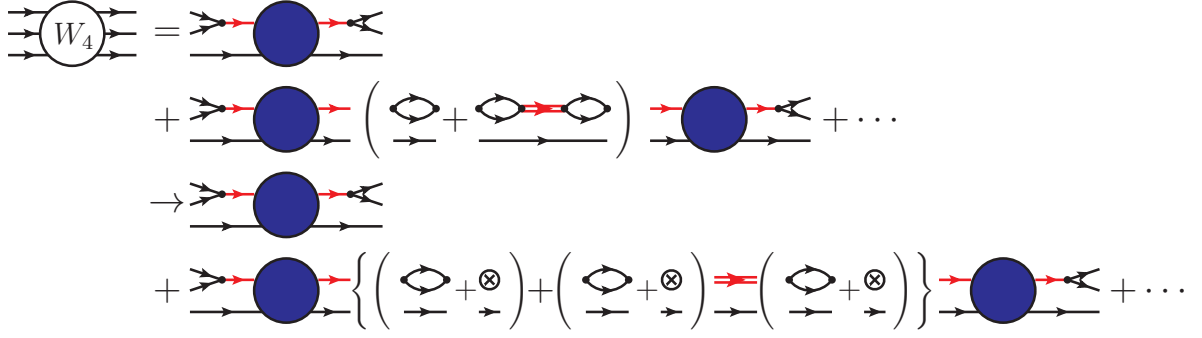


Figure 3.11: One of the diagrammatic representation of the  $W_4(E)$

A diagrammatic representation of this equation is given in figure 3.9. The above equation should be countertermed as below

$$W_4(E) = G_0^{(3)}(E) V^{(32)} \mathcal{G}(E) \frac{1}{1 - (\Sigma(E) + \Delta) G_\Sigma^{(2)}(E) (\Sigma(E) + \Delta) \mathcal{G}(E)} V^{(23)} G_0^{(3)}(E) \quad (3.106)$$

substituting the explicit form of  $\mathcal{G}(E)$ , we obtain

$$\begin{aligned} W_4(E) &= G_0^{(3)}(E) V^{(32)} \mathcal{G}(E) \frac{1}{1 - (\Sigma(E) + \Delta) G_\Sigma^{(2)}(E) (\Sigma(E) + \Delta) \mathcal{G}(E)} V^{(23)} G_0^{(3)}(E) \\ &= G_0^{(3)}(E) V^{(32)} \bar{G}^{(2)}(E) \\ &\times \frac{1}{1 - \left( (\Sigma(E) + \Delta) + (\Sigma(E) + \Delta) G_\Sigma^{(2)}(E) (\Sigma(E) + \Delta) \right) \bar{G}^{(2)}(E)} V^{(23)} G_0^{(3)}(E) \end{aligned}$$

where  $\bar{G}^{(2)}(E)$  is defined in equation (3.74). A diagrammatic representation of this equation is given in the first to the second row in figure 3.11. The last equation can be transformed into a more intuitive one. Substituting the definition of  $\bar{G}^{(2)}(E)$  in equation (3.74), we obtain

$$\begin{aligned} &\bar{G}^{(2)}(E) \frac{1}{1 - \left( (\Sigma(E) + \Delta) + (\Sigma(E) + \Delta) G_\Sigma^{(2)}(E) (\Sigma(E) + \Delta) \right) \bar{G}^{(2)}(E)} \\ &= G_0^{(2)}(E) t^{(2)}(E) \\ &\times \frac{1}{1 - G_0^{(2)}(E) \left( (\Sigma(E) + \Delta) + (\Sigma(E) + \Delta) G_\Sigma^{(2)}(E) (\Sigma(E) + \Delta) \right) G_0^{(2)}(E) t^{(2)}(E)} \\ &\times G_0^{(2)}(E) \end{aligned} \quad (3.107)$$

Here we note that the Dyson-Schwinger equation which  $G_\Sigma^{(2)}(E)$  satisfies gives the following identity

$$G_0^{(2)}(E) \left( (\Sigma(E) + \Delta) + (\Sigma(E) + \Delta) G_\Sigma^{(2)}(E) (\Sigma(E) + \Delta) \right) G_0^{(2)}(E) = G_\Sigma^{(2)}(E) - G_0^{(2)}(E)$$

which simplifies the equation (3.107) as below

$$G_0^{(2)}(E) t^{(2)}(E) \frac{1}{1 - \left( G_\Sigma^{(2)}(E) - G_0^{(2)}(E) \right) t^{(2)}(E)} G_0^{(2)}(E) \quad (3.108)$$

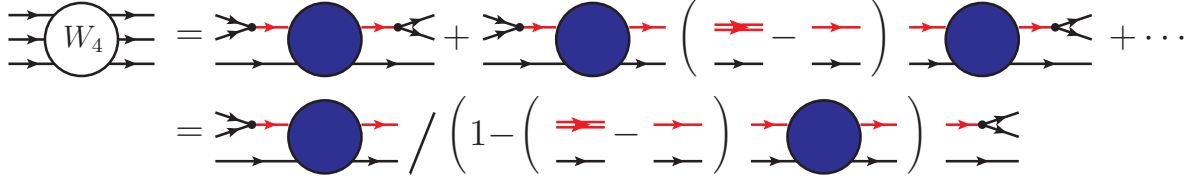


Figure 3.12: One of the diagrammatic representation of the  $W_4(E)$

The  $W_4(E)$  can now be rewritten into an intuitive expression below

$$W_4(E) = G_0^{(3)}(E) V^{(32)} G_0^{(2)}(E) t^{(2)}(E) \times \frac{1}{1 - \left( G_\Sigma^{(2)}(E) - G_0^{(2)}(E) \right) t^{(2)}(E)} G_0^{(2)}(E) V^{(23)} G_0^{(3)}(E) \quad (3.109)$$

The above equation clearly shows what the  $W_4(E)$  is. The three-body state propagates freely and goes to the two-body state. After that, the two-body  $T$ -matrix  $t^{(2)}(E)$  is summed inserting the dressed two-body propagator  $G_\Sigma^{(2)}(E)$  from which free propagation part  $G_0^{(2)}(E)$  is subtracted  $G_\Sigma^{(2)}(E) - G_0^{(2)}(E)$ .  $W_4(E)$  is written in the form of geometric expansion as below

$$W_4(E) = G_0^{(3)}(E) V^{(32)} G_0^{(2)}(E) \times \left( t^{(2)}(E) + t^{(2)}(E) \left( G_\Sigma^{(2)}(E) - G_0^{(2)}(E) \right) t^{(2)}(E) + \dots \right) G_0^{(2)}(E) V^{(23)} G_0^{(3)}(E)$$

A diagrammatic representation of  $W_4(E)$  is given in figure 3.12.

$W_4(E)$  can also be interpreted as  $\psi_3\phi_3$  two-body  $T$ -matrix whose propagator is replaced by the dressed one  $G_\Sigma^{(2)}(E)$  multiplied by  $G_0^{(3)}(E) V^{(32)} G_0^{(2)}(E)$  from both sides as shown below

$$\begin{aligned} W_4(E) &= G_0^{(3)}(E) V^{(32)} G_0^{(2)}(E) \\ &\times t^{(2)}(E) \frac{1}{1 - \left( G_\Sigma^{(2)}(E) - G_0^{(2)}(E) \right) t^{(2)}(E)} G_0^{(2)}(E) V^{(23)} G_0^{(3)}(E) \\ &= G_0^{(3)}(E) V^{(32)} G_0^{(2)}(E) V^{(2)} \frac{1}{1 - G_\Sigma^{(2)}(E) V^{(2)}} G_0^{(2)}(E) V^{(23)} G_0^{(3)}(E) \end{aligned} \quad (3.110)$$

where we have substituted the definition of  $t^{(2)}(E)$  in equation (3.71). We denote the intermediate factor in the above equation as  $t_\Sigma^{(2)}(E)$

$$t_\Sigma^{(2)}(E) = V^{(2)} \frac{1}{1 - G_\Sigma^{(2)}(E) V^{(2)}} \quad (3.111)$$

We note that it satisfies the Lippmann-Schwinger equation

$$t_\Sigma^{(2)}(E) = V^{(2)} + V^{(2)} G_\Sigma^{(2)}(E) t_\Sigma^{(2)}(E) \quad (3.112)$$

$W_4(E)$  is then expressed as the last line in figure 3.13

$$W_4(E) = G_0^{(3)}(E) V^{(32)} G_0^{(2)}(E) t_\Sigma^{(2)}(E) G_0^{(2)}(E) V^{(23)} G_0^{(3)}(E) \quad (3.113)$$

Interpretations between equation (3.109) and equation (3.113) is, the former first sum two-body interaction between  $\psi_3\phi_3$  which we denote  $V_4$  to give  $t^{(2)}(E)$  then sum  $t^{(2)}(E)$  up inserting



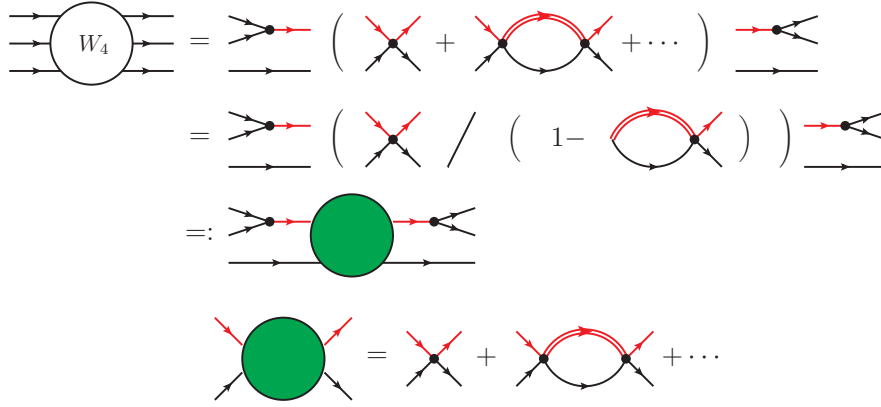


Figure 3.13: One of the diagrammatic representation of the  $W_4(E)$

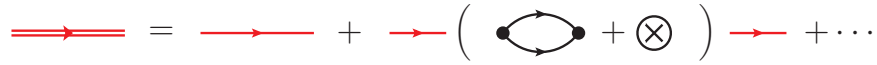


Figure 3.14: A diagrammatic representation of the counterterm dressed propagator of  $\psi_3$

dressed propagator  $G_\Sigma^{(2)}(E)$  from which the free propagator  $G_0^{(2)}(E)$  part is subtracted  $G_\Sigma^{(2)}(E) - G_0^{(2)}(E)$  while the latter first sum the self-energy to give  $G_\Sigma^{(2)}(E)$  and then sum  $V_4$ .

We want to find a way to incorporate those counterterms by modifying  $Z_4(E)$  while keeping the structure of the (Faddeev-)AGS equations the same. This can be achieved in the following reorganization of each terms. We start from the following expression for  $W_4(E)$

$$W_4(E) = G_0^{(3)}(E) V^{(32)} G_0^{(2)}(E) \times t^{(2)}(E) \frac{1}{1 - \left( G_\Sigma^{(2)}(E) - G_0^{(2)}(E) \right) t^{(2)}(E)} G_0^{(2)}(E) V^{(23)} G_0^{(3)}(E) \quad (3.114)$$

we then define  $\sigma(E)$  as below

$$\begin{aligned} G_\Sigma^{(2)}(E) - G_0^{(2)}(E) &= G_0^{(2)}(E) \left( (\Sigma(E) + \Delta) + (\Sigma(E) + \Delta) G_\Sigma^{(2)}(E) (\Sigma(E) + \Delta) \right) G_0^{(2)}(E) \\ &= G_0^{(2)}(E) \left( \sigma(E) + \Sigma(E) G_\Sigma^{(2)}(E) \Sigma(E) \right) G_0^{(2)}(E) \end{aligned} \quad (3.115)$$

or written explicitly,

$$\begin{aligned} \sigma(E) &= (\Sigma(E) + \Delta) + (\Sigma(E) + \Delta) G_\Sigma^{(2)}(E) (\Sigma(E) + \Delta) - \Sigma(E) G_\Sigma^{(2)}(E) \Sigma(E) \\ &= \Sigma(E) + \Delta + \Sigma(E) G_\Sigma^{(2)}(E) \Delta + \Delta G_\Sigma^{(2)}(E) \Sigma(E) + \Delta G_\Sigma^{(2)}(E) \Delta \end{aligned} \quad (3.116)$$

The motivation we have defined  $\sigma(E)$  is that the last term in equation (3.115) appears in  $Z_4(E) t_3^{(3)}(E) Z_4(E)$ , more specifically, the right-most structure of the first factor is multiplied by  $t_3^{(3)}(E)$  and the left-most structure in the last factor. To be more simple, the last term in equation (3.115) appears when the (Faddeev-)AGS equations are iterated while the remaining terms including counterterms do not which makes us to put them into  $Z_4(E)$ .  $W_4(E)$  is then

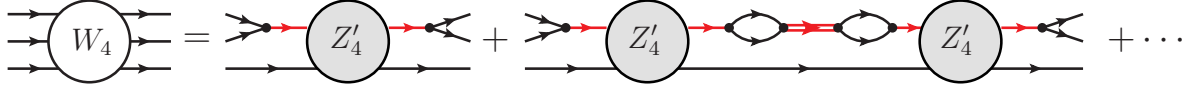


Figure 3.15: A diagrammatic representation of the  $W_4(E)$  in terms of the modified driving term  $Z_4(E)$

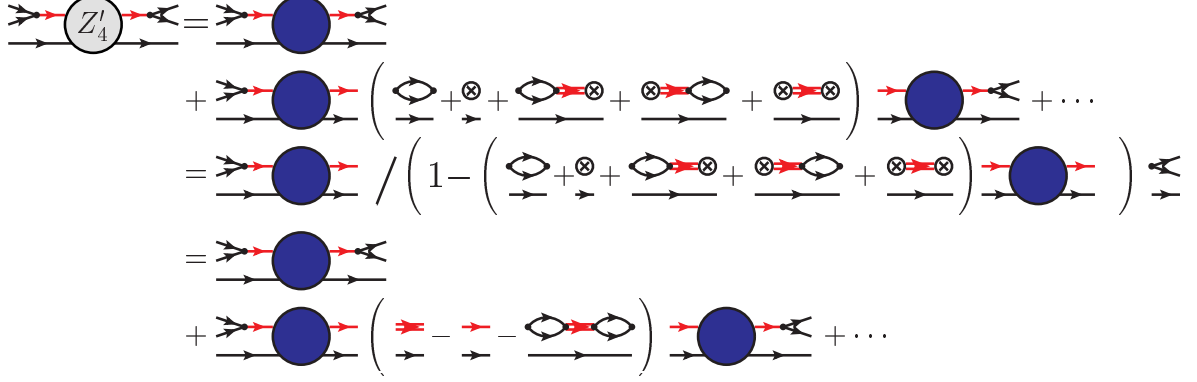


Figure 3.16: A diagrammatic representation of the modified driving term  $Z_4(E)$

rewritten as below

$$\begin{aligned}
 W_4(E) &= G_0^{(3)}(E) V^{(32)} G_0^{(2)}(E) \\
 &\times t^{(2)}(E) \frac{1}{1 - \left( G_\Sigma^{(2)}(E) - G_0^{(2)}(E) \right) t^{(2)}(E)} G_0^{(2)}(E) V^{(23)} G_0^{(3)}(E) \\
 &= Z'_4(E) \frac{1}{1 - t_3^{(3)}(E) Z'_4(E)} \quad (3.117)
 \end{aligned}$$

where  $Z'_4(E)$  is defined as

$$Z'_4(E) := G_0^{(3)}(E) V^{(32)} \mathcal{G}'(E) V^{(23)} G_0^{(3)}(E) \quad (3.118)$$

$$\begin{aligned}
 \mathcal{G}'(E) &:= \bar{G}^{(2)}(E) \frac{1}{1 - \sigma(E) \bar{G}^{(2)}(E)} \\
 &= G_0^{(2)}(E) \\
 &\times t^{(2)}(E) \frac{1}{1 - \left( G_\Sigma^{(2)}(E) - G_0^{(2)}(E) - G_0^{(2)}(E) \Sigma(E) G_\Sigma^{(2)}(E) \Sigma(E) G_0^{(2)}(E) \right) t^{(2)}(E)} \\
 &\times G_0^{(2)}(E) \quad (3.119)
 \end{aligned}$$

We have put all counterterms needed to be added to the self-energies into the new driving term  $Z'_4(E)$  while keeping the structure of the (Faddeev-)AGS equations the same. We can see that the original  $\mathcal{G}(E)$  contains the factor  $\Sigma(E) + \Delta$  and the factor is replaced by  $\sigma(E)$ , that is, the modified one contains the counterterms which need to be added to the iteratively appearing self-energies. The modified driving term and the original one is related by the following equation

$$\mathcal{G}'(E) = \mathcal{G}(E) \frac{1}{1 - (\sigma(E) - (\Sigma(E) + \Delta)) \mathcal{G}(E)} \quad (3.120)$$

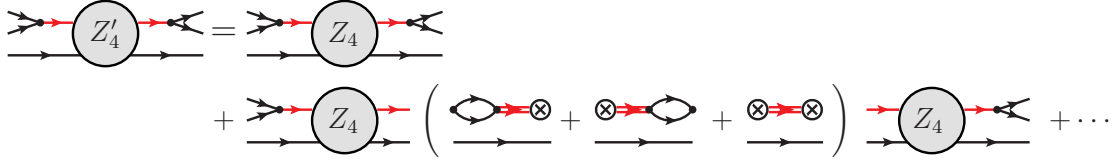


Figure 3.17: A diagrammatic representation of a relation between the modified and the original driving term  $Z_4(E)$

or written explicitly,

$$\begin{aligned} Z'_4(E) &= G_0^{(3)}(E) V^{(32)} \mathcal{G}' V^{(23)} G_0^{(3)}(E) \\ &= G_0^{(3)}(E) V^{(32)} \mathcal{G}(E) \frac{1}{1 - (\sigma(E) - (\Sigma(E) + \Delta)) \mathcal{G}(E)} V^{(23)} G_0^{(3)}(E) \end{aligned}$$

If we expand the second equation in the above equation as geometric series, the first term in the expansion is  $Z_4(E)$  itself and the subsequent terms are roughly geometric series of  $Z_4(E)$  whose intermediate self-energies are  $\sigma(E) - (\Sigma(E) + \Delta)$ , that is, the difference between factors one in the original  $Z_4(E)$  and the other in the modified one  $Z'_4(E)$ .

We have seen that we can add counterterms to the self-energies which appear in  $W_4(E)$  by modifying the driving term  $Z_4(E)$  in an appropriate way. The remaining problematic self-energies are those appearing in the left- and right-most parts in equation (3.100). We have so far have not been considering the matrix structures because they are all proportional to  $1_{ij}$ , the matrix whose all  $3 \times 3$  components are 1 as mentioned earlier. In the following however, we notify the reader that quantities appearing in the below are all  $3 \times 3$  matrices.

We recall that the additional self-energies always appear as a set shown below (3.100)

$$\begin{aligned} &(1 + Z_0(E) T_3(E)) W_4(E) (T_3(E) Z_0(E) + 1) \\ &= G_0^{(3)}(E) V^{(32)} \left(1 + \bar{\delta} I_3 G_\Sigma^{(2)}(E) \Sigma(E)\right) G_0^{(2)}(E) t_\Sigma^{(2)}(E) G_0^{(2)}(E) \\ &\times \left(\Sigma(E) G_\Sigma^{(2)}(E) I_3 \bar{\delta} + 1\right) V^{(23)} G_0^{(3)}(E) \end{aligned} \quad (3.121)$$

where we have defined matrices  $\bar{\delta}$  and  $I_3$  originating in  $Z_0(E)$  and  $T_3(E)$  respectively as

$$\bar{\delta} = \begin{pmatrix} 0 & 1 & 1 \\ 1 & 0 & 1 \\ 1 & 1 & 0 \end{pmatrix} \quad I_3 = \begin{pmatrix} 0 & 0 & 0 \\ 0 & 0 & 0 \\ 0 & 0 & 1 \end{pmatrix} \quad (3.122)$$

and used the fact that

$$Z_0(E) = \bar{\delta} G_0^{(3)}(E) \quad (3.123)$$

and similarly for  $t_3^{(3)}(E)$ ,

$$t_3^{(3)}(E) = I_3 V^{(32)} G_\Sigma^{(2)}(E) V^{(23)} \quad (3.124)$$

The set in equation (3.121) should be countertermed as below

$$\begin{aligned} G_0^{(3)}(E) V^{(32)} \left(1 + \bar{\delta} I_3 G_\Sigma^{(2)}(E) (\Sigma(E) + \Delta)\right) &\times G_0^{(2)}(E) t_\Sigma^{(2)}(E) G_0^{(2)}(E) \\ &\times \left((\Sigma(E) + \Delta) G_\Sigma^{(2)}(E) I_3 \bar{\delta} + 1\right) V^{(23)} G_0^{(3)}(E) \end{aligned}$$

It is also possible to incorporate those counterterms in the above equation by modifying the

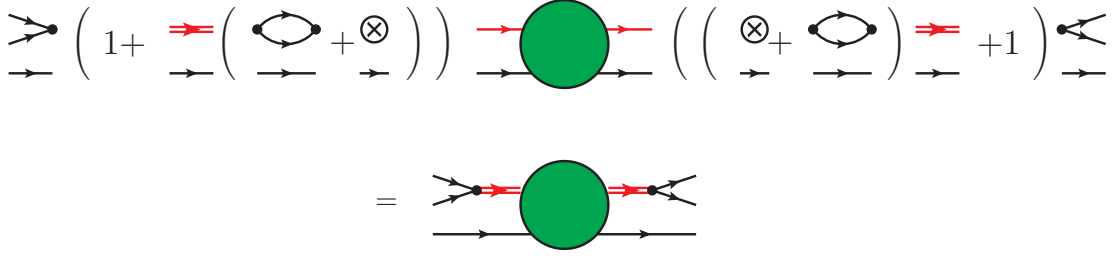


Figure 3.18: A diagrammatic representation of a set of self-energies

driving term  $Z_4(E)$  as below.

$$\begin{aligned}
Z'_4(E) &= \left( G_0^{(3)}(E) V^{(32)} + Z_0(E) I_3 V^{(32)} G_\Sigma^{(2)}(E) \Delta \right) \mathcal{G}'(E) \\
&\times \left( \Delta G_\Sigma^{(2)}(E) V^{(23)} I_3 Z_0(E) + V^{(23)} G_0^{(3)}(E) \right) \\
&= G_0^{(3)}(E) V^{(32)} \left( 1 + \bar{\delta} I_3 G_\Sigma^{(2)}(E) \Delta \right) \mathcal{G}'(E) \left( \Delta G_\Sigma^{(2)}(E) I_3 \bar{\delta} + 1 \right) V^{(23)} G_0^{(3)}(E)
\end{aligned}$$

In the above modification, we just added the counterterms which need to be added to the corresponding self-energies. Then we might worry about double-counting problem. It is however, as shown in the following, the characteristics of  $Z_0(E)$  or equivalently  $\bar{\delta}$ , that it has only off-diagonal components with respect to channels prevents over counting as demonstrated below. The left-most structure of  $(1 + Z_0(E) T_3(E)) Z'_4(E)$  is,

$$\begin{aligned}
&(1 + Z_0(E) T_3(E)) \left( G_0^{(3)}(E) V^{(32)} + Z_0(E) I_3 V^{(32)} G_\Sigma^{(2)}(E) \Delta \right) \\
&= G_0^{(3)}(E) V^{(32)} + Z_0(E) (E) V^{(32)} G_\Sigma^{(2)}(E) (\Sigma(E) + \Delta)
\end{aligned} \tag{3.125}$$

where we used that

$$I_3 Z_0(E) I_3 = 0 \quad \text{or equivalently,} \quad I_3 \bar{\delta} I_3 = 0 \tag{3.126}$$

We can show that the right-most structure does not overcount in a similar way. We also note that the right-most factor of the first  $Z'_4(E)$  in  $Z'_4(E) T_3(E) Z'_4(E)$  multiplied by  $T_3(E)$  then being multiplied again by the left-most structure of the third factor gives the following factor

$$\begin{aligned}
&1_{ij} \left( \Delta G_\Sigma^{(2)}(E) V^{(23)} I_3 Z_0(E) + V^{(23)} G_0^{(3)}(E) \right) T_3(E) \\
&\times \left( G_0^{(3)}(E) V^{(32)} + Z_0(E) I_3 V^{(32)} G_\Sigma^{(2)}(E) \Delta \right) 1_{ij} \\
&= 1_{ij} V^{(23)} G_0^{(3)}(E) T_3(E) G_0^{(3)}(E) V^{(32)} 1_{ij} \\
&= 1_{ij} V^{(23)} G_0^{(3)}(E) V^{(32)} G_\Sigma^{(2)}(E) V^{(23)} I_3 G_0^{(3)}(E) V^{(32)} 1_{ij} \\
&= \Sigma(E) G_\Sigma^{(2)}(E) \Sigma(E) 1_{ij}
\end{aligned} \tag{3.127}$$

We can see that intermediate factors in  $Z'_4(E) T_3(E) Z'_4(E)$  remain proportional to  $1_{ij}$  which ensures that the modification we discussed in this subsection is still valid. Note also that the counterterms to be added to the self-energies above are contained in  $\mathcal{G}'(E)$ .

To summarize, the modification we need to do is,

$$\begin{aligned}
Z_4(E) &= G_0^{(3)}(E) V^{(32)} \mathcal{G}(E) V^{(23)} G_0^{(3)}(E) \\
&\rightarrow \left( G_0^{(3)}(E) V^{(32)} + Z_0(E) I_3 V^{(32)} G_\Sigma^{(2)}(E) \Delta \right) \mathcal{G}'(E) \\
&\times \left( \Delta G_\Sigma^{(2)}(E) V^{(23)} I_3 Z_0(E) + V^{(23)} G_0^{(3)}(E) \right)
\end{aligned}$$



Figure 3.19: A diagrammatic representation of the fully-modified driving term  $Z_4(E)$

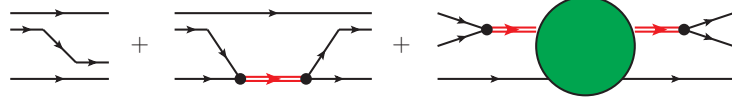


Figure 3.20: A diagrammatic representation of  $X_3(E)$

where  $\mathcal{G}'$  is given in equation (3.119).

## Chapter 4

# The Effective AGS Approach to The Near-Threshold $S$ -Matrix Behavior

In the last chapter, we developed the effective AGS equations in which no unphysical singularities are contained.

In this chapter, we finally implement close analysis of the two-body and three-body coupled-channels system whose thresholds are degenerate. We start from reviewing single-channel two-body as well as single-channel three-body system focusing on how poles of the  $S$ -matrix behave near the thresholds. We then analyze the  $S$ -matrix pole trajectories when two-body and three-body channels are coupled using the two-body and three-body coupled-channel (Faddeev-)AGS equations.

### 4.1 The $S$ -Matrix Behavior for Single-Channel Two-Body and Three-Body System

In this section, we briefly review a single-channel two-body as well as three-body system focusing on the  $S$ -matrix pole behavior near threshold.

#### 4.1.1 $\psi_3\phi_3$ Two-Body System

We first briefly discuss how the  $S$ -matrix poles behave near the threshold for a single-channel two-body system. How poles of the single-channel two-body  $S$ -matrix behave near the threshold is well known and can be discussed with the effective range expansion [67]

$$\begin{aligned} T_\ell(E) &= \frac{p^{2\ell}}{p^{2\ell+1} \cot \delta_\ell - ip^{2\ell+1}} \\ &= \frac{p^{2\ell}}{-\frac{1}{a_\ell} + \frac{r_\ell}{2}p^2 + \dots - ip^{2\ell+1}} \end{aligned} \quad (4.1)$$

We discuss the  $S$ -matrix pole behavior in the complex momentum plane whose origin is taken to be the threshold.

In case of relative angular momentum is in  $s$ -wave, the pole on the complex momentum plane approaches the threshold from the negative imaginary axis which corresponds to virtual state, going through the threshold and keep going upward on the positive imaginary axis which corresponds to bound state.

In case of higher-partial-wave state, poles approach to the threshold one from the fourth quadrant and the other from the third quadrant of the complex momentum plane. The two



The unphysical complex energy sheet

The physical complex energy sheet

Figure 4.1: The  $S$ -matrix pole trajectories for a single-channel two-body system in  $s$ -wave. The pole approaches the threshold from negative real axis on the unphysical complex energy sheet and become a boundstate going along the negative real axis on the physical complex energy sheet.



The unphysical complex energy sheet

The physical complex energy sheet

Figure 4.2: The  $S$ -matrix pole trajectories for a single-channel two-body system in higher-partial-wave. The pole approaches the threshold from the fourth quadrant on the unphysical complex energy sheet which might become resonance if it lies close enough to physical energy region. The pole becomes a boundstate if the interaction is attractive enough and going along the negative real axis on the physical complex energy sheet.

poles are negative complex conjugate of the other. They merge at the threshold one going upward to become bound state while the other going downward to become a anti-bound state. See figure 4.1 The optical theorem tells us the leading behavior of the spectral function to be

$$\begin{aligned}
 \text{Im}T(E) &= \int p^2 dp |T_\ell(E)|^2 \delta\left(E - \frac{p^2}{2\mu}\right) \\
 &\sim k^2 \left(k^{2\ell}\right)^2 \frac{1}{k} \Theta(E) \\
 &= k^{4\ell+1} \Theta(E) \\
 &\sim E^{2\ell+\frac{1}{2}} \Theta(E)
 \end{aligned} \tag{4.2}$$

that is, the leading behavior of the spectral function is half-integer powered with respect to  $E$ .

### 4.1.2 $\phi_1\phi_2\phi_3$ Three-Body System

In this subsection, we briefly review a  $\phi_1\phi_2\phi_3$  three-body system focusing on the  $S$ -matrix pole trajectories near the three-body threshold.

When it comes to consider multi-body systems, it is convenient to introduce the generalized spherical coordinate called the hyperspherical coordinate. The radial part of the Schrödinger equation in  $D$ -dimensional hyperspherical coordinate without interaction is expressed as follows [66]

$$\left\{ -\frac{d^2}{d\rho^2} + \frac{\mathcal{L}(\mathcal{L}+1)}{\rho^2} \right\} u(\rho) = k^2 u(\rho) \quad (4.3)$$

where  $\mathcal{L}$  is defined as

$$\mathcal{L} = L + \frac{D-3}{2} \quad (4.4)$$

and plays a similar role as centrifugal barrier in higher partial-wave two-body systems.  $D$  is a dimension of the system and  $L$  is the total orbital angular momentum. In the three-body center-of-mass systems,  $D = 6$ . That is, even in the absence of orbital angular momentum excitation, three-body systems have effective centrifugal barrier which leads to higher partial-wave-like behavior of the  $S$ -matrix pole near the threshold. We can also see that the effective relative angular momentum takes *half-integer* values while in the two-body systems, relative angular momentum takes only integer values. This causes different consequences for the  $S$ -matrix pole behavior near the threshold as shown in figure 4.2. The leading behavior of the spectral function for three-body system is therefore evaluated as follows

$$\begin{aligned} \text{Im}T(E) &= \int q^2 dq p^2 dp |T(E)|^2 \delta\left(E - \frac{q^2}{2M} - \frac{p^2}{2\mu}\right) \\ &\sim \int \rho^5 d\rho \rho^{4\mathcal{L}} \delta(k^2 - \rho^2) \\ &\sim k^5 k^{4\mathcal{L}} \frac{1}{k} \Theta(k) \sim E^{2\mathcal{L}+2} \Theta(E) \end{aligned} \quad (4.5)$$

As we can see, for a single-channel three-body system, the leading behavior of the spectral function is integer-powered with respect to  $E$  while in case of a single-channel two-body system, it is half-integer-powered with respect to  $E$  as we saw in the previous subsection.

## 4.2 Explicit Expressions of Matrix Elements in The effective AGS equations

In the following section, we investigate the two-body and three-body coupled-channels system applying the effective AGS equations we have developed in the last chapter. We focus on  $\phi_1\phi_2\phi_3 - \psi_3\phi_3$  coupled-channels system in which  $\psi_3$  couples to  $\phi_1\phi_2$  and the two-body and the three-body thresholds are degenerate. We assume there are no relative angular momenta excitation in the three-body as well as in the two-body channels and all particles have spin zero.

In this section, we present explicit expressions of the matrix elements which appear in the effective AGS equations. In the following, we calculate matrix elements of the bare and the effective interactions, the  $T$ -matrices in the three-body as well as the two-body channel and the driving terms of the effective AGS equations.

### The Bare and The Effective Interactions

In section 2.2, we saw that the (Faddeev-)AGS equations formally reduce to the multi-channel Lippmann-Schwinger equation when the two-body interactions are separable. We employ the



following separable interactions as two-body interactions in the three-body channel

$$V_i^{(3)} = \int q_i^2 dq_i |q_i g\rangle \lambda_i^{(3)} \langle q_i g| \quad (4.6)$$

where  $|q_i g\rangle$  is the form factor of the Yamaguchi-type

$$\langle q_i p_i | q_i' g \rangle = \frac{1}{q_i^2} \delta(q_i - q_i') g(p_i) \quad g(p_i) = \frac{\Lambda^2}{p_i^2 + \Lambda^2} \quad (4.7)$$

$|q_i p_i\rangle$  is  $\phi_i \phi_j \phi_k$  three-body partial-wave basis in which quantum numbers such as total and relative angular momentum or spin are suppressed since we assume they are all zero. Matrix elements of the bare interactions are therefore,

$$\langle q_i p_i | V_i^{(3)} | q_i' p_i' \rangle = g(p_i) \lambda_i^{(3)} g(p_i') \frac{1}{q_i^2} \delta(q_i - q_i') \quad (4.8)$$

We assume that  $\psi_3$  couples to  $\phi_1 \phi_2$  through the interaction  $V^{(32)}$  and  $V^{(23)}$

$$V^{(32)} = \Gamma |g\rangle \quad \text{and} \quad V^{(23)} = \langle g | \Gamma \quad (4.9)$$

whose matrix elements are

$$\langle q_3 p_3 | V^{(32)} | q_3' \rangle = \Gamma g(p_3) \frac{1}{q_3^2} \delta(q_3 - q_3') \quad \text{and} \quad \langle q_3 | V^{(23)} | q_3' p_3' \rangle = \frac{1}{q_3^2} \delta(q_3 - q_3') g(p_3') \Gamma \quad (4.10)$$

where  $|q_3\rangle$  is  $\psi_3 \phi_3$  two-body  $s$ -wave partial-wave state. The above matrix element is proportional to delta function  $\delta(q_i - q_i')$  since the two-body and the three-body thresholds are degenerated (see section 3.1). We assume the two-body interaction between  $\psi_3 \phi_3$ , that is, two-body interaction in the two-body channel is also separable as shown below.

$$\langle q_i | V^{(2)} | q_i' \rangle = g(q_i) \lambda^{(2)} g(q_i') \quad (4.11)$$

The full Hamiltonian written in a matrix form is therefore

$$H = \begin{pmatrix} H_0^{(3)} + \sum_{i=1}^3 V_i^{(3)} & V^{(32)} \\ V^{(23)} & H_0^{(2)} + V^{(2)} \end{pmatrix} \quad (4.12)$$

Each components refer to two-body and three-body channels respectively.  $H_0^{(3)}$  and  $H_0^{(2)}$  are kinetic energies of the three-body and two-body channels respectively whose explicit forms are

$$H_0^{(3)} = \sum_{i=1}^3 \frac{k_i^2}{2m_i} \quad (4.13)$$

$$H_0^{(2)} = \frac{K_3^2}{2\mathcal{M}_3} + \frac{k_3^2}{2m_3} \quad (4.14)$$

As we have been discussing so far, we reformulate the two-body and three-body coupled-channels problem as an effective three-body problem. The effects induced by the coupling to the two-body channel is embedded in the effective interactions in the three-body channel. The three effective two-body interactions are,

$$U_1(E) = V_1^{(3)} \quad (4.15)$$

$$U_2(E) = V_2^{(3)} \quad (4.16)$$

$$U_3(E) = V_3^{(3)} + V^{(32)} G_0^{(2)}(E) V^{(23)} \quad (4.17)$$

$$(4.18)$$

The effective three-body interaction is,

$$U_4(E) = V^{(32)} G_0^{(2)}(E) t^{(2)}(E) G_0^{(2)}(E) V^{(23)} \quad (4.19)$$

where  $G_0^{(2)}(E)$  is the free propagator of the two-body channel.

$$G_0^{(2)}(E) = \frac{1}{E - \frac{K_3^2}{2\mathcal{M}_3} - \frac{k_3^2}{2m_3}} \quad (4.20)$$

We deal with the problem in the  $\phi_1\phi_2\phi_3$  three-body center-of-mass frame. Since the two-body and three-body systems are degenerate, it is also the two-body center-of-mass frame. The matrix element of  $G_0^{(2)}(E)$  above then becomes

$$\langle q_3 | G_0^{(2)}(E) | q'_3 \rangle = \frac{1}{E - \frac{q_3^2}{2\nu_3}} \delta(q_3 - q'_3) = G_0^{(2)}(Eq_3) \frac{1}{q_3^2} \delta(q_3 - q'_3) \quad (4.21)$$

where  $\nu_3$  is a reduced mass of  $\psi_3\phi_3$

$$\nu_3^{-1} = \mathcal{M}_3^{-1} + m_3^{-1} \quad (4.22)$$

We note that since the interaction between  $\psi_3\phi_3$  is separable, the  $T$ -matrix in the two-body channel  $t^{(2)}(E)$  can be expressed as below (see appendix E for derivation).

$$t^{(2)}(E) = |g\rangle \tau^{(2)}(E) \langle g| \quad (4.23)$$

where  $\tau^{(2)}(E)$  is given as below

$$\left(\tau^{(2)}(E)\right)^{-1} = \left(\lambda^{(2)}\right)^{-1} - \langle g | G_0^{(2)}(E) | g \rangle = \left(\lambda^{(2)}\right)^{-1} - \frac{\pi}{2} \frac{\nu_3 \Lambda^3}{(k + i\Lambda)^2} \quad (4.24)$$

$k$  is a relative momentum between  $\psi_3\phi_3$  whose definition is

$$E = \frac{k^2}{2\nu_3} \quad (4.25)$$

Matrix elements of the effective interactions are given as below

$$\langle q_1 p_1 | U_1(E) | q'_1 p'_1 \rangle = g(p_1) \lambda_1^{(3)} g(p'_1) \frac{1}{q_1^2} \delta(q_1 - q'_1) \quad (4.26)$$

$$\langle q_2 p_2 | U_2(E) | q'_2 p'_2 \rangle = g(p_2) \lambda_2^{(3)} g(p'_2) \frac{1}{q_2^2} \delta(q_2 - q'_2) \quad (4.27)$$

$$\langle q_3 p_3 | U_3(E) | q'_3 p'_3 \rangle = g(p_3) \left( \lambda_3^{(3)} + \Gamma G_0^{(2)}(Eq_3) \Gamma \right) g(p'_3) \frac{1}{q_3^2} \delta(q_3 - q'_3) \quad (4.28)$$

$$\langle q_3 p_3 | U_4(E) | q'_3 p'_3 \rangle = \Gamma G_0^{(2)}(Eq_3) g(q_3) \tau^{(2)}(E) g(q'_3) G_0^{(2)}(Eq'_3) \Gamma \quad (4.29)$$

### The Two-Body and The Three-Body $T$ -Matrices

The two-body  $T$ -matrix in the three-body channel which we need to input into the effective AGS equations are therefore

$$t_i^{(3)}(Eq_i p_i q'_i p'_i) = g(p_i) \tau_i^{(3)} \left( E - \frac{q_i^2}{2M_i} \right) g(p'_i) \frac{1}{q_i^2} \delta(q_i - q'_i) \quad (4.30)$$

Since the two-body interactions are separable, analytic form of  $\tau_i(E)$  can be obtained as below

$$\left(\tau_i^{(3)}\left(E - \frac{q_i^2}{2M_i}\right)\right)^{-1} = \left(\lambda_i^{(3)}\right)^{-1} - \langle g|G_0^{(3)}(Eq_i)|g\rangle \quad i = 1, 2 \quad (4.31)$$

$$\left(\tau_3^{(3)}\left(E - \frac{q_3^2}{2M_3}\right)\right)^{-1} = \left(\lambda_3^{(3)} + \Gamma G_0^{(2)}(Eq_3)\Gamma\right)^{-1} - \langle g|G_0^{(3)}(Eq_3)|g\rangle \quad (4.32)$$

In the following, we often encounter the matrix elements

$$\langle g|G_0^{(3)}(Eq_i)|g\rangle = \int_0^\infty p_i^2 dp_i g^2(p_i) G_0^{(3)}(Eq_i p_i) \quad (4.33)$$

Since we employ the Yamaguchi-type form factor, the integration can be performed analytically as shown below

$$\langle g|G_0^{(3)}(Eq_i)|g\rangle = \frac{\pi}{2} \frac{\mu_i \Lambda^2}{(k_i + i\Lambda)^2} \quad (4.34)$$

where  $k_i$  is defined as

$$E = \frac{q_i^2}{2M_i} + \frac{k_i^2}{2\mu_i} \quad (4.35)$$

Explicit expressions of  $\tau_i^{(3)}(E - q_i^2/2M_i)$  for  $i = 1, 2$  are therefore

$$\tau_i^{(3)}\left(E - \frac{q_i^2}{2M_i}\right) = \frac{\lambda_i^{(3)}}{1 - \lambda_i^{(3)} \frac{\pi}{2} \frac{\mu_i \Lambda^3}{(k_i + i\Lambda)^2}} = \frac{2}{\pi} \frac{1}{\mu_i \Lambda} \frac{g_i^{(3)}}{1 - g_i^{(3)} \frac{\Lambda^2}{(k_i + \Lambda)^2}} \quad (4.36)$$

where, in the second equation, we introduced dimensionless coupling constant  $g_i^{(3)}$ . For  $g_i^{(3)} \leq -1$ , the  $\phi_j \phi_k$  two-body  $T$ -matrix has bound state (virtual state) pole at

$$k_i = (\sqrt{-g} - 1) \Lambda \quad (k_i = (-\sqrt{-g} - 1) \Lambda) \quad (4.37)$$

in complex momentum plane.

As we saw in chapter 3, the  $\phi_1 \phi_2$  two-body matrix contains the self-energy which shifts the mass of  $\psi_3$  from the bare one. As we discussed in the previous chapter, we deal with this problem by decomposing the mass term of  $\psi_3$  into the physical mass and the counterterm. It is then necessary to add counterterms every time the self energies appear. As we mentioned, it is convenient to write  $\tau_3(E)$  in a different way considering that we need to add counterterms to the self-energies appearing in  $\tau_3(E)$  as follows

$$\begin{aligned} \tau_3^{(3)}\left(E - \frac{q_3^2}{2M_3}\right) &= \tau_3^{(0)}\left(E - \frac{q_3^2}{2M_3}\right) \\ &+ \left(1 + \tau_3^{(0)}\left(E - \frac{q_3^2}{2M_3}\right) \langle g|G_0^{(3)}(Eq_3)|g\rangle\right) \Gamma G_\Sigma^{(2)}(Eq_3) \Gamma \\ &\times \left(\langle g|G_0^{(3)}(Eq_3)|g\rangle \tau_3^{(0)}\left(E - \frac{q_3^2}{2M_3}\right) + 1\right) \end{aligned}$$

where  $\tau_3^{(0)}(E - q_3^2/2M_3)$  is  $\phi_1 \phi_2$  two-body  $T$ -matrix in the three-body channel whose interaction is the bare interaction between  $\phi_1 \phi_2$  we denote  $\lambda_3$ .  $G_\Sigma^{(2)}(Eq_3)$  is the dressed  $\psi_3 \phi_3$  two-body propagator in which counterterms are added to the self-energies.

$$\left(\tau_3^{(0)}\left(E - \frac{q_3^2}{2M_3}\right)\right)^{-1} = \left(\lambda_3^{(3)}\right)^{-1} - \langle g|G_0^{(3)}(Eq_3)|g\rangle \quad (4.38)$$

$$\left(G_\Sigma^{(2)}(Eq_3)\right)^{-1} = \left(G_0^{(2)}(Eq_3)\right)^{-1} - (\Sigma(Eq_3) + \Delta) \quad (4.39)$$

The self-energy is calculated as follows

$$\langle q_3 | V^{(23)} G_3^{(3)}(E) V^{(32)} | q'_3 \rangle = \frac{1}{q_3^2} \delta(q_3 - q'_3) \Gamma \langle g | G_3^{(3)}(E q_3) | g \rangle \Gamma =: \frac{1}{q_3^2} \delta(q_3 - q'_3) \Sigma(E q_3) \quad (4.40)$$

where  $G_3^{(3)}(E)$  satisfies the following Dyson-Schwinger equation

$$G_3^{(3)}(E) = G_0^{(3)}(E) + G_0^{(3)}(E) V_3^{(3)} G_3^{(3)}(E) \quad (4.41)$$

We impose the following mass renormalization condition to determine the counterterm  $\Delta$

$$\left( G_\Sigma^{(2)}(E q_3) \right)^{-1} = 0 \quad \text{as} \quad E \rightarrow \frac{q_3^2}{2\nu_3} \quad (4.42)$$

This renormalization condition determines the counterterm to be

$$\Delta = \Gamma^2 \frac{\pi}{2} \mu \Lambda \quad (4.43)$$

If there is no bare interaction between  $\phi_1 \phi_2$ ,  $\tau_3 \left( E - \frac{q_3^2}{2M_3} \right)$  becomes simply

$$\tau_3^{(3)} \left( E - \frac{q_3^2}{2M_3} \right) = \Gamma G_\Sigma^{(2)}(E q_3) \Gamma \quad (4.44)$$

We also need to calculate three-body  $T$ -matrix which the effective three-body interaction  $U_4(E)$  is summed.

$$\begin{aligned} t_4^{(3)}(E) &= U_4(E) + U_4(E) G_0^{(3)}(E) U_4(E) + \dots \\ &= \Gamma |g\rangle G_0^{(2)}(E) |g\rangle \tau^{(2)}(E) \langle g | G_0^{(2)}(E) \langle g | \Gamma \\ &+ \Gamma |g\rangle G_0^{(2)}(E) |g\rangle \tau^{(2)}(E) \langle g | G_0^{(2)}(E) \langle g | \Gamma G_0^{(3)}(E) \Gamma |g\rangle \\ &\times G_0^{(2)}(E) |g\rangle \tau^{(2)}(E) \langle g | G_0^{(2)}(E) \langle g | \Gamma \\ &+ \dots \end{aligned} \quad (4.45)$$

The matrix elements which appear in intermediate part is evaluated as below

$$\langle g | G_0^{(2)}(E) \langle g | \Gamma G_0^{(3)}(E) \Gamma |g\rangle G_0^{(2)}(E) |g\rangle = \langle g | G_0^{(2)}(E) \Sigma(E) G_0^{(2)}(E) |g\rangle \quad (4.46)$$

whose explicit expression is calculated as below

$$\langle g | G_0^{(2)}(E) \Sigma(E) G_0^{(2)}(E) |g\rangle = \int q_3^2 dq_3 g(q_3) G_0^{(2)}(E q_3) \Sigma(E q_3) G_0^{(2)}(E q_3) g(q_3) \quad (4.47)$$

As we discussed in the chapter 3, we modify the above matrix element

$$\langle g | G_0^{(2)}(E) \langle g | \Gamma G_0^{(3)}(E) \Gamma |g\rangle G_0^{(2)}(E) |g\rangle = \langle g | G_0^{(2)}(E) \Sigma(E) G_0^{(2)}(E) |g\rangle \quad (4.48)$$

$$\Rightarrow \langle g | G_0^{(2)}(E) \left( \Sigma(E) + \Delta + \Delta G_\Sigma^{(2)}(E) \Sigma(E) + \Delta G_\Sigma^{(2)}(E) \Sigma(E) + \Delta G_\Sigma^{(2)}(E) \Delta \right) G_0^{(2)}(E) |g\rangle \quad (4.49)$$

We denote it as  $\mathcal{V}(E)$

$$\begin{aligned} \mathcal{V}(E) &= \int q_3^2 dq_3 g(q_3) G_0^{(2)}(E q_3) \left( \Sigma(E q_3) + \Delta + \Sigma(E q_3) G_\Sigma^{(2)}(E q_3) \Delta \right. \\ &\quad \left. + \Delta G_\Sigma^{(2)}(E q_3) \Sigma(E q_3) + \Delta G_\Sigma^{(2)}(E q_3) \Delta \right) G_0^{(2)}(E q_3) g(q_3) \end{aligned} \quad (4.50)$$

The three-body  $T$ -matrix in which the effective interactions are summed is therefore written as

$$t_4^{(3)}(E) = \Gamma |g\rangle G_0^{(2)}(E) |g\rangle \tau^{(2)}(E) \frac{1}{1 - \mathcal{V}(E) \tau^{(2)}(E)} \langle g | G_0^{(2)}(E) \langle g | \Gamma \quad (4.51)$$

Using  $\mathcal{G}'(E)$  introduced in the previous chapter, we can write it as

$$t_4^{(3)}(E) = \Gamma |g\rangle \mathcal{G}'(E) \langle g | \Gamma \quad (4.52)$$

where,

$$\mathcal{G}'(E) = G_0^{(2)}(E) |g\rangle \tau^{(2)}(E) \frac{1}{1 - \mathcal{V}(E) \tau^{(2)}(E)} \langle g | G_0^{(2)}(E) \quad (4.53)$$

Its matrix element is therefore,

$$\begin{aligned} \langle q_3 p_3 | t_4^{(3)}(E) | q'_3 p'_3 \rangle &= \Gamma g(p_3) G_0^{(2)}(E q_3) g(q_3) \\ &\times \tau^{(2)}(E) \frac{1}{1 - \mathcal{V}(E) \tau^{(2)}(E)} g(q'_3) G_0^{(2)}(E q'_3) g(p'_3) \Gamma \\ &= \Gamma g(p_3) \mathcal{G}'(E q_3 q'_3) g(p'_3) \Gamma \end{aligned} \quad (4.54)$$

### The Driving Terms and Kernels

The remaining matrix elements we need to solve the effective AGS equations are the driving terms. Matrix elements of one of the driving term which is often called the exchange diagram and denoted as  $Z_0(E)$  is calculated as below

$$\langle q_i g | Z_0(E) | q_j g \rangle = Z_0(E q_i q_j) = \frac{\bar{\delta}_{ij}}{2} \int_{-1}^1 dx \frac{g(p_i) g(p_j)}{E - \frac{q_i^2}{2m_i} - \frac{q_j^2}{2m_j} - \frac{(\mathbf{q}_i + \mathbf{q}_j)^2}{2m_k}} \quad (4.55)$$

where we have introduced  $x$ ,  $p_i$  and  $p_j$  defined as below

$$x = \hat{\mathbf{q}}_i \cdot \hat{\mathbf{q}}_j \quad (4.56)$$

$$p_i = \left| -\frac{m_j}{m_j + m_k} \mathbf{q}_i - \mathbf{q}_j \right| \quad (4.57)$$

$$p_j = \left| \mathbf{q}_i + \frac{m_k}{m_k + m_i} \mathbf{q}_j \right| \quad (4.58)$$

Matrix elements of another driving term which we have been denoting  $Z_4(E)$  is, noting its definition is  $G_0^{(3)}(E) t^{(2)}(E) G_0^{(3)}(E)$ , calculated as below

$$\begin{aligned} \langle q_3 g | Z_4(E) | q'_3 g \rangle &= \int_0^\infty p_3^2 dp_3 G_0^{(3)}(E q_3 p_3) g(p_3) \Gamma g(p_3) \times \mathcal{G}'(E q_3 q'_3) \\ &\times \int_0^\infty p_3'^2 dp_3' g(p'_3) \Gamma g(p'_3) G_0^{(3)}(E q'_3 p'_3) \end{aligned} \quad (4.59)$$

Other corresponding matrix elements such as  $\langle q_i g | Z_4(E) | q_j g \rangle$  contains additional angular integrations.

As we saw in the chapter 3, it is also necessary to add counterterms on the left- and right-most parts

$$\begin{aligned} Z_4(E) &= G_0^{(3)}(E) \Gamma |g\rangle \left( I + \bar{\delta} I_3 G_\Sigma^{(2)}(E) \Delta \right) \mathcal{G}'(E) 1_{ij} \left( \Delta G_\Sigma^{(2)}(E) I_3 \bar{\delta} + I \right) \langle g | \Gamma G_0^{(3)}(E) \\ &=: G_0^{(3)}(E) \Gamma |g\rangle \mathcal{G}''(E) \langle g | \Gamma G_0^{(3)}(E) \end{aligned} \quad (4.60)$$

where  $I$  is a  $3 \times 3$  unit matrix,  $\bar{\delta}$  and  $I_3$  are  $3 \times 3$  matrices defined in the previous section. We present an explicit form of  $\mathcal{G}''(E)$  in the following

$$\begin{aligned}
(\mathcal{G}''(E))_{11} &= (\mathcal{G}''(E))_{12} = (\mathcal{G}''(E))_{21} = (\mathcal{G}''(E))_{22} \\
&= \mathcal{G}'(E) + G_{\Sigma}^{(2)}(E) \Delta \mathcal{G}'(E) + \mathcal{G}'(E) \Delta G_{\Sigma}^{(2)}(E) + G_{\Sigma}^{(2)}(E) \Delta \mathcal{G}'(E) \Delta G_{\Sigma}^{(2)}(E) \\
(\mathcal{G}''(E))_{13} &= (\mathcal{G}''(E))_{23} \\
&= \mathcal{G}'(E) + G_{\Sigma}^{(2)}(E) \Delta \mathcal{G}'(E) \\
(\mathcal{G}''(E))_{31} &= (\mathcal{G}''(E))_{32} \\
&= \mathcal{G}'(E) + \mathcal{G}'(E) \Delta G_{\Sigma}^{(2)}(E) \\
(\mathcal{G}''(E))_{33} &= \mathcal{G}'(E)
\end{aligned}$$

The driving term  $Z(E)$  is composed of two-parts we have calculated

$$(Z(E))_{ij} = \langle q_i g | (Z_0(E))_{ij} | q_j g \rangle + \langle q_i g | (Z_4(E))_{ij} | q_j g \rangle \quad (4.61)$$

while the kernel is just matrix product of the driving term  $Z(E)$  and the two-body  $T$ -matrix

$$K_{ij}(E) = \sum_{k=1}^3 (Z(E))_{ik} t_k^{(3)}(E) \quad (4.62)$$

which can be written in a matrix form as below

$$K(E) = Z(E) T(E) \quad (4.63)$$

where  $Z(E)$  and  $T(E)$  are  $3 \times 3$  matrix defined as below

$$(Z(E))_{ij} = \langle q_i g | Z(E) | q_j g \rangle \quad (T(E))_{ij} = \delta_{ij} t_i^{(3)}(E) \quad (4.64)$$

### 4.3 The $S$ -Matrix Pole Trajectories Near The Thresholds

We have calculated the kernel of the effective AGS equations. We are now ready to search the poles of the  $S$ -matrix. The effective AGS equations in its operator form is

$$X(E) = Z(E) + K(E) X(E) \quad (4.65)$$

and it has the formal solution

$$X(E) = \frac{1}{1 - K(E)} Z(E) \quad (4.66)$$

On the other hand, the eigenvalue equation of the kernel  $K(E)$  is written as

$$K(E) |\phi_n\rangle = \eta_n(E) |\phi_n\rangle \quad (4.67)$$

As we saw in section ( ref section ), the formal solution ( ref equation ), can be written as

$$X(E) = \sum_n \frac{|\phi_n\rangle \langle \phi_n|}{1 - \eta_n(E)} Z(E) \quad (4.68)$$

The pole of the transition amplitude  $E_p$  obviously satisfies

$$\eta_n(E_p) = 1 \quad (4.69)$$

We therefore focus on the eigenvalue equation of the effective AGS equations instead of the equation itself. The eigenvalue equation after taking appropriate matrix elements is expressed as

$$\sum_{j=1}^3 \int_0^\infty q_j^2 dq_j Z_{ij}(E q_i q_j) \tau_j^{(3)} \left( E - \frac{q_j^2}{2M_j} \right) \phi_j(q_j) = \eta(E) \phi_i(q_i) \quad (4.70)$$

where  $\phi_j(q_j)$  and  $\eta(E)$  are eigenfunctions and eigenvalues respectively. Each factors in the above eigenvalue equation is given in the previous section.

#### 4.3.1 Analytic Continuation to The Unphysical Complex Energy Sheet

Poles corresponding to bound states are given as energies which satisfy (4.69) and are negative real number. However, if we are interested in the poles lying on the unphysical complex energy sheets, such as virtual state or resonances, we need to perform analytic continuation of the eigenvalue equation (4.70). There are several ways of analytic continuation such as contour deformation [65, 66] or contour rotation [63, 64]. We adopt contour rotation method because it is simple to implement though it restricts the complex energy region we can search poles for.

The contour rotation method is executed in the following manner. We first rotate the integration contour by an amount of  $\theta$  clock-wise. Since our model contains the Yamaguchi-type form factor (4.7), the amount we can rotate is restricted to be  $-\pi/2 < \theta < \pi/2$ . After that, we perform the change of variables to obtain the following analytically continued eigenvalue equations.

$$\sum_{j=1}^3 \int_0^\infty e^{-3i\theta} q_j^2 dq_j Z_{ij}(E e^{-i\theta} q_i e^{-i\theta} q_j) \tau_j \left( E - e^{-2i\theta} \frac{q_j^2}{2M_j} \right) \phi_j(e^{-i\theta} q_j) = \eta(E) \phi_i(e^{-i\theta} q_i) \quad (4.71)$$

The branch cut on the complex energy plane corresponding to the three-body scattering state is now rotated from the real axis whose amount of rotation is  $2\theta$  clock-wise. This can be seen if we consider  $\Lambda \rightarrow \infty$  limit of, for example,  $Z_0(E)$

$$\begin{aligned} Z_0(E q_i q_j) &= \frac{\bar{\delta}_{ij}}{2} \int_{-1}^1 dx \frac{g(p_i) g(p_j)}{E - \frac{q_i^2}{2m_i} - \frac{q_j^2}{2m_j} - \frac{(\mathbf{q}_i + \mathbf{q}_j)^2}{2m_k}} \\ &\rightarrow \frac{\bar{\delta}_{ij}}{2} \int_{-1}^1 dx \frac{1}{E - \frac{q_i^2}{2m_i} - \frac{q_j^2}{2m_j} - \frac{(\mathbf{q}_i + \mathbf{q}_j)^2}{2m_k}} \quad \text{as } \Lambda \rightarrow \infty \\ &= \frac{\bar{\delta}_{ij}}{2} \frac{m_k}{q_i q_j} \log \frac{E - \frac{q_i^2}{2\mu_j} - \frac{q_j^2}{2\mu_i} + \frac{q_i q_j}{m_k}}{E - \frac{q_i^2}{2\mu_j} - \frac{q_j^2}{2\mu_i} - \frac{q_i q_j}{m_k}} \end{aligned} \quad (4.72)$$

$Z_0(E q_i q_j)$  obviously has branch cut starting from  $E = 0$  along the real axis if we integrate  $Z_0(E q_i q_j)$  with respect to  $q_i$  and  $q_j$  from 0 to  $\infty$ . However, after the contour rotation, in equation (4.71),  $Z_0(E q_i q_j)$  becomes

$$Z_0(E q_i q_j) = \frac{\bar{\delta}_{ij}}{2} \frac{m_k}{q_i q_j} \log \frac{E - e^{-2i\theta} \left( \frac{q_i^2}{2\mu_j} + \frac{q_j^2}{2\mu_i} - \frac{q_i q_j}{m_k} \right)}{E - e^{-2i\theta} \left( \frac{q_i^2}{2\mu_j} + \frac{q_j^2}{2\mu_i} + \frac{q_i q_j}{m_k} \right)} \quad (4.73)$$

Integrating the above expression with respect to  $q_i$  and  $q_j$  from 0 to  $\infty$ , the branch cut that the integrated quantity has starts from  $E = 0$  along the rotated line whose amount of rotation is  $2\theta$  clock-wise.

### 4.3.2 Numerical Results and Discussion

We solve the analytically continued eigenvalue equation (4.71) numerically on a complex energy plane and search the energies which the eigenvalue  $\eta_n(E)$  becomes 1. To be more specific, we calculate an absolute value of the so-called Fredholm determinant defined as  $\Pi_n(1 - \eta_n(E))$  for equally spaced lattice on the complex energy plane and search the energy which the Fredholm determinant becomes minimum and identify it to be an approximate pole position. We set the masses of the three particles in the three-body channel  $\phi_1$ ,  $\phi_2$  and  $\phi_3$  to be 1, that is, we regard the masses of  $\phi_i$  to be the unit energy. The mass of  $\psi_3$  is therefore 2 in this unit.

We set the interaction strength between  $\phi_2$  and  $\phi_3$  which we denote as  $\lambda_1^{(3)}$  and the one between  $\phi_3$  and  $\phi_1$  which we denote as  $\lambda_2^{(3)}$  to be equal, that is,  $\lambda_1^{(3)} = \lambda_2^{(3)}$ . We set the bare interaction between  $\phi_1$  and  $\phi_2$  which we denote as  $\lambda_3^{(3)}$  to be zero  $\lambda_3^{(3)} = 0$ . The off-diagonal interaction strength  $\Gamma$  is set to be  $0.1 \times \sqrt{4\pi}$  and the cut-off  $\Lambda$  is taken to be 1 in a unit we consider.

The approximate pole trajectories for different coupling constants near the threshold are given in figure 4.3. Each points in the different color corresponds to different two-body interactions in the three-body channel  $\lambda_1^{(3)} = \lambda_2^{(3)}$ . Each points in the same color corresponds to different two-body interaction in the two-body channel  $\lambda^{(2)}$ . The error bars are taken to be the lattice length. The approximate pole energies for each parameters are also listed in the table 4.1. In the table 4.1, we list approximate pole energies for each interaction strength  $g_1^{(3)} = g_2^{(3)}$  and  $g^{(2)}$  which are dimensionless coupling constants defined as  $g = \pi\mu\lambda\Lambda/2$  (see equation (4.36)).

In figure 4.3, we can see that as we gradually increase the interaction strength  $\lambda^{(2)}$  in an attractive way, poles approach to the threshold and become bound state if the interaction  $\lambda^{(2)}$  is attractive enough. We can see that the poles get close to the threshold from the fourth quadrant of the unphysical energy sheet which might become resonances if they lie close enough to the real axis which corresponds to two-body and three-body scattering energy.

This behavior is in contrast to a single-channel two-body  $s$ -wave scattering. In that case, the pole of the  $S$ -matrix approaches the threshold from negative real axis in the unphysical energy sheet and becomes a bound state if the interaction is attractive enough. In a single-channel two-body systems, resonances appear when the system contains relative angular momentum excitation which generates the centrifugal barrier. It can be shown that in systems in which two-body  $s$ -wave and higher-partial-wave states are coupled, the pole shows  $s$ -wave like behavior near the two-body  $s$ -wave threshold in general. The  $S$ -matrix pole behavior we demonstrated is quite opposite and therefore is peculiar in the two-body and three-body coupled-channels system whose thresholds are degenerate. The same circumstances might be realized in exotic hadron spectroscopy, that is, one might find resonance in the vicinity of hadronic two-body  $s$ -wave threshold if hadronic three-body thresholds lie nearby. We also notice that when poles are very close to threshold, they lie on a same curve shown as solid line in figure 4.3.2. We therefore expect that in the degenerate two-body and three-body coupled-channels system, poles lying near the threshold behave universally just as they do in a single-channel two-body system near the thresholds.

In appendix F, we show that the leading behavior of the inverse of the  $T$ -matrix near the threshold is expressed as

$$(T(E))^{-1} \sim c_0 - c_1 E \log(-E) \quad (4.74)$$

The  $S$ -matrix pole trajectories close to the threshold is then universal as shown below. The  $S$ -matrix poles  $E_p$  are determined by the equation

$$c_0 - c_1 E_p \log(-E_p) = 0 \quad (4.75)$$



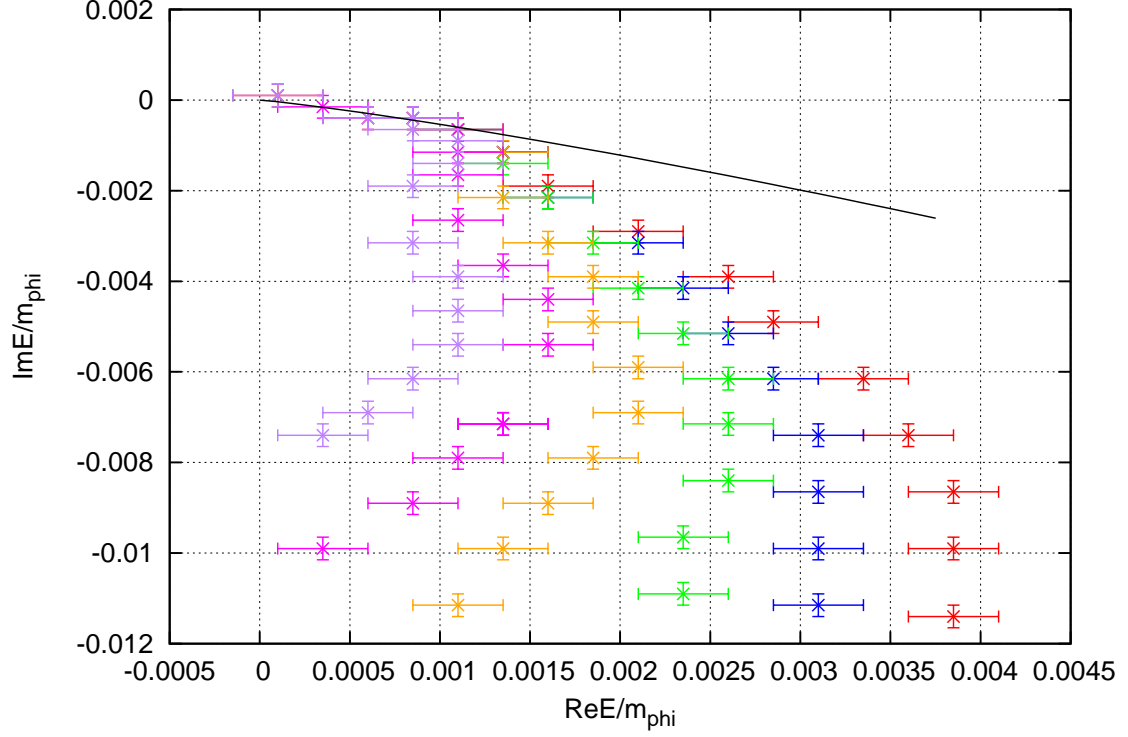


Figure 4.3: The above figure shows the  $S$ -matrix pole trajectories near the threshold on the dimensionless unphysical complex energy sheet for various coupling constants. Colored points with error bars are numerically calculated approximate pole positions while black curve is the universal behavior near the threshold  $c/W(-c)$ . Different colors correspond to different  $g^{(3)}$ , the interaction strength in the three-body channel and different points in the same color correspond to different  $g^{(2)}$ , the interaction strength of the two-body channel. As we gradually increase  $g^{(2)}$  in an attractive way, poles get close to the threshold and eventually become bound states. We can see that, in contrast to two-body  $s$ -wave system, poles approach the threshold from the fourth quadrant of the unphysical energy sheet which might become resonances if they lie close enough to the physical energy region. We can also see that when poles are close enough to the threshold, they lie on the universal curve characterized by  $c/W(-c)$  where  $W(c)$  is the Lambert  $W$  function defined in equation (4.77)

$g^{(2)} \backslash g^{(3)}$	$-0.15$	$-0.20$	$-0.25$
$-1.19$		$(0.00310, -0.01150)$	$(0.00235, -0.00950)$
$-1.21$	$(0.00385, -0.01140)$	$(0.00310, -0.00990)$	$(0.00260, -0.00840)$
$-1.23$	$(0.00385, -0.00990)$	$(0.00310, -0.00865)$	$(0.00260, -0.00715)$
$-1.25$	$(0.00385, -0.00865)$	$(0.00310, -0.00740)$	$(0.00260, -0.00615)$
$-1.27$	$(0.00360, -0.00740)$	$(0.00285, -0.00615)$	$(0.00235, -0.00515)$
$-1.29$	$(0.00335, -0.00490)$	$(0.00260, -0.00515)$	$(0.00210, -0.00415)$
$-1.31$	$(0.00285, -0.00290)$	$(0.00235, -0.00415)$	$(0.00185, -0.00315)$
$-1.33$	$(0.00260, -0.00190)$	$(0.00210, -0.00315)$	$(0.00160, -0.00215)$
$-1.35$	$(0.00210, -0.00190)$	$(0.00160, -0.00215)$	$(0.00135, -0.00140)$
$-1.37$	$(0.00160, -0.00190)$	$(0.00135, -0.00115)$	$(0.00110, -0.00065)$
$-1.39$	$(0.00135, -0.00190)$	$(0.00110, -0.00065)$	$(0.00035, -0.00040)$
$-1.41$	$(0.00010, -0.00190)$	$(0.00000, -0.00000)$	
$g^{(2)} \backslash g^{(3)}$	$-0.30$	$-0.35$	$-0.40$
$-1.11$		$(0.00035, -0.00990)$	$(0.00035, -0.00740)$
$-1.13$	$(0.00110, -0.01115)$	$(0.00085, -0.00890)$	$(0.00060, -0.00690)$
$-1.15$	$(0.00135, -0.00990)$	$(0.00110, -0.00790)$	$(0.00085, -0.00615)$
$-1.17$	$(0.00160, -0.00890)$	$(0.00135, -0.00715)$	$(0.00110, -0.00540)$
$-1.19$	$(0.00185, -0.00790)$	$(0.00135, -0.00715)$	$(0.00110, -0.00465)$
$-1.21$	$(0.00210, -0.00690)$	$(0.00160, -0.00540)$	$(0.00110, -0.00390)$
$-1.23$	$(0.00210, -0.00590)$	$(0.00160, -0.00440)$	$(0.00085, -0.00315)$
$-1.25$	$(0.00185, -0.00490)$	$(0.00135, -0.00365)$	$(0.00085, -0.00190)$
$-1.27$	$(0.00185, -0.00390)$	$(0.00110, -0.00265)$	$(0.00110, -0.00140)$
$-1.29$	$(0.00160, -0.00315)$	$(0.00110, -0.00165)$	$(0.00110, -0.00089)$
$-1.31$	$(0.00135, -0.00215)$	$(0.00110, -0.00115)$	$(0.00085, -0.00065)$
$-1.33$	$(0.00135, -0.00115)$	$(0.00110, -0.00065)$	$(0.00085, -0.00040)$
$-1.35$	$(0.00110, -0.00065)$	$(0.00085, -0.00040)$	$(0.00060, -0.00065)$
$-1.37$	$(0.00085, -0.00040)$	$(0.00060, -0.00040)$	$(0.00010, -0.00010)$

Table 4.1: Approximate pole positions on the unphysical complex energy sheet on which resonances lie for various coupling constants are shown in the above table. Each row corresponds to each  $g^{(2)}$  while each column corresponds to each  $g^{(3)}$ .

The poles are then expressed in a simple form using the so-called Lambert W function.

$$E_p \simeq \frac{g}{W(-g)} \quad \text{as} \quad E_p \sim 0 \quad \text{where,} \quad g = \frac{c_0}{c_1} \quad (4.76)$$

where the Lambert W function is defined so as to satisfy the following equation

$$z = W(z) e^{W(z)} \quad (4.77)$$

We can see that the leading pole trajectories close to threshold are universal in a sense that they all lie on an identical curve determined in equation (4.76). In figure 4.3, we present pole trajectories for various coupling constants with the universal curve (4.76). We can see, as is expected, multiple pole trajectories lie on the same universal curve and they diverge as they get away from the threshold. In appendix F, we demonstrate how this low-energy  $T$ -matrix behavior (4.76) is derived and their characteristics in detail.

## Chapter 5

# Summary and Conclusion

### Exotic Hadrons and Hadronic Two-Body and Three-Body Thresholds Nearby

Since the monumental discovery of the  $X(3872)$  in 2003 by the Belle collaboration, a lot of candidates for the exotic hadron have been observed especially in the energy regions above the double open charm or bottom thresholds. Those exotic candidates seem to lie around the energy regions where two-body and three-body hadronic thresholds lie close to each other. For example, the mass of the  $X(3872)$ ,  $3871.69 \pm 0.17$  MeV is very close to  $\bar{D}^{*0}D^0$  threshold  $\simeq 3871.8$  MeV and it is also very close to  $D^\pm \bar{D}^0 \pi^\mp$  *three-body* threshold  $\simeq 3874.0$  MeV. Other charmonium- and bottomonium-like exotic candidates seem to have more or less similar circumstances. We also note that besides those exotic candidates above the double open charm and bottom thresholds, other exotic candidates such as the possible dibaryon state lying near the  $\Delta N$  threshold and  $\Lambda(1405)N$  threshold couple hadronic three-body state lying nearby.

This feature is characteristic in QCD which originates in a fact that the QCD scale  $\simeq 200$  [MeV] is comparable to light pseudo scalar mesons such as pion or kaon. The mass differences of a hadron and its excited state is therefore comparable to the masses of pion and kaon which causes hadronic one-body and multi-body thresholds to be close to each other. This fact has motivated us to study two-body and three-body coupled-channels system whose thresholds lie close to each other and see if there exists new insight characteristic in such a system.

### The effective AGS equations

Motivated by such circumstances, we considered a general two-body and three-body coupled-channels problem in this thesis. To that end, we consider three-body elastic scattering whose transition amplitudes satisfy the (Faddeev-)AGS equations. Coupling to the two-body channel is taken into account as effective interactions in the three-body channel constructed with the Feshbach projection method.

### The Unphysical Singularities Problem and Its Solution

We denote three particles in the three-body channel as  $\phi_1\phi_2\phi_3$  and the two-body channel which couples to it as  $\psi_3\phi_3$ . We further assume  $\psi_3$  couples  $\phi_1\phi_2$ . The physical mass of  $\psi_3$  is then shifted from the bare one due to the self-energy correction induced by the coupling to  $\phi_1\phi_2$ . The transition amplitudes have of course physical singularities that is, it has poles in the complex energy plane which correspond to bound states, resonances or virtual states and those do not correspond to any of these. They also have branch cuts along the physical energy regions whose branch points correspond to the  $\phi_1\phi_2\phi_3$  three-body as well as the physical  $\psi_3\phi_3$  two-body thresholds.

However, we solve the eigenvalue equation of the (Faddeev-)AGS equations to search poles of the transition amplitudes instead of the scattering equation itself. Though the transition amplitudes have the physical singularities, the kernel of the (Faddeev-)AGS equations does have the unphysical singularities if we naïvely write down the equation. In quantum field theory, we often encounter such self-energy correction to the bare mass and we usually treat it by the mass and the field renormalization. Once the renormalization is done, the bare mass does not appear anywhere in the theory. It is however, necessary to add counterterms every time the self-energies appear.

In perturbative calculations, it is straightforward to add counterterm. However, we solve the effective AGS equations numerically, that is, we sum every single diagrams generated by the assumed interactions. Due to characteristic structure of the two-body and three-body coupled-channels equations, the self-energies also appear when the scattering equations are *iterated* as well as in the kernel of the equations. We therefore need to find a way to incorporate those counterterms which must be added to the iteratively appearing self-energies into what we can input into the scattering equations, namely the kernel of the equations. This is achieved by an appropriate reorganization of each diagrams generated by the scattering equations. Noting that the iteratively-appearing self-energies are generated when  $Z_4(E)$ , one of the driving term and  $t_3(E)$ ,  $\phi_1\phi_2$  two-body  $T$ -matrix is multiplied, we first sum diagrams made from  $Z_4(E)$  and  $t_3(E)$ . The sum of those diagrams can be expressed, after an appropriate transformation, in a quite intuitive way. As we showed in chapter 3, it is possible to incorporate those counterterms which should be added to the iteratively appearing self-energies into the modified driving term  $Z_4(E)$  whose explicit expression is given in equation (3.128) and in figure 3.19. We have also shown that the scattering equation can also be written in a form which does not contain the iteratively-appearing self-energies as in equation (D.43).

### The $S$ -Matrix Pole Behavior Near The Threshold

Since the candidates for the exotic states lie around the energy regions where hadronic two-body and three-body thresholds lie close to each other, we investigated the  $S$ -matrix pole behavior near the thresholds of degenerate  $\phi_1\phi_2\phi_3 - \psi_3\phi_3$  coupled-channels system which contains no relative angular momentum excitations and all particles have spin zero, specifying the model interactions in chapter 4. The poles of the  $S$ -matrix approaches thresholds from fourth quadrant of the unphysical complex energy plane which might become resonances if they lie close enough to the real axis which correspond to two-body and three-body scattering energies. This is in contrast to degenerate coupled-channels two-body system in which one of channels are in  $s$ -wave. In that case, the  $S$ -matrix pole approaches the thresholds from the negative real axis on unphysical complex energy sheet and turn back at the threshold upon the negative real axis on physical complex energy sheet to become a bound state. Numerical results we presented is quite opposite. Our result indicates that even in the vicinity of the two-body  $s$ -wave threshold, if three-body thresholds lie nearby, resonances might appear. Our numerical result also showed that if the  $S$ -matrix pole reside very close to the thresholds, it lie on an identical, universal curve which is determined by the equation (4.76).

### Conclusion

In this thesis, we presented a new method which is able to perform fully-coupled two-body and three-body coupled-channels calculations. In our formulation, two-body and three-body coupled-channels system is treated as an effective three-body scattering problem in which the effects induced by the coupling to two-body state is embedded as effective interactions in the three-body channel. With the method we presented, we studied the  $S$ -matrix pole behavior

near the thresholds in case of two thresholds are degenerate. We showed that the  $S$ -matrix pole approaches the threshold from the fourth quadrant of the unphysical energy sheet which might become resonance if it lies close enough to the physical energy region. This behavior is quite different compared to two-body coupled-channels system which contains two-body  $s$ -wave state and whose thresholds are degenerate. In that case, the  $S$ -matrix behavior is dominated by the two-body  $s$ -wave state and pole approaches the thresholds from the negative axis in the unphysical energy sheet, and consequently resonances do not appear. We also confirmed numerically that poles very close to the threshold behave universally in the sense that they lie on an identical curve and do not depend on details of the system. To summarize, we have found a new form of resonance that lie in the vicinity of the two-body  $s$ -wave threshold generated by the presence of three-body threshold lying nearby and they it behaves universally very close to thresholds. This mechanism might be realized in a real-world hadron spectroscopy for exotic candidates residing near the two-body and three-body thresholds that are lying close to each other.

## Future

The question everyone asks when we discuss exotic hadron candidates is, “Are they hadronic molecule or something like more compact thing which we can refer to as tetraquark, pentaquark, dibaryon, hybrid or gluball?”. We consider Weinberg had given some hints to resolve the debate in his papers [68], [69].

In his papers, he argued if the deuteron is an elementary, compact state or  $NN$  two-body molecular state which we usually imagine when we hear the name of it. He constructed a “sum-rule” which the elementary and  $NN$  molecular, composite components in the deuteron state satisfy.

$$Z + \int d\alpha |\langle \alpha | d \rangle|^2 = 1 \quad (5.1)$$

where  $|\alpha\rangle$  is  $NN$  two-body scattering state and  $Z$  is a squared absolute value of elementary components in the deuteron state  $|d\rangle$ . He defines  $1 - Z$  as “compositness” for obvious reasons.

He showed that under mild assumptions, the compositness can be represented with the scattering length and the lowest-order effective range as follows.

$$a = 2 \frac{1 - Z}{2 - Z} R + O(m_\pi^{-1}) \quad (5.2)$$

$$r = -\frac{Z}{1 - Z} R + O(m_\pi^{-1}) \quad (5.3)$$

This result is interesting in a sense that the internal structure of the deuteron is determined by the low-energy scattering quantities. Our common sense is that we need to perform higher energy experiment if we want to know finer internal structures. The result he had given is quite opposite.

A sum rule we should be interested in is, given the discrete energy eigenstate of the full Hamiltonian in a two-body and three-body coupled-channels system, how much two-body and three-body components the state contains. Systematic studies in this direction might be one of our future research perspective.

Other subjects we are interested in is, to name a few, a deeper understanding of a relation between the Efimov physics and a degenerate two-body and three-body coupled-channels system, a reformulation of our current coupled-channels formulation in terms of an effective field theory and application of our method to realistic channels.

# Appendix A

## Notations

In this appendix, we summarize the notations we use throughout this thesis.

### A.1 Channels

We consider a two-body and a three-body systems which couple with each other. We denote the three particles in the three-body channel as  $\phi_1\phi_2\phi_3$ . We assume  $\phi_1\phi_2$  couple to another particle  $\psi_3$ . The two-body channel is therefore consists of two particles  $\psi_3\phi_3$ . The channels are summarized in the table ( ref table ) below.

### A.2 Three-Body channel

We denote the masses of  $\phi_1\phi_2\phi_3$  as  $m_1, m_2$  and  $m_3$  respectively. In three-body problems, we often introduce the Jacobi coordinates. Let  $\mathbf{x}_1, \mathbf{x}_2$  and  $\mathbf{x}_3$  be position vectors in the Cartesian coordinate. The Jacobi coordinates are then defined as

$$\mathbf{R} = \frac{\sum_i m_i \mathbf{x}_i}{\sum_i m_i} \quad (\text{A.1})$$

$$\mathbf{R}_i = \mathbf{x}_i - \frac{m_j \mathbf{x}_j + m_k \mathbf{x}_k}{m_j + m_k} \quad (\text{A.2})$$

$$\mathbf{r}_i = \mathbf{x}_j - \mathbf{x}_k \quad (\text{A.3})$$

$\mathbf{R}, \mathbf{R}_i$  and  $\mathbf{r}_i$  are center of mass, relative coordinate between  $\phi_i$  and the pair of  $\phi_j\phi_k$  and relative coordinate between  $\phi_j$  and  $\phi_k$  respectively.  $i, j$  and  $k$  are cyclic permutation of  $1, 2, 3$ .

Three-body channel	Two-body channel
$\phi_1\phi_2\phi_3$	$\psi_3\phi_3$

Table A.1: The two-body and three-body channels

Let  $\mathbf{k}_1$ ,  $\mathbf{k}_2$  and  $\mathbf{k}_3$  be momenta in Cartesian coordinate. The Jacobi momenta are then,

$$\mathbf{P} = \sum_i \mathbf{k}_i \quad (\text{A.4})$$

$$\mathbf{q}_i = \frac{(m_j + m_k) \mathbf{k}_i - m_i (\mathbf{k}_j + \mathbf{k}_k)}{\sum_i m_i} \quad (\text{A.5})$$

$$\mathbf{p}_i = \frac{m_j \mathbf{k}_j - m_k \mathbf{k}_k}{m_j + m_k} \quad (\text{A.6})$$

where  $\mathbf{P}$  is the center of mass momentum,  $\mathbf{q}_i$  are the relative momenta between  $\phi_i$  and the pair of  $\phi_j \phi_k$  and  $\mathbf{p}_i$  are relative momenta between  $\phi_j$  and  $\phi_k$ .

We consider the problem in the three-body center-of-mass frame in which  $\mathbf{P} = \mathbf{0}$ . The kinetic energy in the three-body system which we denote as  $H_0^{(3)}$  then is

$$H_0^{(3)} = \sum_{i=1}^3 \frac{k_i^2}{2m_i} = \frac{P^2}{2M} + \frac{q_i^2}{2M_i} + \frac{p_i^2}{2\mu_i} = \frac{q_i^2}{2M_i} + \frac{p_i^2}{2\mu_i} \quad (\text{A.7})$$

where,  $M$ ,  $M_i$  and  $\mu_i$  are defined as below

$$M = m_1 + m_2 + m_3 \quad (\text{A.8})$$

$$M_i^{-1} = m_i^{-1} + (m_j + m_k)^{-1} \quad (\text{A.9})$$

$$\mu_i^{-1} = m_j^{-1} + m_k^{-1} \quad (\text{A.10})$$

$M$  is the total mass,  $M_i$  is the reduced mass between  $\phi_i$  and the pair of  $\phi_j$  and  $\phi_k$  while  $\mu_i$  is the reduced mass between  $\phi_j$  and  $\phi_k$ .

We next present notations for interactions and related quantities. We denote bare two-body interactions between  $\phi_j \phi_k$  as  $V_i^{(3)}$ .

$$V_i^{(3)} = V_{jk}^{(3)} = V_{\phi_j \phi_k}^{(3)}, \quad i = 1, 2, 3 \quad (\text{A.11})$$

The (Faddeev-)AGS equation contains three two-body  $T$ -matrices which are sums of each interactions  $V_i$  and we denote them as  $t_i^{(3)}(E)$  which satisfy the Lippmann-Schwinger equations

$$t_i^{(3)}(E) = V_i^{(3)} + V_i^{(3)} G_0^{(3)}(E) t_i^{(3)}(E), \quad i = 1, 2, 3 \quad (\text{A.12})$$

where we have introduced the three-body free Green function  $G_0^{(3)}(E)$  defined as below

$$G_0^{(3)}(E) = \frac{1}{E - H_0^{(3)}} \quad (\text{A.13})$$

An explicit expression in the momentum space is,

$$\begin{aligned} \langle \mathbf{q}_i \mathbf{p}_i | G_0^{(3)}(E) | \mathbf{q}_i' \mathbf{p}_i' \rangle &= \frac{1}{E - \frac{q_i^2}{2M_i} - \frac{p_i^2}{2\mu_i}} \delta(\mathbf{q}_i - \mathbf{q}_i') \delta(\mathbf{p}_i - \mathbf{p}_i') \\ &= G_0^{(3)}(E q_i p_i) \delta(\mathbf{q}_i - \mathbf{q}_i') \delta(\mathbf{p}_i - \mathbf{p}_i') \end{aligned} \quad (\text{A.14})$$



### A.3 Two-Body Channel

The two particles in the two-body channel are  $\psi_3$  and  $\phi_3$ . We denote their masses  $\eta_3$  and  $m_3$  and their position vectors in the Cartesian coordinate as  $\mathbf{X}_3$  and  $\mathbf{x}_3$  respectively. The center-of-mass and relative coordinates are,

$$\mathbf{R} = \frac{\mathcal{M}_3 \mathbf{X}_3 + m_3 \mathbf{x}_3}{\mathcal{M}_3 + m_3} \quad (\text{A.15})$$

$$\mathbf{r}_3 = \mathbf{X}_3 - \mathbf{x}_3 \quad (\text{A.16})$$

The center-of-mass momentum and the relative momentum are

$$\mathcal{P} = \mathbf{K}_3 + \mathbf{k}_3 \quad (\text{A.17})$$

$$\mathbf{Q}_3 = \frac{m_3 \mathbf{K}_3 - \mathcal{M}_3 \mathbf{k}_3}{\mathcal{M}_3 + m_3} \quad (\text{A.18})$$

In the two-body center-of-mass system, the center-of-mass momentum is zero  $\mathcal{P} = 0$  and therefore the kinetic energy which we denote as  $H_0^{(2)}$  becomes

$$H_0^{(2)} = \frac{\mathbf{K}_3^2}{2\mathcal{M}_3} + \frac{\mathbf{k}_3^2}{2m_3} = \frac{\mathcal{P}^2}{2\mathcal{M}} + \frac{\mathbf{Q}_3^2}{2\nu_3} = \frac{\mathbf{Q}_3^2}{2\nu_3} \quad (\text{A.19})$$

where  $\mathcal{M}$  and  $\nu_3$  are the total mass and the reduced mass of  $\psi_3$  and  $\phi_3$  respectively.

$$\mathcal{M} = \mathcal{M}_3 + m_3 \quad (\text{A.20})$$

$$\nu_3^{-1} = \mathcal{M}_3^{-1} + m_3^{-1} \quad (\text{A.21})$$

We denote the bare two-body interaction between  $\psi_3\phi_3$  as  $V^{(2)}$ .

$$V^{(2)} = V_{\psi_3\phi_3} \quad (\text{A.22})$$

The  $T$ -matrix in which  $V^{(2)}$  is summed is then expressed as  $t^{(2)}(E)$

$$t^{(2)}(E) = V^{(2)} + V^{(2)} G_0^{(2)}(E) t^{(2)}(E) \quad (\text{A.23})$$

with the non-interacting  $\psi_3\phi_3$  two-body Green function defined as below

$$G_0^{(2)}(E) = \frac{1}{E - H_0^{(2)}} \quad (\text{A.24})$$

An explicit representation in the momentum space is,

$$\langle \mathbf{Q} | G_0^{(2)}(E) | \mathbf{Q}' \rangle = \frac{1}{E - \frac{Q^2}{2\nu_3}} \delta(\mathbf{Q} - \mathbf{Q}') = G_0^{(2)}(EQ) \delta(\mathbf{Q} - \mathbf{Q}') \quad (\text{A.25})$$

### A.4 Two-Body and Three-Body Coupled-Channels

We denote the interaction which couples  $\phi_1\phi_2$  and  $\psi_3$  as  $V^{(23)}$

$$V^{(23)} = V_{\phi_1\phi_2\phi_3 \rightarrow \psi_3\phi_3} \quad \text{and} \quad V^{(32)} = V_{\phi_1\phi_2\phi_3 \rightarrow \psi_3\phi_3} \quad (\text{A.26})$$

The matrix element of this interaction is diagonal with respect to momentum of  $\phi_3$ , that is, the momentum of  $\phi_3$  conserves because  $\phi_3$  does not interact with other particles

$$\langle \mathbf{k}_1 \mathbf{k}_2 \mathbf{k}_3 | V^{(32)} | \mathbf{K}_3 \mathbf{k}_3' \rangle \propto \delta(\mathbf{k}_3 - \mathbf{k}_3') \quad (\text{A.27})$$

where  $\mathbf{k}_i$  are three Cartesian momenta of  $\phi_i$  in the three-body system while  $\mathbf{K}_3$  is Cartesian momentum of  $\psi_3$ .

In case the three-body and two-body thresholds are degenerated, that is,

$$\mathcal{M}_3 = m_1 + m_2 \quad (\text{A.28})$$

the reduced mass in two-body  $\psi_3\phi_3$  channel denoted as  $\nu_3$  is equal to reduced mass between  $\phi_3$  and the pair of  $\phi_1\phi_2$  which we denote  $M_3$

$$\begin{aligned} \nu_3 &= \frac{\mathcal{M}_3 m_3}{\mathcal{M}_3 + m_3} \\ &= \frac{(m_1 + m_2) m_3}{m_1 + m_2 + m_3} = M_3 \end{aligned} \quad (\text{A.29})$$

We also note that if the two thresholds are degenerated, the momentum of  $\psi_3$  which we denote  $\mathbf{K}_3$  is equal to the sum of momenta of  $\phi_1$  and  $\phi_2$

$$\mathbf{K}_3 = \mathbf{k}_1 + \mathbf{k}_2 \quad (\text{A.30})$$

The matrix element of  $V^{(32)}$  is then proportional also to  $\delta(\mathbf{K}_3 - \mathbf{k}_1 - \mathbf{k}_2)$

$$\langle \mathbf{k}_1 \mathbf{k}_2 \mathbf{k}_3 | V^{(32)} | \mathbf{K}_3 \mathbf{k}'_3 \rangle \propto \delta(\mathbf{K}_3 - \mathbf{k}_1 - \mathbf{k}_2) \delta(\mathbf{k}_3 - \mathbf{k}'_3) = \delta(\mathbf{P} - \mathcal{P}) \delta(\mathbf{k}_3 - \mathbf{k}'_3) \quad (\text{A.31})$$

The last equality indicates that the center-of-mass momentum in both of the two-body and the three-body channel are equal

$$\mathbf{P} = \mathcal{P} \quad (\text{A.32})$$

If we consider in the two-body as well as the three-body center-of-mass coordinate, that is,  $\mathbf{P} = \mathcal{P} = \mathbf{0}$ , the relative momentum between  $\psi_3$  and  $\phi_3$  which we denote  $\mathbf{Q}_3$  is equal to ( up to sign ) the relative momentum between  $\phi_3$  and the pair of  $\phi_1\phi_2$

$$\begin{aligned} \mathbf{Q}_3 &= \frac{m_3 \mathbf{K}_3 - \mathcal{M}_3 \mathbf{k}_3}{\mathcal{M}_3 + m_3} \\ &= \frac{m_3 (\mathbf{k}_1 + \mathbf{k}_2) - (m_1 + m_2) \mathbf{k}_3}{m_1 + m_2 + m_3} \\ &= -\mathbf{q}_3 \end{aligned} \quad (\text{A.33})$$

## A.5 The Effective Interactions in The Three-Body Channel

We concentrate on the elastic  $\phi_1\phi_2\phi_3$  three-body scattering and we embed effects due to coupling to the  $\psi_3\phi_3$  two-body channels into interactions utilizing the *Feshbach projection* method. The Feshbach projection method is reviewed in the appendix ( ref appendix ). We regard the three-body channel as  $P$ -channel and the two-body channel as  $Q$ -channel. The effective interactions in the three-body channel is therefore, (see appendix ( ref appendix ))

$$\begin{aligned} U(E) &= \sum_{i=1}^3 V_i^{(3)} + V^{(32)} G^{(2)}(E) V^{(23)} \\ &= \sum_{i=1}^3 V_i^{(3)} + V^{(32)} G_0^{(2)}(E) V^{(23)} + V^{(32)} \left( G^{(2)}(E) - G_0^{(2)}(E) \right) V^{(23)} \\ &= \sum_{i=1}^3 V_i + V^{(32)} G_0^{(2)}(E) V^{(23)} + V^{(32)} G_0^{(2)}(E) t^{(2)}(E) G_0^{(2)}(E) V^{(23)} \end{aligned} \quad (\text{A.34})$$

where we have introduced the full Green function in two-body channel which satisfies the Dyson-Schwinger equation

$$G^{(2)}(E) = G_0^{(2)}(E) + G_0^{(2)}(E) V^{(2)} G^{(2)}(E) \quad (\text{A.35})$$

and used the fact that it has the following formal solution

$$G^{(2)}(E) = G_0^{(2)}(E) + G_0^{(2)}(E) t^{(2)}(E) G_0^{(2)}(E) \quad (\text{A.36})$$

where  $t^{(2)}(E)$  is the  $T$ -matrix in two-body channel we presented in the previous subsection. The three effective two-body interaction in the three-body channel are therefore

$$U_1(E) = V_1^{(3)} \quad (\text{A.37})$$

$$U_2(E) = V_2^{(3)} \quad (\text{A.38})$$

$$U_3(E) = V_3^{(3)} + V^{(32)} G_0^{(2)}(E) V^{(23)} \quad (\text{A.39})$$

while the effective three-body interaction is given as

$$U_4(E) = V^{(32)} G_0^{(2)}(E) t^{(2)}(E) G_0^{(2)}(E) V^{(23)} \quad (\text{A.40})$$

By performing the Feshbach projection procedure above, we now have reformulated the two-body and three-body coupled-channels problem as an effective three-body problem whose effects due to coupling to the two-body channels are embedded into the effective interactions in three-body channels. Diagrammatic representation of the effective interactions are given in figure (ref figure).

The elements in the (Faddeev-)AGS equations are modified accordingly. Specifically, three two-body  $T$ -matrices which we denote  $t_k^{(2)}(E)$   $k = 1, 2, 3$  and the three-body  $T$ -matrix sandwiched by  $G_0^{(3)}(E)$  which we denote as  $Z_4(E)$  are modified as shown in figure (ref figure).

$$t_i^{(3)}(E) = U_i(E) + U_i(E) G_0^{(3)}(E) t_i^{(3)}(E) \quad i = 1, 2, 3, 4 \quad (\text{A.41})$$

$$Z_4(E) = G_0^{(3)} t_4^{(3)}(E) G_0^{(3)}(E) \quad (\text{A.42})$$

The energies  $E$  which have appeared so far does not necessarily be the  $q_i^2/2M_i - \epsilon_i$  in case of the fragmentation scattering or  $q_i^2/2M_i + p_i^2/2\mu_i$  in case of free three-body scattering. When the energy is those we mentioned, we need to replace  $E$  with  $E + i\epsilon$  which ensures that the transition amplitudes are actually the physical one.

## Appendix B

# Some Algebras Related to the Feshbach Projection

Our objective is to develop a two-body and three-body coupled-channels scattering equations. To achieve that, we employ the Feshbach projection formalism developed by Feshbach [53], [54]. The Feshbach projection embed the effects due to coupling to other channels into interactions of the channel we focus on. In our case, we consider three-body elastic scattering in which the effects due to two-body channels are embedded as effective interactions in three-body channels. In this appendix, we introduce the Feshbach projection procedure in detail and see how effects due to couplings to other channels are embedded as effective interactions in the channel we are interested in.

### B.1 The Feshbach Projection

We start from the general perspective not limited to two-body and three-body coupled-channels system. To simplify the argument, we consider a system in which two channels are coupled. Let  $H$  be a full Hamiltonian of the system.  $H$  contains the kinetic term  $H_0$  and the interaction  $V$ .

$$H = H_0 + V \quad (\text{B.1})$$

where  $V$  contains interactions which couple two channels in addition to interactions within each channels. The  $T$ -matrix, from which we can extract scattering quantities such as scattering cross sections, phase shift and decay width satisfies the Lippmann-Schwinger equation

$$T(E) = V + VG_0(E)T(E) \quad (\text{B.2})$$

where  $G_0(E)$  is the free Green function

$$G_0(E) = \frac{1}{E - H_0} \quad (\text{B.3})$$

which has a formal solution below

$$T(E) = V + VG(E)V \quad (\text{B.4})$$

where  $G(E)$  is the full Green function

$$G(E) = \frac{1}{E - H} = \frac{1}{E - H_0 - V} \quad (\text{B.5})$$

where  $E$  is a total energy of the system. The expression above is valid for analytically continued off-shell  $T$ -matrix while if we are interested in physical energy regions, we need to introduce the infinitesimal quantity  $\epsilon$  and replace the argument by  $E + i\epsilon$ . We next define the projection operators which project any state into each channels.

$$P = |\text{channel 1}\rangle\langle\text{channel 1}| \quad (\text{B.6})$$

$$Q = |\text{channel 2}\rangle\langle\text{channel 2}| \quad (\text{B.7})$$

where  $P$  and  $Q$  satisfies the relation

$$P + Q = 1 \quad (\text{B.8})$$

In the remaining part of this section, we call each channels as  $P$ -channel and  $Q$ -channel which is often-used terminology.  $P$ -channel elastic scattering amplitude is obtained by sandwiching eq ( ref eq ) from both sides with  $P$

$$T(E) = V + VG(E)V \quad (\text{B.9})$$

where  $V$  is the interaction and  $G(E)$  is a full Green function whose explicit expression is

$$G(E) = \frac{1}{E - H_0 - V} \quad (\text{B.10})$$

With the aid of an identity for operators

$$\frac{1}{A - B} = \frac{1}{A} + \frac{1}{A}B\frac{1}{A - B} \quad (\text{B.11})$$

$G$  can be shown to satisfy the equation

$$G(E) = G_0(E) + G_0(E)VG(E) \quad (\text{B.12})$$

This equation leads to the Lippmann-Schwinger equation

$$T(E) = V + VG_0(E)T(E) \quad (\text{B.13})$$

The elastic scattering  $T$ -matrix for the channel  $P$  is obtained by applying the projection operator  $P$  from left and right and using the identity  $P + Q = 1$

$$T_{PP}(E) = V_{PP} + V_{PP}G_{PP}(E)V_{PP} + V_{PQ}G_{QP}(E)V_{QP} + V_{PP}G_{PQ}(E)V_{QP}V_{PQ}G_{QQ}(E)V_{QP} \quad (\text{B.14})$$

We now need expressions for  $G_{PP}$ , etc. Applying  $P$  and  $Q$  from left and right to the equation (B.12), following simultaneous set of equations are obtained

$$\begin{aligned} G_{PP}(E) &= G_0^P(E) + G_0^P(E)(V_{PP}G_{PP}(E) + V_{PQ}G_{QQ}(E)) \\ G_{PQ}(E) &= G_0^P(E)(V_{PQ}G_{QQ}(E) + V_{PP}G_{PQ}(E)) \\ G_{QP}(E) &= G_0^Q(E)(V_{QP}G_{PP}(E) + V_{QQ}G_{QP}(E)) \\ G_{QQ}(E) &= G_0^Q(E) + G_0^Q(E)(V_{QP}G_{PQ}(E) + V_{QQ}G_{QQ}(E)) \end{aligned}$$

which lead to

$$\begin{aligned} G_{PP}(E) &= \frac{1}{G_0^P(E)^{-1} - V_{PP}} (1 + V_{PQ}G_{QQ}(E)) =: G_P + G_P V_{PQ}G_{QQ} \\ G_{PQ}(E) &= \frac{1}{G_0^P(E)^{-1} - V_{PP}} V_{PQ}G_{QQ}(E) =: G_P(E) V_{PQ}G_{QQ}(E) \\ G_{QP}(E) &= \frac{1}{G_0^Q(E)^{-1} - V_{QQ}} V_{QP}G_{PP}(E) =: G_Q(E) V_{QP}G_{PP}(E) \\ G_{QQ}(E) &= \frac{1}{G_0^Q(E)^{-1} - V_{QQ}} (1 + V_{QP}G_{PQ}(E)) =: G_Q(E) + G_Q(E) V_{QP}G_{PQ}(E) \end{aligned}$$

where we have defined the channel Green functions  $G_P$  and  $G_Q$  as

$$G_P(E) = \frac{1}{E - H_0^P - V_{PP}} \quad (\text{B.15})$$

$$G_Q(E) = \frac{1}{E - H_0^Q - V_{QQ}} \quad (\text{B.16})$$

The simultaneous set of equations can be solved to give the following expressions

$$\begin{aligned} G_{PP}(E) &= G_P(E) + G_P(E) V_{PQ} G_Q(E) V_{QP} G_{PP}(E) \\ G_{PQ}(E) &= \frac{1}{G_P(E)^{-1} - V_{PQ} G_Q(E) V_{QP}} V_{PQ} G_Q(E) \\ G_{QP}(E) &= \frac{1}{G_Q(E)^{-1} - V_{QP} G_P(E) V_{PQ}} V_{QP} G_P(E) \\ G_{QQ}(E) &= G_Q(E) + G_Q(E) V_{QP} \frac{1}{G_P(E)^{-1} - V_{PQ} G_Q(E) V_{QP}} V_{PQ} G_Q(E) \end{aligned} \quad (\text{B.17})$$

Substituting the expressions for  $G_{PP}$ ,  $G_{PQ}$ ,  $G_{QP}$  and  $G_{QQ}$  into eq ( ref eq ), we finally obtain

$$T_{PP}(E) = U_{PP}(E) + U_{PP}(E) \frac{1}{E - H_0^P - U_{PP}(E)} U_{PP}(E) \quad (\text{B.18})$$

$U_{PP}$  is the effective interactions in the channel  $P$  and we can see that the coupling to the channel  $Q$  are embedded into the effective interactions.

$$U_{PP}(E) = V_{PP} + V_{PQ} G_Q(E) V_{QP} \quad (\text{B.19})$$

where  $G_Q(E)$  is the Green function in  $Q$ -channel

$$G_Q(E) = G_0^Q(E) + G_0^Q(E) T_Q(E) G_0^Q(E) \quad (\text{B.20})$$

where  $T_Q(E)$  is the  $T$ -matrix in the  $Q$ -channel which satisfies the Lippmann-Schwinger equation

$$T_Q(E) = V_{QQ} + V_{QQ} G_0^Q(E) T_Q(E) \quad (\text{B.21})$$

We can see that the effective interaction in the  $P$ -channel  $U_{PP}(E)$  consists of two parts. The first term is bare interactions in the  $P$ -channel while the other is an effective interaction which is *induced* due to the coupling to the  $Q$ -channel. The second term is a sum of interactions which contain transition to  $Q$ -channel *once*. That is, a  $P$ -channel state transfer to  $Q$ -channel state, then particles in the  $Q$ -channel fully propagate with the interactions in the  $Q$ -channel which we denote  $V_{QQ}$  and transfer back to  $P$ -channel state. Processes that contain more than once transition between the  $P$ -channel and the  $Q$ -channel appears when the scattering equation is iterated. We show a diagrammatic expression of the example scattering equation after the Feshbach projection in figure 2.1.

It is sometimes useful to represent  $T_{PP}(E)$  with  $G_{QQ}(E)$  and  $T_P(E)$  and  $G_P(E)$  as follows

$$\begin{aligned} T_{PP} &= P(V + VGV)P \\ &= V_{PP} + V_{PP} G_{PP} V_{PP} + V_{PQ} G_{QP} V_{PP} + V_{PP} G_{PQ} V_{QP} + V_{QQ} G_{QQ} V_{QQ} \\ &= V_{PP} + V_{PP} (G_P + G_P V_{PQ} G_{QQ} V_{QP} G_P) V_{PP} + V_{PQ} G_{QQ} V_{QP} G_P V_{PP} \\ &\quad + V_{PP} G_P V_{PQ} G_{QQ} V_{QP} + V_{QQ} G_{QQ} V_{QQ} \\ &= V_{PP} + V_{PP} G_P V_{PP} + (1 + V_{PP} G_P) V_{PQ} G_{QQ} V_{QP} (G_P V_{PP} + 1) \\ &= T_P + (1 + T_P G_0^P) V_{PQ} G_{QQ} V_{QP} (G_0^P T_P + 1) \end{aligned} \quad (\text{B.22})$$

we note that

$$G_{QQ} = G_0^Q \frac{1}{1 - V_{QP} G_P V_{PQ} G_0^Q} = \left( G_0^{Q-1} - V_{QP} G_P V_{PQ} \right)^{-1} \quad (\text{B.23})$$

## B.2 Notes on the Induced Interaction

In this subsection, we focus on the induced interaction and briefly discuss its notable physical consequences. The full propagator  $G(E) = (E - H)^{-1}$  is replaced by the full propagator of the  $P$ -channel  $G_{PP}(E) = (E - H_0^P - U_{PP}(E))^{-1}$  whose interaction is also replaced by the effective interaction  $U_{PP}(E)$ . We can see that effects due to the coupling to  $Q$ -channel is embedded in the effective interaction  $U_{PP}(E)$  and do not appear elsewhere in the equation. As we mentioned in the previous subsection, the induced interactions are sum of scattering processes that transfer to  $Q$ -channel *once* in intermediate state and processes that transfer to the  $Q$ -channel more than once appears when the scattering equation is iterated. The above discussion clarifies the meaning of the Feshbach projection, that is, the procedure can be considered as a simple re-organization of the scattering processes.

Whether the induced interaction is attractive or repulsive depends only on the relation between the two thresholds. We consider the  $Q$ -channel problem without the coupling to the  $P$ -channel. The full Hamiltonian in the  $Q$ -channel is  $QHQ =: H_{QQ}$  and it has, as energy eigenstates, scattering state which we denote  $|\mathbf{p}\rangle$  and if the interaction in the  $Q$ -channel  $V_{QQ}$  is attractive enough, it also has bound states.

$$H_{QQ}|b\rangle = E_b|b\rangle \quad (\text{B.24})$$

$$H_{QQ}|\mathbf{p}\rangle = E_p|\mathbf{p}\rangle \quad (\text{B.25})$$

which forms the complete set of basis

$$\sum_b |b\rangle\langle b| + \int d\mathbf{p} |\mathbf{p}\rangle\langle \mathbf{p}| = 1 \quad (\text{B.26})$$

The full Green function for the  $Q$ -channel  $G_Q(E)$  is then be represented in a spectral form

$$G_Q(E) = \frac{Q}{E - H_{QQ}} = \sum_b \frac{|b\rangle\langle b|}{E - E_b} + \int d\mathbf{p} \frac{|\mathbf{p}\rangle\langle \mathbf{p}|}{E - E_p} \quad (\text{B.27})$$

Let  $|\psi\rangle$  be an arbitrary state and the expectation value of the induced interaction is

$$\langle \psi | PVQ \frac{Q}{E - H_{QQ}} QVP | \psi \rangle = \sum_b \frac{|\langle \psi | PVQ | b \rangle|^2}{E - E_b} + \int d\mathbf{p} \frac{|\langle \psi | PVQ | \mathbf{p} \rangle|^2}{E - E_p} \quad (\text{B.28})$$

which becomes negative when the energy of the system  $E$  is lower than the lowest eigenenergy of the  $Q$ -channel. Therefore, from the variational method point of view, the induced interaction is attractive for the energy  $E < E_b$  if the bound state in  $Q$ -channel exists or for  $E < 0$  if the  $Q$ -channel has only scattering states as eigenstates. The conclusion is true no matter how much the interactions in  $Q$ -channel are strong. In particular, the induced interaction might be attractive (repulsive) if the  $Q$ -channel interactions are infinitely repulsive (attractive).

## Appendix C

# Two More Derivations of The (Faddeev-)AGS Equations

In subsection 2.2.2, we derived the Faddeev equations from the fundamental set of Lippmann-Schwinger equations, that is, by considering the boundary conditions the three-body scattering amplitudes must satisfy. In this appendix, we introduce two more derivations of the Faddeev equations.

### C.1 Derivation By Considering Disconnected Processes

The definition of  $|\psi_{i,i}\rangle$  and Faddeev decomposition (2.80) enable us to write

$$|\psi_{i,i}\rangle = G_0(E) V_i |\Psi_i\rangle^{(+)} = G_0(E) V_i \sum_j |\psi_{i,j}\rangle = G_0(E) V_i \sum_j G_0(E) V_j \sum_k |\psi_{i,k}\rangle \quad (\text{C.1})$$

repeating the same procedure leads to series like

$$G_0(E) V_i G_0(E) V_j G_0(E) V_k \dots \quad (\text{C.2})$$

in which contains a special term that particle  $i$  does not interact at all.

$$G_0(E) V_i G_0(E) V_i G_0(E) V_i \dots \quad (\text{C.3})$$

we then transpose this special term to the left-hand-side to give

$$\begin{aligned} |\psi_{i,i}\rangle - G_0(E) V_i |\psi_{i,i}\rangle &= G_0(E) V_i \sum_{j \neq i} |\psi_{i,j}\rangle \\ \Leftrightarrow (1 - G_0(E) V_i) |\psi_{i,i}\rangle &= G_0(E) V_i \sum_{j \neq i} |\psi_{i,j}\rangle \end{aligned} \quad (\text{C.4})$$

This equation can be solved for  $|\psi_{i,i}\rangle$  by noting that  $1 + G_i(E) V_i = (1 - G_0(E) V_i)^{-1}$

$$|\psi_{i,i}\rangle = (1 + G_i(E) V_i) G_0(E) V_i \sum_{j \neq i} |\psi_{i,j}\rangle \quad (\text{C.5})$$

The resolvent identity  $G_0(E) + G_i(E) V_i G_0(E) = G_i(E)$  let the above equation be simplified as

$$|\psi_{i,i}\rangle = G_i(E) V_i \sum_{j \neq i} |\psi_{i,j}\rangle \quad (\text{C.6})$$



We must note that  $|\phi_i\rangle$  do satisfy the homogeneous version of ( ref equation ), that is,

$$(1 - G_0(E) V_i) |\phi_i\rangle = 0 \quad (\text{C.7})$$

the general solution of the equation ( ref equation ) is therefore given by

$$|\psi_{i,i}\rangle = |\phi_i\rangle + G_i(E) V_i \sum_{j \neq i} |\psi_{i,j}\rangle \quad (\text{C.8})$$

## C.2 Derivation Based on Reorganization of The Green Function

Another derivation focuses on diagrammatic structure of a three-body scattering. The following argument is closer to that in the original Faddeev's article [55].

The diagrammatic derivation explained above is equivalent to the following algebraic one. We start from the resolvent identity

$$\begin{aligned} G(E) &= G_0(E) + G_0(E) V G(E) \\ &= G_0(E) + G_0(E) \sum_{i=1}^3 V_i G(E) \\ &=: G_0(E) + \sum_{i=1}^3 G^{(i)}(E) \end{aligned} \quad (\text{C.9})$$

Here we note the fact that  $G^{(i)}$ , the green function which the leftmost interaction is  $V_i$  is expressed as  $G_0 V_i G$ . We next use another resolvent identity for  $G$  to obtain

$$G^{(i)}(E) = G_0(E) V_i G(E) = G_0(E) V_i (G_i(E) + G_i(E) V^i G(E)) \quad (\text{C.10})$$

The first term is rewritten using the resolvent identity as

$$G_0(E) V_i G_i(E) = G_i(E) - G_0(E) \quad (\text{C.11})$$

and the second term as

$$G_0(E) V_i G_i(E) V^i G(E) = G_i(E) V_i G_0(E) (V_j + V_k) G(E) = G_i(E) V_i (G^{(j)}(E) + G^{(k)}(E)) \quad (\text{C.12})$$

We thus obtain the three coupled equations for  $G^{(i)}$

$$G^{(i)}(E) = G_i(E) - G_0(E) + G_i(E) V_i (G^{(j)}(E) + G^{(k)}(E)) \quad (\text{C.13})$$

$$G^{(j)}(E) = G_j(E) - G_0(E) + G_j(E) V_j (G^{(k)}(E) + G^{(i)}(E)) \quad (\text{C.14})$$

$$G^{(k)}(E) = G_k(E) - G_0(E) + G_k(E) V_k (G^{(i)}(E) + G^{(j)}(E)) \quad (\text{C.15})$$

Here we note that applying  $i\epsilon G^{(j)}$  to  $|\phi_i\rangle$  gives  $|\psi_{i,j}\rangle$ . Indeed,

$$i\epsilon G^{(j)}(E) |\phi_i\rangle = G_0(E) V_j i\epsilon G(E) |\phi_i\rangle = G_0(E) V_i |\Psi_i\rangle^{(+)} = |\psi_{i,j}\rangle \quad (\text{C.16})$$

We also note that applying  $i\epsilon |\phi_i\rangle$  to the equation  $G = G_0 + \sum_i G^{(i)}$  and noting that  $i\epsilon G_0 |\phi_i\rangle = 0$ , we retrieve the Faddeev decomposition

$$i\epsilon G(E) |\phi_i\rangle = |\Psi_i\rangle^{(+)} = \sum_j i\epsilon G^{(j)}(E) |\phi_i\rangle = \sum_j |\psi_{i,j}\rangle \quad (\text{C.17})$$

equation (C.13)  $\times i\epsilon|\phi_i\rangle$  with equations  $i\epsilon G_j(E)|\phi_i\rangle = \delta_{ij}|\phi_i\rangle$  leads to

$$|\psi_{i,i}\rangle = |\phi_i\rangle + G_i(E) V_i (|\psi_{i,j}\rangle + |\psi_{i,k}\rangle) \quad (\text{C.18})$$

$$|\psi_{i,i}\rangle = G_j(E) V_j (|\psi_{i,k}\rangle + |\psi_{i,i}\rangle) \quad (\text{C.19})$$

$$|\psi_{i,i}\rangle = G_k(E) V_k (|\psi_{i,i}\rangle + |\psi_{i,j}\rangle) \quad (\text{C.20})$$

which is equivalent to the Faddeev equations ( ref equation ) in the previous subsection.

## Appendix D

# Reorganization Procedure with Detailed Calculations

### D.1 Detailed Calculation in section 3.3

In this appendix, we present detailed calculations of reorganization procedure we discussed in chapter 3.

We first present reorganization procedure when  $V_3 = 0$ .

$$\begin{aligned}
 t_3^{(3)}(E) &= V^{(32)} G_0^{(2)}(E) V^{(23)} + V^{(32)} G_0^{(2)}(E) V^{(23)} \cdot G_0^{(3)}(E) \cdot V^{(32)} G_0^{(2)}(E) V^{(23)} + \dots \\
 &= V^{(32)} \left( G_0^{(2)}(E) + G_0^{(2)}(E) \Sigma(E) G_0^{(2)}(E) + \dots \right) V^{(23)} \\
 &= V^{(32)} G_0^{(2)}(E) \frac{1}{1 - \Sigma(E) G_0^{(2)}(E)} V^{(23)} \\
 &\rightarrow V^{(32)} G_0^{(2)}(E) \frac{1}{1 - (\Sigma(E) + \Delta) G_0^{(2)}(E)} V^{(23)} \\
 &= V^{(32)} G_\Sigma^{(2)}(E) V^{(23)}
 \end{aligned} \tag{D.1}$$

The useful identity (3.95) is obtained as follows

$$\begin{aligned}
 A + A(B + C)A + \dots &= A \frac{1}{1 - (B + C)A} = A \frac{1}{(1 - BA) - CA} \\
 &= A \frac{1}{\left(1 - CA \frac{1}{1 - BA}\right) (1 - BA)} = A \frac{1}{1 - BA} \frac{1}{1 - CA \frac{1}{1 - BA}} \\
 &= S_B \frac{1}{1 - CS_B}
 \end{aligned} \tag{D.2}$$

equation (3.104) is derived as follows

$$\begin{aligned}
 \mathcal{G}(E) &= \bar{G}^{(2)}(E) \frac{1}{1 - (\Sigma(E) + \Delta) \bar{G}^{(2)}(E)} \\
 &= G_0^{(2)}(E) t^{(2)}(E) G_0^{(2)}(E) \frac{1}{1 - (\Sigma(E) + \Delta) G_0^{(2)}(E) t^{(2)}(E) G_0^{(2)}(E)} \\
 &= G_0^{(2)}(E) t^{(2)}(E) \frac{1}{1 - G_0^{(2)}(E) (\Sigma(E) + \Delta) G_0^{(2)}(E) t^{(2)}(E)} G_0^{(2)}(E)
 \end{aligned} \tag{D.3}$$

equation (3.106) is derived as follows

$$\begin{aligned}
W_4(E) &= Z_4(E) + Z_4(E) T_3(E) Z_4(E) + \dots \\
&= G_0^{(3)}(E) V^{(32)} \mathcal{G}(E) V^{(23)} G_0^{(3)}(E) \\
&+ G_0^{(3)}(E) V^{(32)} \mathcal{G}(E) V^{(23)} G_0^{(3)}(E) \times V^{(32)} G_\Sigma^{(2)}(E) V^{(23)} \\
&\times G_0^{(3)}(E) V^{(32)} \mathcal{G}(E) V^{(23)} G_0^{(3)}(E) + \dots \\
&= G_0^{(3)}(E) V^{(32)} \left( \mathcal{G}(E) + \mathcal{G}(E) \Sigma(E) G_\Sigma^{(2)}(E) \Sigma(E) \mathcal{G}(E) + \dots \right) V^{(32)} G_0^{(3)}(E) \\
&= G_0^{(3)}(E) V^{(32)} \mathcal{G}(E) \frac{1}{1 - \Sigma(E) G_\Sigma^{(2)}(E) \Sigma(E) \mathcal{G}(E)} V^{(32)} G_0^{(3)}(E) \quad (D.4)
\end{aligned}$$

Adding the appropriate counterterms, we obtain

$$\begin{aligned}
W_4(E) &= G_0^{(3)}(E) V^{(32)} \mathcal{G}(E) \frac{1}{1 - (\Sigma(E) + \Delta) G_\Sigma^{(2)}(E) (\Sigma(E) + \Delta) \mathcal{G}(E)} V^{(23)} G_0^{(3)}(E) \\
&= G_0^{(3)}(E) V^{(32)} \bar{G}^{(2)}(E) \frac{1}{1 - (\Sigma(E) + \Delta) \bar{G}^{(2)}(E)} \\
&\times \frac{1}{1 - (\Sigma(E) + \Delta) G_\Sigma^{(2)}(E) (\Sigma(E) + \Delta) \bar{G}^{(2)}(E) \frac{1}{1 - (\Sigma(E) + \Delta) \bar{G}^{(2)}(E)}} V^{(23)} G_0^{(3)}(E) \\
&= G_0^{(3)}(E) V^{(32)} \bar{G}^{(2)}(E) \\
&\times \frac{1}{1 - \left( (\Sigma(E) + \Delta) + (\Sigma(E) + \Delta) G_\Sigma^{(2)}(E) (\Sigma(E) + \Delta) \right) \bar{G}^{(2)}(E)} V^{(23)} G_0^{(3)}(E)
\end{aligned}$$

The intermediate factor can be represented as follows

$$\begin{aligned}
&\bar{G}^{(2)}(E) \frac{1}{1 - \left( (\Sigma(E) + \Delta) + (\Sigma(E) + \Delta) G_\Sigma^{(2)}(E) (\Sigma(E) + \Delta) \right) \bar{G}^{(2)}(E)} \\
&= G_0^{(2)}(E) t^{(2)}(E) G_0^{(2)}(E) \\
&\times \frac{1}{1 - \left( (\Sigma(E) + \Delta) + (\Sigma(E) + \Delta) G_\Sigma^{(2)}(E) (\Sigma(E) + \Delta) \right) G_0^{(2)}(E) t^{(2)}(E) G_0^{(2)}(E)} \\
&= G_0^{(2)}(E) t^{(2)}(E) \\
&\times \frac{1}{1 - G_0^{(2)}(E) \left( (\Sigma(E) + \Delta) + (\Sigma(E) + \Delta) G_\Sigma^{(2)}(E) (\Sigma(E) + \Delta) \right) G_0^{(2)}(E) t^{(2)}(E)} \\
&\times G_0^{(2)}(E) \quad (D.5)
\end{aligned}$$

notice that the identity holds

$$G_0^{(2)}(E) \left( (\Sigma(E) + \Delta) + (\Sigma(E) + \Delta) G_\Sigma^{(2)}(E) (\Sigma(E) + \Delta) \right) G_0^{(2)}(E) = G_\Sigma^{(2)}(E) - G_0^{(2)}(E) \quad (D.6)$$

then the equation (D.5) becomes

$$G_0^{(2)}(E) t^{(2)}(E) \frac{1}{1 - \left( G_\Sigma^{(2)}(E) - G_0^{(2)}(E) \right) t^{(2)}(E)} G_0^{(2)}(E) \quad (D.7)$$

This can also be written in a following form

$$\begin{aligned}
& G_0^{(2)}(E) t^{(2)}(E) \frac{1}{1 - \left( G_\Sigma^{(2)}(E) - G_0^{(2)}(E) \right) t^{(2)}(E)} G_0^{(2)}(E) \\
= & G_0^{(2)}(E) V^{(2)} \frac{1}{1 - G_0^{(2)}(E) V_4} \frac{1}{1 - \left( G_\Sigma^{(2)}(E) - G_0^{(2)}(E) \right) V^{(2)} \frac{1}{1 - G_0^{(2)}(E) V_4}} G_0^{(2)}(E) \\
= & G_0^{(2)}(E) V^{(2)} \frac{1}{1 - G_0^{(2)}(E) V^{(2)} - \left( G_\Sigma^{(2)}(E) - G_0^{(2)}(E) \right) V^{(2)}} G_0^{(2)}(E) \\
= & G_0^{(2)}(E) V^{(2)} \frac{1}{1 - G_\Sigma^{(2)}(E) V^{(2)}} G_0^{(2)}(E) \\
=: & G_0^{(2)}(E) t_\Sigma^{(2)}(E) G_0^{(2)}(E)
\end{aligned} \tag{D.8}$$

$W_4(E)$  is therefore written as

$$W_4(E) = G_0^{(3)}(E) V^{(32)} G_0^{(2)}(E) t_\Sigma^{(2)}(E) G_0^{(2)}(E) V^{(23)} G_0^{(3)}(E) \tag{D.9}$$

Let us define

$$\bar{G}_\Sigma^{(2)}(E) = G_\Sigma^{(2)}(E) - G_0^{(2)}(E) - G_0^{(2)}(E) \Sigma(E) G_\Sigma^{(2)}(E) \Sigma(E) G_0^{(2)}(E) \tag{D.10}$$

then  $W_4(E)$  is rewritten as follows

$$\begin{aligned}
W_4(E) &= G_0^{(3)}(E) V^{(32)} G_0^{(2)}(E) t^{(2)}(E) \\
&\times \frac{1}{1 - \left( G_\Sigma^{(2)}(E) - G_0^{(2)}(E) \right) t^{(2)}(E)} G_0^{(2)}(E) V^{(23)} G_0^{(3)}(E) \\
&= G_0^{(3)}(E) V^{(32)} G_0^{(2)}(E) t^{(2)}(E) \\
&\times \frac{1}{1 - \left( \bar{G}_\Sigma^{(2)} + G_0^{(2)}(E) \Sigma(E) G_\Sigma^{(2)}(E) \Sigma(E) G_0^{(2)}(E) \right) t^{(2)}(E)} G_0^{(2)}(E) V^{(23)} G_0^{(3)}(E) \\
&= G_0^{(3)}(E) V^{(32)} G_0^{(2)}(E) t^{(2)}(E) \frac{1}{1 - \bar{G}_\Sigma^{(2)}(E) t^{(2)}(E)} \\
&\times \frac{1}{1 - G_0^{(2)}(E) \Sigma(E) G_\Sigma^{(2)}(E) \Sigma(E) G_0^{(2)}(E) t^{(2)}(E) \frac{1}{1 - \bar{G}_\Sigma^{(2)}(E) t^{(2)}(E)}} \\
&\times G_0^{(2)}(E) V^{(23)} G_0^{(3)}(E)
\end{aligned} \tag{D.11}$$

We further define

$$\bar{t}_\Sigma^{(2)}(E) = t^{(2)}(E) \frac{1}{1 - \bar{G}_\Sigma^{(2)}(E) t^{(2)}(E)} \tag{D.12}$$

then  $W_4(E)$  is written as

$$\begin{aligned}
W_4(E) &= G_0^{(3)}(E) V^{(32)} G_0^{(2)}(E) \bar{t}_\Sigma^{(2)}(E) \\
&\times \frac{1}{1 - G_0^{(2)}(E) \Sigma(E) G_\Sigma^{(2)}(E) \Sigma(E) G_0^{(2)}(E) \bar{t}_\Sigma^{(2)}(E)} G_0^{(2)}(E) V^{(23)} G_0^{(3)}(E) \\
&= G_0^{(3)}(E) V^{(32)} G_0^{(2)}(E) \bar{t}_\Sigma^{(2)}(E) G_0^{(2)}(E) \\
&\times \frac{1}{1 - \Sigma(E) G_\Sigma^{(2)}(E) \Sigma(E) G_0^{(2)}(E) \bar{t}_\Sigma^{(2)}(E) G_0^{(2)}(E)} V^{(23)} G_0^{(3)}(E)
\end{aligned} \tag{D.13}$$

then we defined the modified  $\mathcal{G}(E)$

$$\mathcal{G}'(E) = G_0^{(2)}(E) \bar{t}_\Sigma^{(2)}(E) G_0^{(2)}(E) \quad (\text{D.14})$$

$$\begin{aligned} W_4(E) &= G_0^{(3)}(E) V^{(32)} \mathcal{G}'(E) \frac{1}{1 - \Sigma(E) G_\Sigma^{(2)}(E) \Sigma(E) \mathcal{G}'(E)} V^{(23)} G_0^{(3)}(E) \\ &= G_0^{(3)}(E) V^{(32)} \mathcal{G}'(E) \\ &\times \frac{1}{1 - V^{(23)} G_0^{(3)}(E) V^{(32)} G_\Sigma^{(2)}(E) V^{(23)} G_0^{(3)}(E) V^{(32)} \mathcal{G}'(E)} V^{(23)} G_0^{(3)}(E) \\ &= G_0^{(3)}(E) V^{(32)} \mathcal{G}'(E) V^{(23)} G_0^{(3)}(E) \\ &\times \frac{1}{1 - t_3^{(3)}(E) G_0^{(3)}(E) V^{(32)} \mathcal{G}'(E) V^{(23)} G_0^{(3)}(E)} \\ &= Z'_4(E) \frac{1}{1 - t_3^{(3)}(E) Z'_4(E)} \end{aligned} \quad (\text{D.15})$$

where we have defined

$$Z'_4(E) = G_0^{(3)}(E) V^{(32)} \mathcal{G}'(E) V^{(23)} G_0^{(3)}(E) \quad (\text{D.16})$$

A relation between  $\mathcal{G}(E)$

$$\begin{aligned} \mathcal{G}'(E) &= G_0^{(2)}(E) \bar{t}_\Sigma^{(2)}(E) G_0^{(2)}(E) \\ &= \bar{G}^{(2)}(E) \frac{1}{1 - \left( \Sigma(E) + \Delta + \Sigma(E) G_\Sigma^{(2)}(E) \Delta + \Delta G_\Sigma^{(2)}(E) \Sigma(E) \right) \bar{G}^{(2)}(E)} \\ &= \bar{G}^{(2)}(E) \frac{1}{1 - (\Sigma(E) + \Delta) \bar{G}^{(2)}(E)} \\ &\times \frac{1}{1 - \left( \Sigma(E) G_\Sigma^{(2)}(E) \Delta + \Delta G_\Sigma^{(2)}(E) \Sigma(E) \right) \bar{G}^{(2)}(E) \frac{1}{1 - (\Sigma(E) + \Delta) \bar{G}^{(2)}(E)}} \\ &= \mathcal{G}(E) \frac{1}{1 - \left( \Sigma(E) G_\Sigma^{(2)}(E) \Delta + \Delta G_\Sigma^{(2)}(E) \Sigma(E) \right) \mathcal{G}(E)} \end{aligned} \quad (\text{D.17})$$

$$\begin{aligned} &(1 + Z_0(E) T_3(E)) W_4(E) (T_3(E) Z_0(E) + 1) \\ &= \left( 1 + Z_0(E) I_3 t_3^{(3)}(E) \right) G_0^{(3)}(E) V^{(32)} G_0^{(2)}(E) t_\Sigma^{(2)}(E) G_0^{(2)}(E) \\ &\times V^{(23)} G_0^{(3)}(E) \left( t_3^{(3)}(E) I_3 Z_0(E) + 1 \right) \\ &= \left( 1 + Z_0(E) I_3 V^{(32)} G_0^{(2)}(E) V^{(23)} \right) G_0^{(3)}(E) V^{(32)} G_0^{(2)}(E) t_\Sigma^{(2)}(E) G_0^{(2)}(E) V^{(23)} G_0^{(3)}(E) \\ &\times \left( V^{(32)} G_0^{(2)}(E) V^{(23)} I_3 Z_0(E) + 1 \right) \\ &= \left( G_0^{(3)}(E) V^{(32)} + Z_0(E) I_3 V^{(32)} G_0^{(2)}(E) \Sigma(E) \right) G_0^{(2)}(E) t_\Sigma^{(2)}(E) G_0^{(2)}(E) \\ &\times \left( \Sigma(E) G_0^{(2)}(E) V^{(23)} I_3 Z_0(E) + V^{(23)} G_0^{(3)}(E) \right) \end{aligned} \quad (\text{D.18})$$

## D.2 Direct Derivation of the Modified Kernel

We have been exploring how self-energies appear when the effective AGS equations are iterated and how those counterterms can be incorporated into the kernel, that is,  $T_3(E)$  and  $Z_4(E)$ . It is however, possible to derive the modified kernel directly by transforming the bare kernel. The key equation is the following

$$\begin{aligned} G_{\Sigma}^{(2)}(E) &= G_0^{(2)B}(E) \frac{1}{1 - \Sigma(E) G_0^{(2)B}} \\ &= G_0^{(2)}(E) \frac{1}{1 - (\Sigma(E) + \Delta) G_0(E)} \end{aligned} \quad (D.19)$$

where  $G_0^{(2)B}(E)$  and  $G_0^{(2)}(E)$  are the bare and the physical free Green function

$$G_0^{(2)B}(Eq) = \frac{1}{E - \eta_3^B - m_3 - \frac{q^2}{2\nu_3^B}} \quad (\nu_3^B)^{-1} = (\eta_3^B)^{-1} + m_3^{-1} \quad (D.20)$$

$$G_0^{(2)}(Eq) = \frac{1}{E - \eta_3^P - m_3 - \frac{q^2}{2\nu_3^P}} \quad (\nu_3^P)^{-1} = (\eta_3^P)^{-1} + m_3^{-1} \quad (D.21)$$

We expressed the dressed propagator in two ways, one is the bare propagator and the self-energy, while the other is the physical propagator and the self-energy plus counterterm. The second equation can be transformed into the following form

$$G_{\Sigma}^{(2)}(E) = G_0^{(2)}(E) \frac{1}{1 - \Delta G_0^{(2)}(E)} \frac{1}{1 - \Sigma(E) G_0^{(2)}(E) \frac{1}{1 - \Delta G_0^{(2)}(E)}} \quad (D.22)$$

comparing the above equation with the first one, we obtain

$$G_0^{(2)B}(E) = G_0^{(2)}(E) \frac{1}{1 - \Delta G_0^{(2)}(E)} = G_0^{(2)}(E) + G_0^{(2)}(E) \Delta G_0^{(2)}(E) + \dots \quad (D.23)$$

### Counterterms in $\phi_1\phi_2$ Two-Body $T$ -Matrix $t_3^{(3)}(E)$

We first derive the countertermed  $\psi_3\phi_3$  two-body  $T$ -matrix  $t_3^{(3)}(E)$

$$\begin{aligned} t_3^{(3)}(E) &= V^{(32)} G_0^{(2)B}(E) V^{(23)} + V^{(32)} G_0^{(2)B}(E) V^{(23)} G_0^{(3)}(E) V^{(32)} G_0^{(2)B} V^{(23)} + \dots \\ &= V^{(32)} G_0^{(2)B}(E) \frac{1}{1 - \Sigma(E) G_0^{(2)B}(E)} V^{(23)} \end{aligned} \quad (D.24)$$

$$\begin{aligned} &= V^{(32)} G_0^{(2)}(E) \frac{1}{1 - \Delta G_0^{(2)}(E)} \frac{1}{1 - \Sigma(E) G_0^{(2)}(E) \frac{1}{1 - \Delta G_0^{(2)}(E)}} V^{(23)} \\ &= V^{(32)} G_0^{(2)}(E) \frac{1}{1 - \Delta G_0^{(2)}(E) - \Sigma(E) G_0^{(2)}(E)} V^{(23)} \\ &= V^{(32)} G_0^{(2)}(E) \frac{1}{1 - (\Sigma(E) + \Delta) G_0^{(2)}(E)} V^{(23)} \\ &= V^{(32)} G_{\Sigma}^{(2)}(E) V^{(23)} \end{aligned} \quad (D.25)$$

### The Remaining Counterterms; Those in $Z_4(E)$ and in Cross Terms Between $t_3^{(3)}(E)$

In the previous section, we considered the self-energies which appear in  $Z_4(E)$  and in cross terms between  $Z_4(E)$  and  $t_3^{(3)}(E)$  separately. However, we will see it is natural to consider rather both of them at the same time.

Recall that the additional self-energies always appear as a set shown below

$$(1 + Z_0(E) T_3(E)) W_4(E) (T_3(E) Z_0(E) + 1) \quad (\text{D.26})$$

We first consider  $W_4(E)$

$$\begin{aligned} W_4(E) &= Z_4(E) + Z_4(E) T_3(E) Z_4(E) + \cdots \\ &= Z_4(E) \frac{1}{1 - T_3(E) Z_4(E)} \end{aligned} \quad (\text{D.27})$$

Recall that

$$Z_4(E) = G_0^{(3)}(E) V^{(32)} \mathcal{G}(E) V^{(23)} G_0^{(3)}(E) \quad (\text{D.28})$$

$$\mathcal{G}(E) = \bar{G}^{(2)B}(E) \frac{1}{1 - \Sigma(E) \bar{G}^{(2)B}(E)} \quad (\text{D.29})$$

$$\bar{G}^{(2)B}(E) = G_0^{(2)B}(E) t_4^B(E) G_0^{(2)B}(E) \quad (\text{D.30})$$

$$t_4^B(E) = V^{(2)} \frac{1}{1 - G_0^{(2)B}(E)} \quad (\text{D.31})$$

$W_4(E)$  is then rewritten as follows

$$\begin{aligned} W_4(E) &= Z_4(E) \frac{1}{1 - T_3(E) Z_4(E)} \\ &= G_0^{(3)}(E) V^{(32)} \mathcal{G}(E) V^{(23)} G_0^{(3)}(E) \frac{1}{1 - T_3(E) G_0^{(3)}(E) V^{(32)} \mathcal{G}(E) V^{(23)} G_0^{(3)}(E)} \\ &= G_0^{(3)}(E) V^{(32)} \mathcal{G}(E) \frac{1}{1 - V^{(23)} G_0^{(3)}(E) T_3(E) G_0^{(3)}(E) V^{(32)} \mathcal{G}(E)} V^{(23)} G_0^{(3)}(E) \\ &= G_0^{(3)}(E) V^{(32)} \mathcal{G}(E) \frac{1}{1 - \Sigma(E) G_\Sigma^{(2)}(E) \Sigma(E) \mathcal{G}(E)} V^{(23)} G_0^{(3)}(E) \end{aligned} \quad (\text{D.32})$$

where we have used  $T_3(E) = V^{(32)} G_\Sigma^{(2)}(E) V_{23}$  to obtain

$$\begin{aligned} V^{(23)} G_0^{(3)}(E) T_3(E) G_0^{(3)}(E) V^{(32)} &= V^{(23)} G_0^{(3)}(E) V^{(32)} G_\Sigma^{(2)}(E) V^{(23)} G_0^{(3)}(E) V^{(32)} \\ &= \Sigma(E) G_\Sigma^{(2)}(E) \Sigma(E) \end{aligned} \quad (\text{D.33})$$



$W_4(E)$  then becomes

$$\begin{aligned}
W_4(E) &= G_0^{(3)}(E) V^{(32)} \mathcal{G}(E) \frac{1}{1 - \Sigma(E) G_\Sigma^{(2)}(E) \Sigma(E) \mathcal{G}(E)} V^{(23)} G_0^{(3)}(E) \\
&= G_0^{(3)}(E) V^{(32)} \bar{G}^{(2)B}(E) \frac{1}{1 - \Sigma(E) \bar{G}^{(2)B}(E)} \\
&\times \frac{1}{1 - \Sigma(E) G_\Sigma^{(2)}(E) \Sigma(E) \bar{G}^{(2)B}(E) \frac{1}{1 - \Sigma(E) \bar{G}^{(2)B}(E)}} V^{(23)} G_0^{(3)}(E) \\
&= G_0^{(3)}(E) V^{(32)} \bar{G}^{(2)B}(E) \frac{1}{1 - \left( \Sigma(E) + \Sigma(E) G_\Sigma^{(2)}(E) \Sigma(E) \right) \bar{G}^{(2)B}} V^{(23)} G_0^{(3)}(E) \\
&= G_0^{(3)}(E) V^{(32)} G^{(2)B}(E) \\
&\times t_4^B(E) \frac{1}{1 - G_0^{(2)B}(E) \left( \Sigma(E) + \Sigma(E) G_\Sigma^{(2)}(E) \Sigma(E) \right) G_0^{(2)B}(E) t_4^B(E)} \\
&\times G_0^{(2)B}(E) V^{(23)} G_0^{(3)}(E) \\
&= G_0^{(3)}(E) V^{(32)} G^{(2)B}(E) t_4^B(E) \frac{1}{1 - \left( G_\Sigma^{(2)}(E) - G_0^{(2)B}(E) \right) t_4^B(E)} \\
&\times G_0^{(2)B}(E) V^{(23)} G_0^{(3)}(E) \\
&= G_0^{(3)}(E) V^{(32)} G^{(2)B}(E) V^{(2)} \\
&\times \frac{1}{1 - V^{(2)} G_0^{(2)B}(E) - \left( G_\Sigma^{(2)}(E) - G_0^{(2)B}(E) \right) V^{(2)}} G_0^{(2)B}(E) V^{(23)} G_0^{(3)}(E) \\
&= G_0^{(3)}(E) V^{(32)} G_0^{(2)B}(E) V^{(2)} \frac{1}{1 - G_\Sigma^{(2)}(E) V^{(2)}} G_0^{(2)B}(E) V^{(23)} G_0^{(3)}(E) \quad (D.34)
\end{aligned}$$

The left-most structure of  $\left( 1 + G_0(E) t_3^{(3)}(E) \right) W_4(E)$  is,

$$\begin{aligned}
&\left( 1 + G_0^{(3)}(E) V^{(32)} G_\Sigma^{(2)}(E) V^{(23)} \right) G_0^{(3)}(E) V^{(32)} G_0^{(2)B}(E) \\
&= G_0^{(3)}(E) V^{(32)} \left( 1 + G_\Sigma^{(2)}(E) \Sigma(E) \right) G_0^{(2)B}(E) \\
&= G_0^{(3)}(E) V^{(32)} G_\Sigma^{(2)}(E) \quad (D.35)
\end{aligned}$$

The right-most structure of  $W_4(E) \left( 1 + t_3^{(3)}(E) G_0(E) \right)$  is similarly

$$G_0^{(2)B}(E) V^{(23)} G_0^{(3)}(E) \left( V^{(32)} G_\Sigma^{(2)}(E) V^{(23)} G_0^{(3)}(E) G_0^{(3)}(E) + 1 \right) = G_\Sigma^{(2)}(E) V^{(23)} G_0^{(3)}(E) \quad (D.36)$$

$\left( 1 + G_0(E) t_3^{(3)}(E) \right) W_4(E) \left( t_3^{(3)}(E) G_0(E) + 1 \right)$  is therefore

$$\begin{aligned}
&G_0^{(3)}(E) V^{(32)} G_\Sigma^{(2)}(E) V^{(2)} \frac{1}{1 - G_\Sigma^{(2)}(E) V^{(2)}} G_\Sigma^{(2)}(E) V^{(23)} G_0^{(3)}(E) \\
&= G_0^{(3)}(E) V^{(32)} G_\Sigma^{(2)}(E) t_4^\Sigma(E) G_\Sigma^{(2)}(E) V^{(23)} G_0^{(3)}(E) \quad (D.37)
\end{aligned}$$

We now re-organize this using only the renormalized quantities. We first concentrate on  $t_4^\Sigma(E)$

$$\begin{aligned}
t_4^\Sigma(E) &= V^{(2)} \frac{1}{1 - G_\Sigma^{(2)}(E) V^{(2)}} \\
&= V^{(2)} \frac{1}{1 - G_0^{(2)}(E) V^{(2)} - \left( G_\Sigma^{(2)}(E) - G_0^{(2)}(E) \right) V^{(2)}} \\
&= V^{(2)} \frac{1}{1 - G_0^{(2)}(E) V^{(2)}} \frac{1}{1 - \left( G_\Sigma^{(2)}(E) - G_0^{(2)}(E) \right) V^{(2)} \frac{1}{1 - G_0^{(2)}(E) V^{(2)}}} \\
&= t^{(2)}(E) \frac{1}{1 - \left( G_\Sigma^{(2)}(E) - G_0^{(2)}(E) \right) t^{(2)}(E)} \tag{D.38}
\end{aligned}$$

Note that it is written using only the renormalized terms. We further transform the above equation to obtain the re-organized driving term  $Z_4'(E)$  as below

$$\begin{aligned}
G_0^{(2)}(E) t_4^\Sigma(E) G_0^{(2)}(E) &= G_0^{(2)}(E) t^{(2)}(E) \frac{1}{1 - \left( G_\Sigma^{(2)}(E) - G_0^{(2)}(E) \right) t^{(2)}(E)} G_0^{(2)}(E) \\
&= G_0^{(2)}(E) t^{(2)}(E) \\
&\times \frac{1}{1 - \left( G_0^{(2)}(E) \Sigma(E) G_\Sigma^{(2)}(E) \Sigma(E) G_0^{(2)}(E) + \bar{G}_\Sigma^{(2)}(E) \right) t^{(2)}(E)} \\
&\times G_0^{(2)}(E) \\
&= G_0^{(2)}(E) \bar{t}_\Sigma^{(2)}(E) \frac{1}{1 - G_0^{(2)}(E) \Sigma(E) G_\Sigma^{(2)}(E) \Sigma(E) G_0^{(2)}(E) \bar{t}_\Sigma^{(2)}(E)} \\
&\times G_0^{(2)}(E) \\
&= \mathcal{G}'(E) \frac{1}{1 - \Sigma(E) G_\Sigma^{(2)}(E) \Sigma(E) \mathcal{G}'(E)} \tag{D.39}
\end{aligned}$$

we define the first factor, which also appear in the last factor of denominator to be  $\mathcal{T}(E)$

$$\begin{aligned}
\mathcal{T}(E) &= t^{(2)}(E) \frac{1}{1 - \left( G_\Sigma^{(2)}(E) - G_0^{(2)}(E) - G_0^{(2)}(E) \Sigma(E) G_\Sigma^{(2)}(E) \Sigma(E) G_0^{(2)}(E) \right) t^{(2)}(E)} \\
&= t^{(2)}(E) \\
&\times \frac{1}{1 - G_0^{(2)}(E) \left( \Sigma(E) + \Delta + \Sigma(E) G_\Sigma^{(2)}(E) \Delta + \Delta G_\Sigma^{(2)}(E) \Sigma(E) \right) G_0^{(2)}(E) t^{(2)}(E)} \\
&= t^{(2)}(E) \frac{1}{1 - G_0^{(2)}(E) \sigma(E) G_0^{(2)}(E) t^{(2)}(E)} \tag{D.40}
\end{aligned}$$

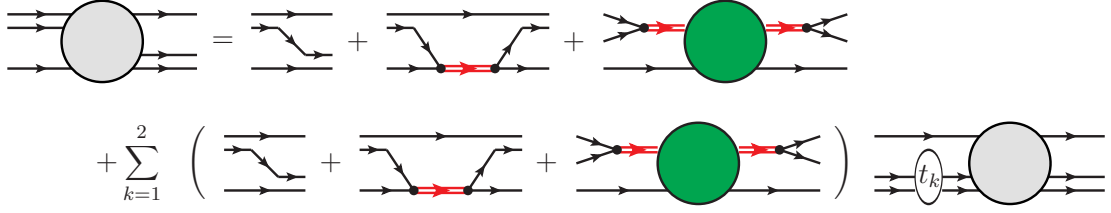


Figure D.1: A diagrammatic representation of another coupled-channels scattering equations

$t_4^\Sigma(E)$  multiplied by  $G_0^{(3)}(E) V^{(32)} G_0^{(2)}(E)$  from both sides then is,

$$\begin{aligned}
& G_0^{(3)}(E) \mathcal{T}(E) \frac{1}{1 - G_0^{(2)}(E) \Sigma(E) G_\Sigma^{(2)}(E) \Sigma(E) G_0^{(2)}(E) \mathcal{T}(E)} G_0^{(3)}(E) \\
&= G_0^{(3)}(E) V^{(32)} G_0^{(2)}(E) \\
&\times \mathcal{T}(E) \frac{1}{1 - G_0^{(2)}(E) V^{(23)} G_0^{(3)}(E) V^{(32)} G_\Sigma^{(2)}(E) V^{(23)} G_0^{(3)}(E) V^{(32)} G_0^{(2)}(E) \mathcal{T}(E)} \\
&\times G_0^{(2)}(E) V^{(23)} G_0^{(3)}(E) \\
&= G_0^{(3)}(E) V^{(32)} G_0^{(2)}(E) \mathcal{T}(E) G_0^{(2)}(E) V^{(23)} G_0^{(3)}(E) \\
&\times \frac{1}{1 - t_3^{(3)}(E) G_0^{(3)}(E) V^{(32)} G_0^{(2)}(E) \mathcal{T}(E) G_0^{(2)}(E) V^{(23)} G_0^{(3)}(E)} \\
&= \mathcal{G}'(E) \frac{1}{1 - t_3^{(3)}(E) \mathcal{G}'(E)} \tag{D.41}
\end{aligned}$$

$$\begin{aligned}
& \left(1 + G_0^{(3)}(E) t_3^{(3)}(E)\right) W_4(E) \left(t_3^{(3)}(E) G_0^{(3)}(E) + 1\right) \\
&= G_0^{(3)}(E) V^{(32)} G_\Sigma^{(2)}(E) t_4^\Sigma(E) G_\Sigma^{(2)}(E) V^{(23)} G_0^{(3)}(E) \\
&= G_0^{(3)}(E) V^{(32)} \left(1 + G_\Sigma^{(2)}(E) (\Sigma(E) + \Delta)\right) G_0^{(3)}(E) t_4^\Sigma(E) G_0^{(3)}(E) \\
&\times \left((\Delta + \Sigma(E)) G_\Sigma^{(2)}(E) + 1\right) V^{(23)} G_0^{(3)}(E) \\
&= G_0^{(3)}(E) V^{(32)} \left(1 + G_\Sigma^{(2)}(E) (\Sigma(E) + \Delta)\right) G_0^{(3)}(E) \mathcal{G}'(E) \frac{1}{1 - t_3^{(3)}(E) \mathcal{G}'(E)} \\
&\times G_0^{(3)}(E) \left((\Delta + \Sigma(E)) G_\Sigma^{(2)}(E) + 1\right) V^{(23)} G_0^{(3)}(E)
\end{aligned}$$

which leads to the modified driving term  $Z'_4(E)$  to be

$$\begin{aligned}
Z'_4(E) &= \left(G_0^{(3)}(E) V^{(32)} + Z_0(E) V^{(32)} I_3 G_\Sigma^{(2)}(E) \Delta\right) \mathcal{G}'(E) \\
&\times \left(\Delta G_\Sigma^{(2)}(E) I_3 V^{(23)} Z_0(E) + V^{(23)} G_0^{(3)}(E)\right)
\end{aligned}$$

### D.3 Another Two-Body and Three-Body Coupled-Channels Equations

In the previous subsection, we saw that the transition amplitude  $X(E)$  is reorganized as a series

$$X(E) = X_3(E) + X_3(E) \bar{T}_3(E) X_3(E) + \dots \tag{D.42}$$

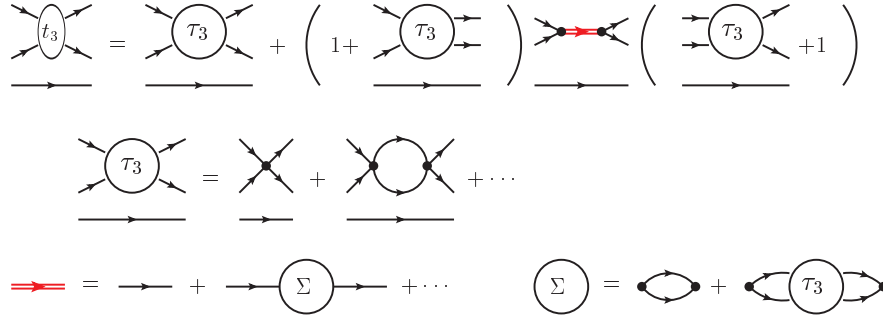


Figure D.2: A diagrammatic representation of  $t_3(E)$

the above series can obviously be rewritten as a following equation

$$X(E) = X_3(E) + X_3(E) \bar{T}_3(E) X(E) \quad (\text{D.43})$$

where  $X_3(E)$  and  $T_3(E)$  is given in equations (3.93) and (3.94) respectively. A diagrammatic representation of the equation (D.43) is given in figure D.1. Written in this form, there are no iteratively appearing self-energies since they are all put into the  $X_3(E)$  as a set.

#### D.4 In Case of $V_3 \neq 0$

We have now obtained the modified or reorganized driving term  $Z'(E)$ . We have however, ignored the bare interaction between  $\phi_1\phi_2$  which we denote  $V_3$ . In this subsection, we briefly present how the modification is modified by the presence of  $V_3$ . Discussion is carried out almost in a parallel manner.

$$t_3^{(3)}(E) = \tau_3^{(3)}(E) + \left(1 + \tau_3^{(3)}(E) G_0^{(3)}(E)\right) V^{(32)} G_\Sigma^{(2)}(E) V^{(23)} \left(G_0^{(3)}(E) \tau_3^{(3)}(E) + 1\right) \quad (\text{D.44})$$

where

$$G_\Sigma^{(2)}(E) = G_0^{(2)}(E) + G_0^{(2)}(E) \Sigma(E) G_0^{(2)}(E) + \dots \quad (\text{D.45})$$

and

$$\Sigma(E) = V^{(23)} G_3(E) V^{(32)} \quad (\text{D.46})$$

where

$$G_3(E) = G_0^{(3)}(E) + G_0^{(3)}(E) \tau_3^{(3)}(E) G_0^{(3)}(E) \quad (\text{D.47})$$

$$\tau_3^{(3)}(E) = V_3^{(3)} + V_3^{(3)} G_0^{(3)}(E) \tau_3^{(3)}(E) \quad (\text{D.48})$$

We decompose the  $\Sigma(E)$  into two terms one the same self-energy which has appeared so far and the other which contain  $\tau_3^{(3)}(E)$  as follows

$$\Sigma(E) = \Sigma_0(E) + \Sigma_V(E) = V^{(23)} G_0^{(3)}(E) V^{(32)} + V^{(23)} G_0^{(3)}(E) \tau_3^{(3)}(E) G_0^{(3)}(E) V^{(32)} \quad (\text{D.49})$$

#### Counterterms in $t_3^{(3)}(E)$

Written in the form (D.44), adding counterterm to self-energies appearing in  $t_3^{(3)}(E)$  is trivial. We just replace the self-energies in  $G_\Sigma^{(2)}(E)$  with the one to which the counterterm is added

$$\Sigma(E) \rightarrow \Sigma(E) + \Delta \quad (\text{D.50})$$



Figure D.3: A diagrammatic representation of  $\Sigma(E) + \Delta$

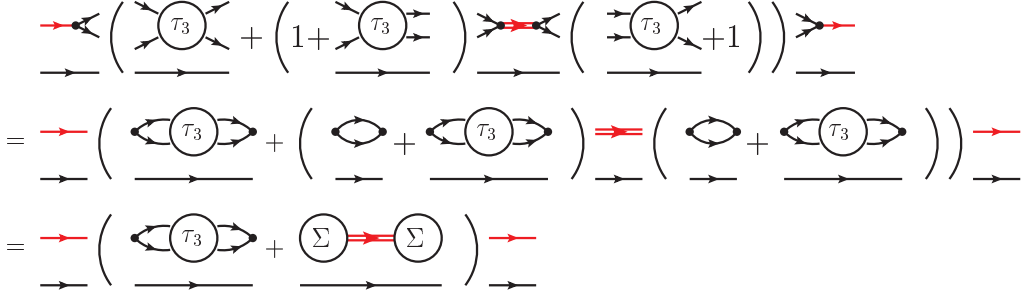


Figure D.4: A diagrammatic representation of equation (D.52)

### Counterterms in $Z_4(E)$ and Others

$Z_4(E)$  is the same as before

$$\begin{aligned}
 Z_4(E) &= G_0^{(3)}(E) V^{(32)} \\
 &\times G_0^{(2)}(E) t^{(2)}(E) G_0^{(2)}(E) \frac{1}{1 - \Sigma_0(E) G_0^{(2)}(E) t^{(2)}(E) G_0^{(2)}(E)} V^{(23)} G_0^{(3)}(E) \\
 &= G_0^{(3)}(E) V^{(32)} \mathcal{G}_0(E) V^{(23)} G_0^{(3)}(E)
 \end{aligned} \tag{D.51}$$

$W_4(E)$  is however,

$$\begin{aligned}
 W_4(E) &= Z_4(E) + Z_4(E) t_3^{(3)}(E) Z_4(E) + \dots \\
 &= Z_4(E) \frac{1}{1 - t_3^{(3)}(E) Z_4(E)} \\
 &= G_0^{(3)}(E) V^{(32)} \mathcal{G}_0(E) \frac{1}{1 - V^{(23)} G_0^{(3)}(E) t_3^{(3)}(E) V^{(23)} G_0^{(3)}(E) \mathcal{G}_0(E)} V^{(23)} G_0^{(3)}(E)
 \end{aligned}$$

The left-most structure  $Z_4(E)$  multiplied by  $t_3^{(3)}(E)$  and the right-most structure of  $Z_4(E)$  is,

$$V^{(23)} G_0^{(3)}(E) t_3^{(3)}(E) V^{(23)} G_0^{(3)}(E) = \Sigma_V(E) + \Sigma(E) G_\Sigma^{(2)}(E) \Sigma(E) \tag{D.52}$$

$W_4(E)$  is therefore,

$$\begin{aligned}
 W_4(E) &= G_0^{(3)}(E) V^{(32)} G_0^{(2)}(E) t^{(2)}(E) G_0^{(2)}(E) \\
 &\times \frac{1}{1 - \left( \Sigma_0(E) + \Sigma_V(E) + \Sigma(E) G_\Sigma^{(2)}(E) \Sigma(E) \right) G_0^{(2)}(E) t^{(2)}(E) G_0^{(2)}(E)} \\
 &\times V^{(23)} G_0^{(3)}(E)
 \end{aligned} \tag{D.53}$$

The self-energies in the denominator become, after adding counterterms,

$$\Sigma(E) + \Delta + (\Sigma(E) + \Delta) G_\Sigma^{(2)}(E) (\Delta + \Sigma(E)) \tag{D.54}$$

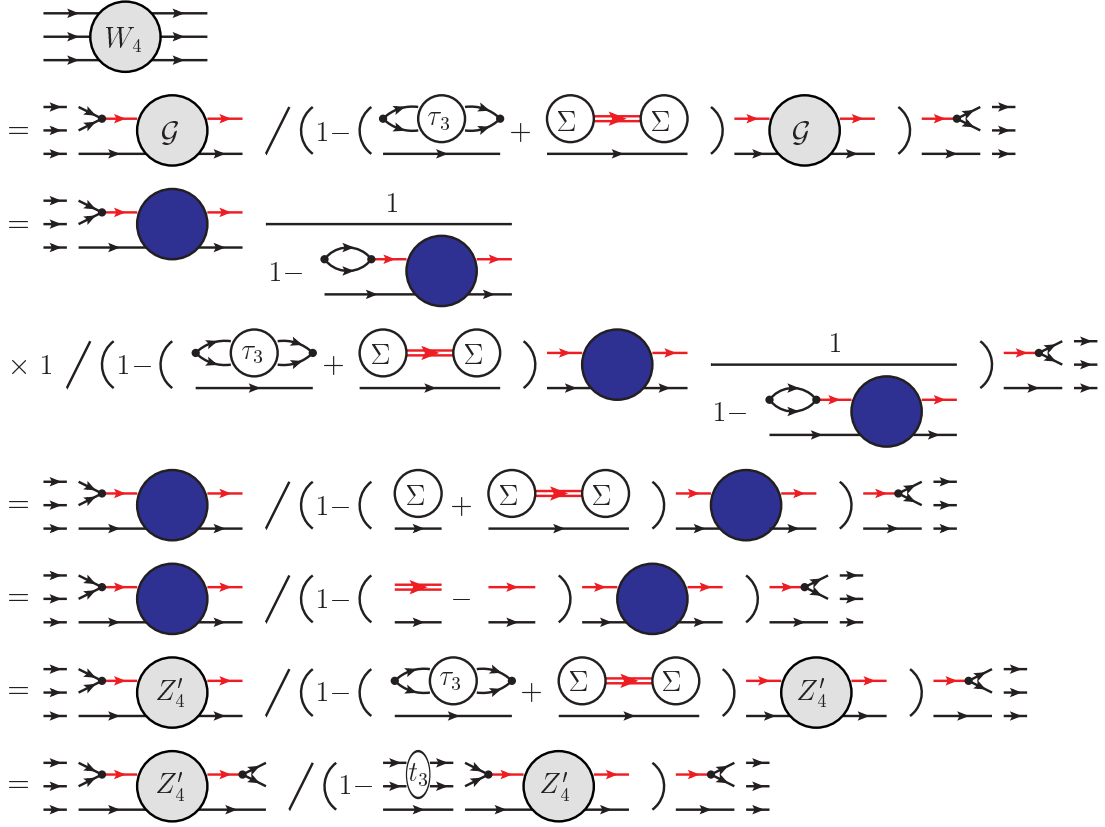


Figure D.5: A diagrammatic representation of equation (D.52)

Noting that

$$G_0^{(2)}(E) \left( \Sigma(E) + \Delta + (\Sigma(E) + \Delta) G_\Sigma^{(2)}(E) (\Delta + \Sigma(E)) \right) G_0^{(2)}(E) = G_\Sigma^{(2)}(E) - G_0^{(2)}(E)$$

$W_4(E)$  becomes simply

$$\begin{aligned} W_4(E) &= G_0^{(3)}(E) V^{(32)} G_0^{(2)}(E) \\ &\times t^{(2)}(E) \frac{1}{1 - (G_\Sigma^{(2)}(E) - G_0^{(2)}(E)) t^{(2)}(E)} G_0^{(2)}(E) V^{(23)} G_0^{(3)}(E) \end{aligned} \quad (\text{D.55})$$

which is formally equivalent to (3.109). It can also be written as

$$\begin{aligned} W_4(E) &= G_0^{(3)}(E) V^{(32)} G_0^{(2)}(E) V^{(2)} \frac{1}{1 - G_\Sigma^{(2)}(E) V^{(2)}} G_0^{(2)}(E) V^{(23)} G_0^{(3)}(E) \\ &= G_0^{(3)}(E) V^{(32)} G_0^{(2)}(E) t_\Sigma^{(2)}(E) G_0^{(2)}(E) V^{(23)} G_0^{(3)}(E) \end{aligned} \quad (\text{D.56})$$

The modified driving term is obtained by an appropriate reorganization

$$\begin{aligned} &t^{(2)}(E) \frac{1}{1 - (G_\Sigma^{(2)}(E) - G_0^{(2)}(E)) t^{(2)}(E)} \\ &= t^{(2)}(E) \frac{1}{1 - \bar{G}_\Sigma^{(2)}(E) t^{(2)}(E)} \\ &\times \frac{1}{1 - G_0^{(2)}(E) \left( \Sigma_V(E) + \Sigma(E) G_\Sigma^{(2)}(E) \Sigma(E) \right) G_0^{(2)}(E) t^{(2)}(E) \frac{1}{1 - \bar{G}_\Sigma^{(2)}(E) t^{(2)}(E)}} \end{aligned}$$

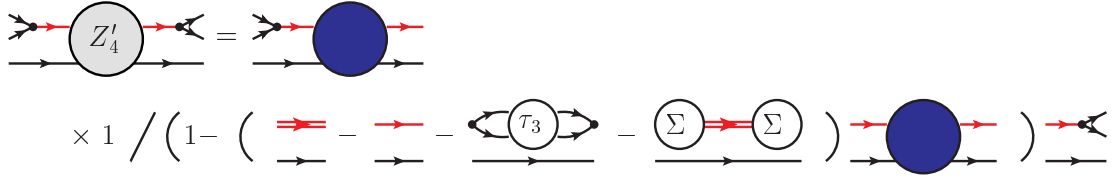


Figure D.6: A diagrammatic representation of the modified  $Z_4(E)$

where we have defined  $\bar{G}_\Sigma^{(2)}(E)$  as

$$G_\Sigma^{(2)}(E) - G_0^{(2)}(E) = \bar{G}_\Sigma^{(2)}(E) + G_0^{(2)}(E) \left( \Sigma_V(E) + \Sigma(E) G_\Sigma^{(2)}(E) \Sigma(E) \right) G_0^{(2)}(E) \quad (\text{D.57})$$

and further define

$$\bar{t}_\Sigma^{(2)}(E) = t^{(2)}(E) \frac{1}{1 - \bar{G}_\Sigma^{(2)}(E) t^{(2)}(E)} \quad (\text{D.58})$$

then,

$$\begin{aligned} & \bar{t}_\Sigma^{(2)}(E) \frac{1}{1 - G_0^{(2)}(E) \left( \Sigma_V(E) + \Sigma(E) G_\Sigma^{(2)}(E) \Sigma(E) \right) G_0^{(2)}(E) \bar{t}_\Sigma^{(2)}(E)} \\ &= \bar{t}_\Sigma^{(2)}(E) \frac{1}{1 - G_0^{(2)}(E) V^{(23)} G_0^{(3)}(E) t_3^{(3)}(E) G_0^{(3)}(E) V^{(32)} G_0^{(2)}(E) \bar{t}_\Sigma^{(2)}(E)} \end{aligned}$$

$W_4(E)$  is therefore written as

$$W_4(E) = Z'_4(E) \frac{1}{1 - t_3^{(3)}(E) Z'_4(E)} \quad (\text{D.59})$$

where  $Z'_4(E)$  is defined as

$$Z'_4(E) = G_0^{(3)}(E) V^{(32)} G_0^{(2)}(E) \bar{t}_\Sigma^{(2)}(E) G_0^{(2)}(E) V^{(23)} G_0^{(3)}(E) \quad (\text{D.60})$$

Modification on the right- and left-most parts are determined by the following arguments. Multiplying  $t_3^{(3)}(E)$  to the left-most structure of  $Z_4(E)$  gives

$$\begin{aligned} & G_0^{(3)}(E) t_3^{(3)}(E) G_0^{(3)}(E) V^{(32)} G_0^{(2)}(E) \\ &= G_0^{(3)}(E) \tau_3^{(3)}(E) G_0^{(3)}(E) V^{(32)} G_0^{(2)}(E) \\ &+ G_0^{(3)}(E) \left( 1 + \tau_3^{(3)}(E) G_0^{(3)}(E) \right) V^{(32)} G_\Sigma^{(2)}(E) \Sigma(E) G_0^{(2)}(E) \end{aligned} \quad (\text{D.61})$$

which should be countertermed as below

$$\begin{aligned} & G_0^{(3)}(E) \tau_3^{(3)}(E) G_0^{(3)}(E) V^{(32)} G_0^{(2)}(E) \\ &+ G_0^{(3)}(E) \left( 1 + \tau_3^{(3)}(E) G_0^{(3)}(E) \right) V^{(32)} G_\Sigma^{(2)}(E) (\Sigma(E) + \Delta) G_0^{(2)}(E) \end{aligned} \quad (\text{D.62})$$

We need to take the last term

$$G_0^{(3)}(E) \left( 1 + \tau_3^{(3)}(E) G_0^{(3)}(E) \right) V^{(32)} G_\Sigma^{(2)}(E) \Delta G_0^{(2)}(E) \quad (\text{D.63})$$

Considering the matrix structure, the modification we need to do is,

$$\begin{aligned}
Z'_4(E) &= \left( G_0^{(3)}(E) + \bar{\delta} I_3 G_0^{(3)}(E) \left( 1 + \tau_3^{(3)}(E) G_0^{(3)}(E) \right) V^{(32)} G_\Sigma^{(2)}(E) \Delta \right) \\
&\times \mathcal{G}'(E) \\
&\times \left( \Delta G_\Sigma^{(2)}(E) V^{(23)} \left( G_0^{(3)}(E) \tau^{(3)}(E) + 1 \right) G_0^{(3)}(E) I_3 \bar{\delta} + G_0^{(3)}(E) \right) \quad (D.64)
\end{aligned}$$

where  $\mathcal{G}'(E)$  is,

$$\begin{aligned}
\mathcal{G}'(E) &= G_0^{(2)}(E) \bar{t}_\Sigma^{(2)}(E) G_0^{(2)}(E) \\
&= G_0^{(2)}(E) t^{(2)}(E) \frac{1}{1 - \bar{G}_\Sigma^{(2)}(E) t^{(2)}(E)} G_0^{(2)}(E) \quad (D.65)
\end{aligned}$$

where,  $\bar{G}_\Sigma^{(2)}(E)$  is defined as

$$\begin{aligned}
\bar{G}_\Sigma^{(2)}(E) &= G_\Sigma^{(2)}(E) - G_0^{(2)}(E) - G_0^{(2)}(E) \left( \Sigma_V(E) + \Sigma(E) G_\Sigma^{(2)}(E) \Sigma(E) \right) G_0^{(2)}(E) \\
&= G_\Sigma^{(2)}(E) - G_0^{(2)}(E) - G_0^{(2)}(E) V^{(23)} G_0^{(3)}(E) t_3^{(3)}(E) G_0^{(3)}(E) V^{(32)} G_0^{(2)}(E)
\end{aligned}$$

A relation between  $\mathcal{G}_0(E)$  and the modified one  $\mathcal{G}'(E)$  is given as below

$$\begin{aligned}
\mathcal{G}'(E) &= G_0^{(2)}(E) t^{(2)}(E) \frac{1}{1 - \bar{G}_\Sigma^{(2)}(E) t^{(2)}(E)} G_0^{(2)}(E) \\
&= \mathcal{G}_0(E) \frac{1}{1 - \left( \Delta + \Delta G_\Sigma^{(2)}(E) \Sigma(E) + \Sigma(E) G_\Sigma^{(2)}(E) \Delta + \Delta G_\Sigma^{(2)}(E) \Delta \right) \mathcal{G}_0(E)}
\end{aligned}$$

In practice, we just replace the original  $Z_4(E)$  with the modified one in (D.64).



## Appendix E

# Formal Treatment of Two-Body Potential Scattering

In this appendix, we briefly review elements of formal potential scattering theory.

### E.1 The Möller Operator and The Green Function

The initial state obeys the following time-dependent Schroedinger equation

$$i\frac{d}{dt}|\psi_0(t)\rangle = H_0|\psi_0(t)\rangle \quad (\text{E.1})$$

where  $H_0$  is the free Hamiltonian

$$H_0 = \frac{p^2}{2m} \quad (\text{E.2})$$

As the particle enters into the region where it feels the potential, the initial state  $|\psi_0\rangle$  develops into the state which obeys the full time-dependent Schroedinger equation

$$i\frac{d}{dt}|\psi(t)\rangle = H|\psi(t)\rangle \quad (\text{E.3})$$

$H$  is the full Hamiltonian including the potential

$$H = H_0 + V \quad (\text{E.4})$$

the question is, how is  $|\psi\rangle$  related to the initial state  $|\psi_0\rangle$ ? Since  $|\psi\rangle$  coincide with  $|\psi_0\rangle$  in the infinite past, we require the following equation to be satisfied

$$\lim_{t \rightarrow -\infty} \| |\psi(t)\rangle - |\psi_0(t)\rangle \| = 0 \quad (\text{E.5})$$

let us remind that  $|\psi_0\rangle$  and  $|\psi\rangle$  can be formally solved and written as

$$|\psi(t)\rangle = e^{-iHt}|\psi(0)\rangle \quad (\text{E.6})$$

$$|\psi_0(t)\rangle = e^{-iH_0t}|\psi_0(0)\rangle \quad (\text{E.7})$$

(E.5) then equals to

$$\lim_{t \rightarrow -\infty} \| |\psi(0)\rangle - e^{iHt}e^{-iH_0t}|\psi_0(0)\rangle \| = 0 \quad (\text{E.8})$$

where we have used the fact that  $e^{-iHt}$  is a unitary operator. We thus arrive at an equation which relates the initial state and the full scattering state

$$|\psi(0)\rangle = \Omega^{(+)}|\psi_0(0)\rangle \quad (\text{E.9})$$

$\Omega^{(+)}$  is called the Moeller operator and defined as follows

$$\Omega^{(+)} = \lim_{t \rightarrow -\infty} e^{iHt} e^{-iH_0 t} \quad (\text{E.10})$$

Since the above expression is not practical, we use the identity

$$\lim_{t \rightarrow -\infty} f(t) = \lim_{\epsilon \rightarrow -\infty} \epsilon \int_{-\infty}^0 dt e^{\epsilon t} f(t) \quad (\text{E.11})$$

and rewrite (E.9)

$$\begin{aligned} |\psi(0)\rangle &= \lim_{t \rightarrow -\infty} e^{iHt} e^{-iH_0 t} |\psi_0(0)\rangle \\ &= \lim_{\epsilon \rightarrow 0} \epsilon \int_{-\infty}^0 dt e^{\epsilon t} e^{iHt} e^{-iH_0 t} |\psi_0(0)\rangle \\ &= \lim_{\epsilon \rightarrow 0} \epsilon \int_{-\infty}^0 dt e^{\epsilon t} e^{iHt} \int d\mathbf{p} e^{-iE_p t} |\mathbf{p}\rangle \langle \mathbf{p} | \psi_0(0)\rangle \\ &= \lim_{\epsilon \rightarrow 0} \int d\mathbf{p} \frac{i\epsilon}{E_p + i\epsilon - H} |\mathbf{p}\rangle \langle \mathbf{p} | \psi_0(0)\rangle \end{aligned} \quad (\text{E.12})$$

which leads to the equation relating momentum representations of each states

$$\langle \mathbf{p} | \psi \rangle = \lim_{\epsilon \rightarrow 0} \frac{i\epsilon}{E_p + i\epsilon - H} \langle \mathbf{p} | \psi_0 \rangle \quad (\text{E.13})$$

Now we are facing the Green function which plays the central role in the scattering theory.

$$G(z) = \frac{1}{z - H} \quad (\text{E.14})$$

Here we defined  $G(z)$  on the complex energy  $z$ . This generalization is necessary when we consider resonances as well as bound states. Obviously,  $z$  cannot lie on the spectrum of the  $H$ .

We now define

$$\begin{aligned} |\mathbf{p}\rangle^{(+)} &= \lim_{\epsilon \rightarrow 0} \frac{i\epsilon}{E_p + i\epsilon - H} |\mathbf{p}\rangle \\ &= \lim_{\epsilon \rightarrow 0} i\epsilon G(E_p + i\epsilon) |\mathbf{p}\rangle \end{aligned} \quad (\text{E.15})$$

In the following, we omit  $\lim_{\epsilon \rightarrow 0}$  for the notational simplicity and always assume that  $\epsilon \rightarrow 0$  limit is taken. Note that  $|\mathbf{p}\rangle^{(+)}$  is an eigenstate of the full Hamiltonian  $H$ .

$$(H - E_p) |\mathbf{p}\rangle^{(+)} = 0 \quad (\text{E.16})$$

$|\mathbf{p}\rangle^{(+)}$  thus form the complete set of states.

$$\int d\mathbf{p} |\mathbf{p}\rangle^{(+)} \langle \mathbf{p}| = 1 \quad (\text{E.17})$$

## E.2 Transition Amplitude

The Transition Amplitude at time  $t$  is defined as a probability of finding plane-wave state with momentum  $\mathbf{p}$  in  $|\Psi(t)\rangle$ .

$$\begin{aligned} A_{\mathbf{p}_f}(t) &= \langle \mathbf{p}_f(t) | \Psi(t) \rangle \\ &= -i \langle \mathbf{p}_f(0) | e^{iH_0 t} e^{-Ht} | \Psi(0) \rangle \end{aligned} \quad (\text{E.18})$$

Scattering Cross section, which is observed in experiments, is proportional to  $d/dt|A|^2$ . Thus we also need time derivative of the transition amplitude

$$\begin{aligned}\frac{d}{dt}A_{\mathbf{p}_f}(t) &= -i\langle\mathbf{p}_f(0)|e^{iH_0t}Ve^{-Ht}|\Psi(0)\rangle \\ &= -i\int d\mathbf{p}e^{i(E_{p_f}-E_p)t}\langle\mathbf{p}_f(0)|V|\mathbf{p}\rangle^{(+)}\langle\mathbf{p}|\Psi(0)\rangle\end{aligned}\quad (\text{E.19})$$

The matrix element  $\langle\mathbf{p}_f|V|\mathbf{p}\rangle^{(+)}$  is called the scattering amplitude or the  $T$ -matrix element and written as  $T_{\mathbf{p}_f\mathbf{p}}$

$$T_{\mathbf{p}_f\mathbf{p}} = \langle\mathbf{p}_f|V|\mathbf{p}\rangle^{(+)} \quad (\text{E.20})$$

A physical meaning of the scattering amplitude can be seen from the following discussion. The Green function satisfies the identity  $G = G_0 + G_0VG$  which leads to the scattering equation

$$|\mathbf{p}\rangle^{(+)} = |\mathbf{p}\rangle + G_0V|\mathbf{p}\rangle^{(+)} \quad (\text{E.21})$$

its plane-wave component is,

$$\langle\mathbf{p}_f|\mathbf{p}\rangle^{(+)} = \delta(\mathbf{p}_f - \mathbf{p}) + \frac{\langle\mathbf{p}_f|V|\mathbf{p}\rangle^{(+)}}{E_p - E_{p_f} + i\epsilon} \quad (\text{E.22})$$

That is, the scattering amplitude represents the probability of finding a plane-wave state with momentum  $\mathbf{p}_f$  in the perturbed part of  $|\mathbf{p}\rangle^{(+)}$ .

The transition amplitude is now simply written as

$$\begin{aligned}A_{\mathbf{p}_f}(t) &= \int d\mathbf{p}e^{i(E_{p_f}-E_p)t}\langle\mathbf{p}_f(0)|\mathbf{p}\rangle^{(+)}\langle\mathbf{p}|\Psi(0)\rangle \\ &= \int d\mathbf{p}e^{i(E_{p_f}-E_p)t}\left\{\delta(\mathbf{p}_f - \mathbf{p}) + \frac{T_{\mathbf{p}_f\mathbf{p}}}{E_p - E_{p_f} + i\epsilon}\right\}\langle\mathbf{p}|\Psi(0)\rangle \\ &= \int d\mathbf{p}\left\{\delta(\mathbf{p}_f - \mathbf{p}) - 2\pi i\delta(E_p - E_{p_f})T_{\mathbf{p}_f\mathbf{p}}\right\}\langle\mathbf{p}|\Psi(0)\rangle \\ &= \int d\mathbf{p}S_{\mathbf{p}_f\mathbf{p}}\langle\mathbf{p}|\Psi(0)\rangle\end{aligned}\quad (\text{E.23})$$

where we have defined the  $S$ -matrix element

$$S_{\mathbf{p}_f\mathbf{p}} = \delta(\mathbf{p}_f - \mathbf{p}) - 2\pi i\delta(E_p - E_{p_f})T_{\mathbf{p}_f\mathbf{p}} \quad (\text{E.24})$$

Its physical meaning is obvious that the  $S$ -matrix element is the probability from  $\mathbf{p}$  to  $\mathbf{p}_f$ .

### E.3 Analytic Properties of The Green Function and The $T$ -Matrix

The eigenstates of the free-Hamiltonian  $H_0$  are plane-wave  $|\mathbf{p}\rangle$  which forms the complete set of states.

$$H_0|\mathbf{p}\rangle = E_p|\mathbf{p}\rangle, \quad \int d\mathbf{p}|\mathbf{p}\rangle\langle\mathbf{p}| = 1 \quad (\text{E.25})$$

The corresponding free Green function  $G_0$  can be written as the following spectral representation form

$$G_0(z) = \frac{1}{z - H_0} = \int d\mathbf{p}|\mathbf{p}\rangle\frac{1}{z - E_p}\langle\mathbf{p}| \quad (\text{E.26})$$

Using the above expression and the formula

$$\frac{1}{E \pm i\epsilon - E_p} = \mathcal{P} \frac{1}{E - E_p} \mp i\pi \delta(E - E_p) \quad (\text{E.27})$$

we obtain

$$G_0(E + i\epsilon) - G_0(E - i\epsilon) = -2\pi i \int d\mathbf{p} |\mathbf{p}\rangle \delta(E - E_p) \langle \mathbf{p}| \quad (\text{E.28})$$

which means that the  $G_0$  has a branch cut along the real axis.

Similar argument is carried out for the full Green function  $G$ . The full Hamiltonian  $H$  has the scattering state  $|\mathbf{p}\rangle^{(+)}$  and if the interaction is attractive enough, it also has the bound states  $|b\rangle$  as eigenstates.

$$H|\mathbf{p}\rangle^{(+)} = E_p|\mathbf{p}\rangle^{(+)} \quad (\text{E.29})$$

$$H|b\rangle = E_b|b\rangle \quad (\text{E.30})$$

the spectral representation of the full Green function  $G$  is then

$$G(z) = \sum_b \frac{|b\rangle\langle b|}{z - E_b} + \int d\mathbf{p} \frac{|\mathbf{p}\rangle\langle \mathbf{p}|}{z - E_p} \quad (\text{E.31})$$

We can see that the  $G$  has poles at  $z$  equals to energy of the bound states  $E_b$  in addition to the branch cut along the real axis

## Appendix F

# Analytical Approach to The Near-Threshold $S$ -Matrix Pole Behavior

In this chapter, we investigate the degenerate two-body and three-body coupled-channels system from the dispersion relation and the two-body and three-body coupled-channels optical theorem perspective. We have so far been considering three-body elastic scattering amplitudes. In this chapter however, we focus on two-body elastic scattering amplitudes instead of the three-body scattering amplitudes.

We start our discussion by constructing the elastic two-body  $T$ -matrix by using the Feshbach projection method. We then apply the multi-channel optical theorem we introduced in section 2.1 and examine the leading behavior of the imaginary part of the  $T$ -matrix. Once the leading behavior of the spectral function is obtained, dispersion relation enables us to estimate the leading behavior of inverse of the  $T$ -matrix which gives us behavior of poles of the  $T$ -matrix near the threshold.

### F.1 Elastic Two-Body $T$ -Matrix In The $\phi_1\phi_2\phi_3 - \psi_3\phi_3$ Coupled-Channels System

In this section, we derive the fully-connected elastic two-body  $T$ -matrix using the Feshbach projection method.

Let  $P$  and  $Q$  be projection operators which projects any state into three-body and two-body channels respectively. The Feshbach projection procedure gives the following expression of the elastic two-body  $T$ -matrix which we denote  $T_{QQ}(E)$

$$T_{QQ}(E) = U_{QQ}(E) + U_{QQ}(E) \frac{1}{E - H_0^Q - U_{QQ}(E)} U_{QQ}(E) \quad (\text{F.1})$$

We define the intermediate part of the second terms as  $G_{QQ}(E)$

$$G_{QQ}(E) = \frac{1}{E - H_0^Q - U_{QQ}(E)} \quad (\text{F.2})$$

The effective interactions in the two-body channel  $U_{QQ}$  in which the effects originating from the coupling to the three-body channel are embedded in are,

$$\begin{aligned} U_{QQ}(E) &= V_{QQ} + V_{QP} G_P(E) V_{PQ} \\ &= V^{(2)} + V^{(23)} G_P(E) V^{(32)} \end{aligned} \quad (\text{F.3})$$

$G_P$  is a three-body propagator with the bare interactions in three-body channel

$$G_P(E) = \frac{1}{E - PHP} = \frac{1}{E - H_0^P - V_{PP}} \quad (\text{F.4})$$

and satisfies the Dyson-Schwinger equation

$$G_P(E) = G_0^P(E) + G_0^P(E) V_3 G_P(E) \quad (\text{F.5})$$

$G_P(E)$  can also be expressed with the three-body  $T$ -matrix  $T_P(E)$  as below

$$G_P(E) = G_0^P(E) + G_0^P(E) T_P(E) G_0^P(E) \quad (\text{F.6})$$

where  $T_P(E)$  is the fully-connected three-body scattering  $T$ -matrix whose interactions are bare two-body interactions which we have been denoting  $V_i^{(3)}$ . It is related to the fragmentation amplitudes  $U_{ij}(E)$  which are obtained by solving the (Faddeev-)AGS equations [70]

$$T_P(E) = \sum_{i,j}^3 t_i^{(3)}(E) G_0^{(3)}(E) U_{ij}(E) G_0^{(3)}(E) t_j^{(3)}(E) \quad (\text{F.7})$$

By definition,  $T_P(E)$  formally satisfies the Lippmann-Schwinger equation

$$T_P(E) = V_{PP} + V_{PP} G_0^{(3)}(E) T_P(E) \quad (\text{F.8})$$

The above equation is of course ill-defined and that is the very reason that we need to introduce the (Faddeev-)AGS equations. The above equation is however, still valid keeping in mind that we drop the disconnected parts. We rewrite the equation (F.3) using the equation (F.8) as follows

$$U_{QQ} = V^{(2)} + V^{(23)} G_0^{(3)}(E) V^{(32)} + V^{(23)} G_0^{(3)}(E) T_P(E) G_0^{(3)}(E) V^{(32)} \quad (\text{F.9})$$

The second term is a “disconnected” interaction which is equal to the self-energy  $\Sigma(E)$ . We therefore separate the second term and write  $U_{QQ}(E)$  as

$$U_{QQ}(E) = \mathcal{U}_{QQ}(E) + \Sigma(E) \quad (\text{F.10})$$

The full elastic two-body  $T$ -matrix is then written as

$$T_{QQ}(E) = (\mathcal{U}_{QQ}(E) + \Sigma(E)) + (\mathcal{U}_{QQ}(E) + \Sigma(E)) G_{QQ}(E) (\mathcal{U}_{QQ}(E) + \Sigma(E)) \quad (\text{F.11})$$

The first two terms  $\mathcal{U}_{QQ}(E) + \mathcal{U}_{QQ}(E) G_{QQ}(E) \mathcal{U}_{QQ}(E)$  are fully connected and we denote it as  $T_c(E)$ .

$$T_c(E) = \mathcal{U}_{QQ}(E) + \mathcal{U}_{QQ}(E) G_{QQ}(E) \mathcal{U}_{QQ}(E) \quad (\text{F.12})$$

Here we note that using the identity

$$\frac{1}{A - B} = \frac{1}{A} + \frac{1}{A} \left( B + B \frac{1}{A - B} B \right) \frac{1}{A} \quad (\text{F.13})$$

gives the relation between  $T_c(E)$  and  $G_{QQ}(E)$  shown below

$$\begin{aligned} G_{QQ}(E) &= G_{\Sigma}^{(2)}(E) + G_{\Sigma}^{(2)}(E) (\mathcal{U}_{QQ}(E) + \mathcal{U}_{QQ}(E) G_{QQ}(E) \mathcal{U}_{QQ}(E)) G_{\Sigma}^{(2)}(E) \\ &= G_{\Sigma}^{(2)}(E) + G_{\Sigma}^{(2)}(E) T_c(E) G_{\Sigma}^{(2)}(E) \end{aligned} \quad (\text{F.14})$$

where we have defined  $G_\Sigma^{(2)}(E)$  as the dressed propagator of  $\psi_3\phi_3$  whose explicit expression is

$$G_\Sigma^{-1}(E) = G_0^{-1}(E) - \Sigma(E) \quad (\text{F.15})$$

We also note that the identity

$$\frac{1}{A-B} = \frac{1}{A} + \frac{1}{A}B\frac{1}{A-B} = \frac{1}{A} + \frac{1}{A-B}B\frac{1}{A} \quad (\text{F.16})$$

gives the following equations

$$G_{QQ}(E) = G_\Sigma^{(2)}(E) + G_\Sigma^{(2)}(E)U_{QQ}(E)G_{QQ}(E) \quad (\text{F.17})$$

$$= G_\Sigma^{(2)}(E) + G_{QQ}(E)U_{QQ}(E)G_\Sigma^{(2)}(E) \quad (\text{F.18})$$

comparing with the equation (F.14), we obtain

$$G_{QQ}(E)U_{QQ}(E) = G_\Sigma^{(2)}(E)T_c(E) \quad (\text{F.19})$$

$$U_{QQ}(E)G_{QQ}(E) = T_c(E)G_\Sigma^{(2)}(E) \quad (\text{F.20})$$

Substituting the above expression to equation (F.11), we obtain

$$T_{QQ}(E) = \Sigma(E) + \Sigma(E)G_\Sigma^{(2)}(E)\Sigma(E) + \left(1 + \Sigma(E)G_\Sigma^{(2)}(E)\right)T_c(E)\left(G_\Sigma^{(2)}(E)\Sigma(E) + 1\right) \quad (\text{F.21})$$

The first two terms are the disconnected diagrams and do not contribute to the  $T$ -matrix. The third term contains the factors  $1 + \Sigma(E)G_\Sigma^{(2)}(E)$  and  $G_\Sigma^{(2)}(E)\Sigma(E) + 1$  which are Moeller operators which make the bare propagator  $G_0^{(2)}(E)$  the dressed one  $G_\Sigma^{(2)}(E)$ . They therefore do not contribute to scattering and we drop them. The appropriate  $T$ -matrix we focus on is therefore contained in  $T_c(E)$  in the above equation. The identity (F.16) also gives the following Lippmann-Schwinger equation that  $T_c(E)$  satisfies

$$T_c(E) = \mathcal{U}_{QQ}(E) + \mathcal{U}_{QQ}(E)G_\Sigma^{(2)}(E)T_c(E) \quad (\text{F.22})$$

In the preceding discussion, we followed closely an article by Lee and Matsuyama [71].

## F.2 The Dispersion Relation and The Optical Theorem

In this section, we present another useful methods, the dispersion relation [72, 73, 74] and the optical theorem [75, 76]. The dispersion relation is based only on analyticities of the  $S$ -matrix and all it need is the spectral function which enables us to discuss some physics in a model-independent manner. The optical theorem states that an imaginary part of the  $T$ -matrix is proportional to inclusive scattering cross section. It is this very imaginary part of the  $T$ -matrix which we need to input into the dispersion relation, that is, it is a spectral function. Note also that the optical theorem most manifestly relates the leading behavior of the spectral function with the phase space of the system. In this section, we consider two-body problem for simplicity.

### F.2.1 The Dispersion Relation

Since the  $S$ -matrix and the  $T$ -matrix have the same analyticities, and that we are interested in poles of the  $S$ -matrix, we consider the  $T$ -matrix instead of the  $S$ -matrix. Analyticities of the  $T$ -matrix are most manifestly represented in the form of the spectral decomposition.

$$T(E) = V + \sum_b \frac{V|b\rangle\langle b|V}{E - E_b} + \int d\mathbf{p} \frac{V|\mathbf{p}\rangle^{(+)(+)}\langle\mathbf{p}|V}{E - E_p} \quad (\text{F.23})$$

where  $|b\rangle$  and  $|\mathbf{p}\rangle^{(+)}$  are bound state and scattering state vectors of the full Hamiltonian.

$$H|b\rangle = E_b|b\rangle \quad (\text{F.24})$$

$$H|\mathbf{p}\rangle^{(+)} = E_p|\mathbf{p}\rangle^{(+)} \quad (\text{F.25})$$

The  $T$ -matrix obviously has poles at the energies corresponding to bound states and branch cut starting from the energy corresponding to the two-body threshold. A function which has such analyticities satisfies the so called dispersion relation.

$$\begin{aligned} T(E_0) &= \frac{1}{\pi} \int_0^\infty dE \frac{\text{Im}T(E)}{E - E_0 - i\epsilon} \\ &= \frac{\mathcal{P}}{\pi} \int_0^\infty dE \frac{\text{Im}T(E)}{E - E_0} + i \int_0^\infty dE \text{Im}T(E) \delta(E - E_0) \\ &= \frac{\mathcal{P}}{\pi} \int_0^\infty dE \frac{\text{Im}T(E)}{E - E_0} + i \text{Im}T(E_0) \end{aligned} \quad (\text{F.26})$$

where we have used the fact that

$$\frac{1}{E - E_0 - i\epsilon} = \mathcal{P} \frac{1}{E - E_0} + i\pi \delta(E - E_0) \quad (\text{F.27})$$

The last equation of the dispersion relation shows that the real part of the  $T$ -matrix can be calculated as integration of its imaginary part. The imaginary part of the  $T$ -matrix is therefore called the spectral function. In theoretical calculations in practice, it is often hard to obtain a full spectral function and the dispersive part diverges due to its imperfect form of the spectral function. In such cases, we perform 'subtraction' to obtain finite expressions of the  $T$ -matrix. For example, once subtracted form of the dispersion relation is, for example, given as below

$$T(E_0) = T(0) + E_0 \frac{\mathcal{P}}{\pi} \int_0^\infty dE \frac{1}{E} \frac{\text{Im}T(E)}{E - E_0} + i \text{Im}T(E_0) \quad (\text{F.28})$$

### F.2.2 The Optical Theorem

The optical theorem states that the imaginary part of the  $T$ -matrix is proportional to the cross section. We discuss the optical theorem for a single channel as well as generalized multi-channel case.

#### A Single-Channel Case

The single-channel optical theorem which is identical to the unitary nature of the  $S$ -matrix is derived as follows. Recall that the  $T$ -matrix satisfies the Lippmann-Schwinger equation

$$T(E) = V + V G_0(E) T(E) = V + T(E) G_0(E) V(E) \quad (\text{F.29})$$

$T - T^\dagger$  is calculated as

$$\begin{aligned} T(E) - T^\dagger(E) &= (V + V G_0(E) T(E)) - (V^\dagger + V^\dagger G_0^\dagger(E) T^\dagger(E)) \\ &= V (G_0(E) - G_0^\dagger(E)) T + V G_0^\dagger(E) (T(E) - T^\dagger(E)) \\ \Rightarrow T(E) - T^\dagger(E) &= \frac{1}{1 - V G_0^\dagger(E)} V (G_0(E) - G_0^\dagger(E)) T(E) \end{aligned}$$

where we have used the Hermiticity of the interaction  $V$  which gives the following equation

$$T(E) - T^\dagger(E) = T^\dagger(E) (G_0(E) - G_0^\dagger(E)) T(E) \quad (\text{F.30})$$



$$\text{Im}(\text{diagram}) = \int d\Pi_2 \left| \text{diagram} \right|^2 \delta\left(E - \frac{p^2}{2\mu}\right)$$

Figure F.1: A diagrammatic representation of the single-channel optical theorem

The factor in the center of the equation on the right-hand side gives, after taking matrix element, a condition that the momentum in intermediate state to be that of the external one.

Inserting the completeness relation of the plane-wave states and taking the matrix element of the above equation gives

$$\begin{aligned} 2i \text{Im}T(E\mathbf{p}\mathbf{p}') &= \int d\mathbf{p}'' T^*(E\mathbf{p}\mathbf{p}'') 2i \text{Im}G_0(E\mathbf{p}'') T(E\mathbf{p}''\mathbf{p}') \\ \Rightarrow \text{Im}T(E\mathbf{p}\mathbf{p}') &= -\pi \int d\mathbf{p}'' T^*(E\mathbf{p}\mathbf{p}'') \delta\left(E - \frac{p''^2}{2\mu}\right) T(E\mathbf{p}''\mathbf{p}') \end{aligned}$$

The second equation represents that  $\text{Im}T$  is proportional to absolute value of the on-shell  $T$ -matrix  $|T|^2$  which is why  $\text{Im}T$  is called the spectral function.

### Two-Channels Case

A generalization to multi-channel case is easily done with the Feshbach projection method. We consider a system in which two channels are coupled for simplicity. Sandwiching the equation (F.30) with  $P$  from both sides, we obtain an obvious equation

$$\begin{aligned} T_{PP}(E) - T_{PP}^\dagger(E) &= T_{PP}^\dagger(E) \left( G_0^P(E) - G_0^{P\dagger}(E) \right) T_{PP}(E) \\ &+ T_{PQ}^\dagger(E) \left( G_0^Q(E) - G_0^{Q\dagger}(E) \right) T_{QP}(E) \end{aligned} \quad (\text{F.31})$$

The inelastic operators  $T_{PQ}(E)$  can be re-written as

$$T_{PQ}^\dagger(E) = \left( 1 + T_{PP}^\dagger(E) G_0^{P\dagger}(E) \right) V_{PQ} \left( 1 + G_0^{Q\dagger}(E) T_Q^\dagger(E) \right) \quad (\text{F.32})$$

$$T_{QP}(E) = \left( 1 + T_Q(E) G_0^Q(E) \right) V_{QP} \left( 1 + G_0^P(E) T_{PP}(E) \right) \quad (\text{F.33})$$

See appendix ( ref appendix ) for the derivation. The equation (ref eq) is therefore rewritten as

$$\begin{aligned} T_{PP}(E) - T_{PP}^\dagger(E) &= T_{PP}^\dagger(E) \left( G_0^P(E) - G_0^{P\dagger}(E) \right) T_{PP}(E) \\ &+ \left( 1 + T_{PP}^\dagger(E) G_0^{P\dagger}(E) \right) V_{PQ} \left( 1 + G_0^{Q\dagger}(E) T_Q^\dagger(E) \right) \\ &\times \left( G_0^Q(E) - G_0^{Q\dagger}(E) \right) \\ &\times \left( 1 + T_Q(E) G_0^Q(E) \right) V_{QP} \left( 1 + G_0^P(E) T_{PP}(E) \right) \end{aligned} \quad (\text{F.34})$$

We have decomposed the spectral function into two parts, one is those whose final states are the  $P$ -channel and the other whose final state is the  $Q$ -channel. The first factor in the second term indicates that the left-most interaction is proportional to the full  $T$ -matrix  $T_{PP}(E)$  or not. The term whose left-most interaction is not proportional to  $T_{PP}(E)$  is proportional to interaction which couples  $P$ -channel to  $Q$ -channel.

In chapter F, we apply this multi-channel optical theorem to analyze the two-body and three-body coupled-channels system.

$$\begin{aligned}
\text{Im} \left( \text{diagram} \right) &= \text{diagram} + \text{diagram} \\
&= \int d\Pi_2 \left| \text{diagram} \right|^2 \delta \left( E - \frac{p^2}{2\mu} \right) + \int d\Pi'_2 \left| \text{diagram} \right|^2 \delta \left( E - \Delta - \frac{p'^2}{2\mu'} \right) \\
&= \text{diagram} \\
&\quad + \left( 1 + \text{diagram} \right) \times \left( 1 + \text{diagram} \right) \div \left( \text{diagram} + 1 \right) \times \left( \text{diagram} + 1 \right) \\
&= \int d\Pi_2 \left| \text{diagram} \right|^2 \delta \left( E - \frac{p^2}{2\mu} \right) + \int d\Pi'_2 \left| \left( 1 + \text{diagram} \right) \times \left( 1 + \text{diagram} \right) \right|^2 \delta \left( E - \Delta - \frac{p'^2}{2\mu'} \right) \\
T_Q &= \text{diagram} = \text{diagram} + \text{diagram} + \dots \quad T_{PP} = \text{diagram} \quad T_{PQ} = \text{diagram}
\end{aligned}$$

Figure F.2: A diagrammatic representation of the two-channel optical theorem

$$\text{Im} \left( \text{diagram} \right) = \text{diagram} + \left( 1 + \text{diagram} \right) \overset{T_P}{\text{diagram}} \left( \text{diagram} + 1 \right)$$

Figure F.3: A diagrammatic representation of the coupled-channels optical theorem

### F.3 The Two-Body and Three-Body Coupled-Channels Optical Theorem

Having got rid of the disconnected parts which do not contribute to scattering between  $\psi_3\phi_3$ , our next task is to write down the optical theorem for  $T_c(E)$  and estimate the leading behavior of it near the threshold.  $T_c(E)$  and  $T_c^\dagger(E)$  satisfies the Lippmann-Schwinger equations

$$T_c(E) = \mathcal{U}_{QQ}(E) + \mathcal{U}_{QQ}(E) G_\Sigma^{(2)}(E) T_c(E) \quad (\text{F.35})$$

$$T_c^\dagger(E) = \mathcal{U}_{QQ}^\dagger(E) + \mathcal{U}_{QQ}^\dagger(E) G_\Sigma^{(2)\dagger}(E) T_c^\dagger(E) \quad (\text{F.36})$$

Subtracting the second equation from the first one, we obtain

$$\begin{aligned}
T_c(E) - T_c^\dagger(E) &= T_c^\dagger(E) \left( G_\Sigma^{(2)}(E) - G_\Sigma^{(2)\dagger}(E) \right) T_c(E) \\
&\quad + \left( 1 + T_c^\dagger(E) G_\Sigma^{(2)\dagger}(E) \right) \left( \mathcal{U}_{QQ}(E) - \mathcal{U}_{QQ}^\dagger(E) \right) \left( G_\Sigma^{(2)}(E) T_c(E) + 1 \right)
\end{aligned} \quad (\text{F.37})$$

The second term gives the spectral function whose final state is the three-body state while the first term contains spectrum whose final states are both of two-body and three-body states. In figure F.3, we show a diagrammatic representation of the equation (F.37).

$$\begin{aligned}
G_{\Sigma}^{(2)}(E) - G_{\Sigma}^{(2)\dagger}(E) &= G_0^{(2)}(E) - G_0^{(2)\dagger}(E) + \left(G_0^{(2)}(E) - G_0^{(2)\dagger}(E)\right) \Sigma(E) G_{\Sigma}^{(2)}(E) \\
&+ G_0^{(2)\dagger}(E) \left(\Sigma(E) - \Sigma^{\dagger}(E)\right) G_{\Sigma}^{(2)}(E) \\
&+ G_0^{\dagger}(E) \Sigma^{\dagger}(E) \left(G_{\Sigma}^{(2)}(E) - G_{\Sigma}^{(2)\dagger}(E)\right) \\
G_{\Sigma}^{(2)}(E) - G_{\Sigma}^{(2)\dagger}(E) &= \frac{1}{1 - G_0^{(2)\dagger}(E) \Sigma^{\dagger}(E)} \left( \left(G_0^{(2)}(E) - G_0^{(2)\dagger}(E)\right) \left(\Sigma(E) G_{\Sigma}^{(2)}(E) + 1\right) \right. \\
&+ \left. G_0^{(2)}(E) \left(\Sigma(E) - \Sigma^{\dagger}(E)\right) G_{\Sigma}^{(2)\dagger}(E) \right) \\
G_{\Sigma}^{(2)}(E) - G_{\Sigma}^{(2)\dagger}(E) &= \left(1 + G_{\Sigma}^{(2)\dagger}(E) \Sigma^{\dagger}(E)\right) \left(G_0^{(2)}(E) - G_0^{(2)\dagger}(E)\right) \left(\Sigma(E) G_{\Sigma}^{(2)}(E) + 1\right) \\
&+ G_{\Sigma}^{(2)\dagger}(E) \left(\Sigma(E) - \Sigma^{\dagger}(E)\right) G_{\Sigma}^{(2)}(E) \tag{F.38}
\end{aligned}$$

$$\begin{aligned}
T_{QQ}(E) &= (\mathcal{U}_{QQ}(E) + \Sigma(E)) + (\mathcal{U}_{QQ}(E) + \Sigma(E)) G_{QQ}(E) (\mathcal{U}_{QQ}(E) + \Sigma(E)) \\
&= \mathcal{U}_{QQ}(E) + \mathcal{U}_{QQ}(E) G_{QQ}(E) \mathcal{U}_{QQ}(E) + \Sigma(E) + \Sigma(E) G_{QQ}(E) \Sigma(E) \\
&+ \mathcal{U}_{QQ}(E) G_{QQ}(E) \Sigma(E) + \Sigma(E) G_{QQ}(E) \mathcal{U}_{QQ}(E) \tag{F.39}
\end{aligned}$$

$$\begin{aligned}
T_c(E) - T_c^{\dagger}(E) &= \left(\mathcal{U}_{QQ}(E) - \mathcal{U}_{QQ}^{\dagger}(E)\right) \left(1 + G_{\Sigma}^{(2)}(E) T_c(E)\right) \\
&+ \mathcal{U}_{QQ}^{\dagger}(E) \left(G_{\Sigma}^{(2)}(E) - G_{\Sigma}^{(2)\dagger}(E)\right) T_c(E) \\
&+ \mathcal{U}_{QQ}^{\dagger}(E) G_{\Sigma}^{\dagger}(E) \left(T_c(E) - T_c^{\dagger}(E)\right) \\
\Rightarrow T_c(E) - T_c^{\dagger}(E) &= T_c^{\dagger}(E) \left(G_{\Sigma}^{(2)}(E) - G_{\Sigma}^{(2)\dagger}(E)\right) T_c(E) \\
&+ \left(1 + T_c^{\dagger}(E) G_{\Sigma}^{(2)\dagger}(E)\right) \left(\mathcal{U}_{QQ}(E) - \mathcal{U}_{QQ}^{\dagger}(E)\right) \left(G_{\Sigma}^{(2)}(E) T_c(E) + 1\right) \tag{F.40}
\end{aligned}$$

$$\begin{aligned}
&T_c(E) - T_c^{\dagger}(E) \\
&= T_c^{\dagger}(E) \left(G_{\Sigma}^{(2)}(E) - G_{\Sigma}^{(2)\dagger}(E)\right) T_c(E) \\
&+ \left(1 + T_c^{\dagger}(E) G_{\Sigma}^{(2)\dagger}(E)\right) \left(\mathcal{U}_{QQ}(E) - \mathcal{U}_{QQ}^{\dagger}(E)\right) \left(G_{\Sigma}^{(2)}(E) T_c(E) + 1\right) \\
&= T_c^{\dagger}(E) \left(1 + G_{\Sigma}^{(2)\dagger}(E) \Sigma^{\dagger}(E)\right) \left(G_0^{(2)}(E) - G_0^{(2)\dagger}(E)\right) \left(\Sigma(E) G_{\Sigma}^{(2)}(E) + 1\right) T_c(E) \\
&+ T_c^{\dagger}(E) G_{\Sigma}^{(2)\dagger}(E) \left(\Sigma(E) - \Sigma^{\dagger}(E)\right) G_{\Sigma}^{(2)}(E) T_c(E) \\
&+ \left(1 + T_c^{\dagger}(E) G_{\Sigma}^{(2)\dagger}(E)\right) \left(\mathcal{U}_{QQ}(E) - \mathcal{U}_{QQ}^{\dagger}(E)\right) \left(G_{\Sigma}^{(2)}(E) T_c(E) + 1\right) \\
&= T_c^{\dagger}(E) \left(1 + G_{\Sigma}^{(2)\dagger}(E) \Sigma^{\dagger}(E)\right) \left(G_0^{(2)}(E) - G_0^{(2)\dagger}(E)\right) \left(\Sigma(E) G_{\Sigma}^{(2)}(E) + 1\right) T_c(E) \\
&+ T_c^{\dagger}(E) G_{\Sigma}^{(2)\dagger}(E) V^{(23)} \left(G_0^{(3)}(E) - G_0^{(3)\dagger}(E)\right) V^{(32)} G_{\Sigma}^{(2)}(E) T_c(E) \\
&+ \left(1 + T_c^{\dagger}(E) G_{\Sigma}^{(2)\dagger}(E)\right) V^{(23)} G_0^{(3)}(E) \left(T_P(E) - T_P^{\dagger}(E)\right) \\
&\times G_0^{(3)}(E) V^{(32)} \left(G_{\Sigma}^{(2)}(E) T_c(E) + 1\right)
\end{aligned}$$

We now further decompose the spectrum in equation (F.37) into two-body and three-body channels as follows.  $G_{\Sigma}^{(2)}(E)$  satisfies the Dyson-Schwinger equations

$$G_{\Sigma}^{(2)}(E) = G_0^{(2)}(E) + G_0^{(2)}(E) \Sigma(E) G_{\Sigma}^{(2)}(E) \tag{F.41}$$

$$G_{\Sigma}^{(2)\dagger}(E) = G_0^{(2)\dagger}(E) + G_0^{(2)\dagger}(E) \Sigma^{\dagger}(E) G_{\Sigma}^{(2)\dagger}(E) \tag{F.42}$$

Subtracting the second equation from the first one, we have

$$\begin{aligned} G_{\Sigma}^{(2)}(E) - G_{\Sigma}^{(2)\dagger}(E) &= \left(1 + G_{\Sigma}^{(2)\dagger}(E) \Sigma^{\dagger}(E)\right) \left(G_0^{(2)}(E) - G_0^{(2)\dagger}(E)\right) \left(\Sigma(E) G_{\Sigma}^{(2)}(E) + 1\right) \\ &+ G_{\Sigma}^{(2)\dagger}(E) \left(\Sigma(E) - \Sigma^{\dagger}(E)\right) G_{\Sigma}^{(2)}(E) \end{aligned} \quad (\text{F.43})$$

The first term corresponds to a scattering process whose final state is two-body channel while the second term is those whose final state is three-body channel. Substituting the expression in equation (F.43), equation (F.37) becomes

$$\begin{aligned} &T_c(E) - T_c^{\dagger}(E) \\ &= T_c^{\dagger}(E) \left(1 + G_{\Sigma}^{(2)\dagger}(E) \Sigma^{\dagger}(E)\right) \left(G_0^{(2)}(E) - G_0^{(2)\dagger}(E)\right) \left(\Sigma(E) G_{\Sigma}^{(2)}(E) + 1\right) T_c(E) \\ &+ T_c^{\dagger}(E) G_{\Sigma}^{(2)\dagger}(E) V^{(23)} \left(G_0^{(3)}(E) - G_0^{(3)\dagger}(E)\right) V^{(32)} G_{\Sigma}^{(2)}(E) T_c(E) \\ &+ \left(1 + T_c^{\dagger}(E) G_{\Sigma}^{(2)\dagger}(E)\right) V^{(23)} G_0^{(3)}(E) \left(T_P(E) - T_P^{\dagger}(E)\right) \\ &\times G_0^{(3)}(E) V^{(32)} \left(G_{\Sigma}^{(2)}(E) T_c(E) + 1\right) \end{aligned}$$

Noting that the identity  $T_P(E) - T_P^{\dagger}(E) = T_P^{\dagger}(E) \left(G_0^{(3)}(E) - G_0^{(3)\dagger}(E)\right) T_P(E)$  holds, the last term becomes

$$\begin{aligned} &\left(1 + T_c^{\dagger}(E) G_{\Sigma}^{(2)\dagger}(E)\right) V^{(23)} G_0^{(3)}(E) T_P^{\dagger}(E) \left(G_0^{(3)}(E) - G_0^{(3)\dagger}(E)\right) \\ &\times T_P(E) G_0^{(3)}(E) V^{(32)} \left(G_{\Sigma}^{(2)}(E) T_c(E) + 1\right) \end{aligned} \quad (\text{F.44})$$

The full explicit expression for  $T_c(E) - T_c^{\dagger}(E)$  is therefore,

$$\begin{aligned} &T_c(E) - T_c^{\dagger}(E) \\ &= T_c^{\dagger}(E) \left(1 + G_{\Sigma}^{(2)\dagger}(E) \Sigma^{\dagger}(E)\right) \left(G_0^{(2)}(E) - G_0^{(2)\dagger}(E)\right) \left(\Sigma(E) G_{\Sigma}^{(2)}(E) + 1\right) T_c(E) \\ &+ T_c^{\dagger}(E) G_{\Sigma}^{(2)\dagger}(E) V^{(23)} \left(G_0^{(3)}(E) - G_0^{(3)\dagger}(E)\right) V^{(32)} G_{\Sigma}^{(2)}(E) T_c(E) \\ &+ \left(1 + T_c^{\dagger}(E) G_{\Sigma}^{(2)\dagger}(E)\right) V^{(23)} G_0^{(3)\dagger}(E) T_P^{\dagger}(E) \left(G_0^{(3)}(E) - G_0^{(3)\dagger}(E)\right) \\ &\times T_P(E) G_0^{(3)}(E) V^{(32)} \left(G_{\Sigma}^{(2)}(E) T_c(E) + 1\right) \end{aligned} \quad (\text{F.45})$$

Diagrammatic representation of the above optical theorem is given in figure F.4.

The decomposition we have performed is most intuitively understood in the form of the diagrammatic representation of the equation in figure F.4. The first term gives spectrum corresponding to scattering processes whose final states are  $\psi_3\phi_3$  two-body state while the rest correspond to scattering processes whose final states are  $\phi_1\phi_2\phi_3$  three-body states. The factor in the first term  $(1 + G_{\Sigma}^{(2)}(E) \Sigma(E))$  is the Möller which projects the bare  $\psi_3$  state  $|\mathbf{p}\rangle$  into dressed one  $|\mathbf{p}\rangle^{\Sigma}$  which satisfy

$$H_0^Q |\mathbf{p}\rangle = E_p |\mathbf{p}\rangle \quad \text{and} \quad \left(H_0^Q + \Sigma(E)\right) |\mathbf{p}\rangle^{\Sigma} = E_p |\mathbf{p}\rangle^{\Sigma} \quad (\text{F.46})$$

respectively. The latter eigenstate is expressed with former one as below

$$|\mathbf{p}\rangle^{\Sigma} = \left(1 + G_{\Sigma}^{(2)}(E + i\epsilon) \Sigma(E + i\epsilon)\right) |\mathbf{p}\rangle = i\epsilon G_{\Sigma}^{(2)}(E + i\epsilon) |\mathbf{p}\rangle \quad (\text{F.47})$$

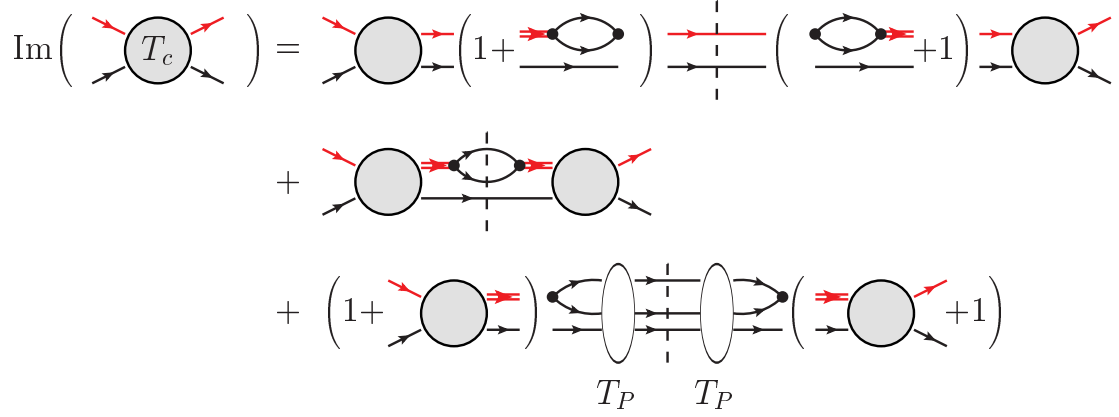


Figure F.4: A diagrammatic representation of the coupled-channels optical theorem

which satisfies

$$\left(G_{\Sigma}^{(2)}(E)\right)^{-1}|\mathbf{p}\rangle^{\Sigma} = \left(E + i\epsilon - H_0^Q - \Sigma(E)\right)i\epsilon G_{\Sigma}^{(2)}(E + i\epsilon)|\mathbf{p}\rangle = i\epsilon|\mathbf{p}\rangle = 0 \quad (\text{F.48})$$

and is equivalent to equation (F.46). The second term in the figure F.4 corresponds to scattering processes which contain no bare interactions in the three-body channel which we have been denoting  $V_1, V_2, V_3$  respectively. Note that there are no “disconnected” term such as  $V^{(23)}G_0^{(3)}(E)V_{32}$  since we have dropped such terms in the previous subsection. The last term in figure F.4 represents the scattering processes whose final states are the three-body ones which contain the bare interactions in the three-body channel. We can see that it is composed of two parts, that is, the part whose initial state is proportional to the full  $T$ -matrix  $T_c(E)$  and the part which is not.

## F.4 The Leading Behavior of The Spectral Function and The $S$ -Matrix Near The Threshold

Having introduced the two-body and three-body coupled-channels optical theorem and its decomposition to each channel, we now turn to examining the leading behavior of the spectral function near the threshold. The self energy of  $\psi_3$  induced by the coupling to the  $\phi_1\phi_2$  two-body  $s$ -wave state has in general following form for energies close to the threshold.

$$\Sigma(E) = c_0 + c_1 i\sqrt{E} + \mathcal{O}(E) \quad (\text{F.49})$$

where we have suppressed the index of momentum by assuming  $\psi_3$  is in the rest frame. Since two-body and three-body thresholds are degenerate, we subtract the constant term using the counter term to obtain the dressed Green function  $G_{\Sigma}^{(2)}(E)$  which therefor behaves as below

$$G_{\Sigma}^{(2)}(E) \sim \frac{1}{E + i\epsilon - c_1 i\sqrt{E} + i\epsilon} \quad \text{as } E \sim 0 \quad (\text{F.50})$$

The crucial point is that for energies close to the threshold, in this case, when  $E \sim 0$  the self-energy part dominates the  $(G_0(E))^{-1} = E$  part and thus the dressed propagator and its imaginary part behaves

$$G_{\Sigma}^{(2)}(E) \sim \frac{1}{\sqrt{E}} \quad \text{and} \quad \text{Im}G_{\Sigma}^{(2)}(E) \sim \frac{1}{\sqrt{E}} \quad \text{as } E \sim 0 \quad (\text{F.51})$$

We will see how this behavior of the dressed Green function affects the imaginary part of the  $T$ -matrix in the following. We examine a leading behavior of each terms in equation (F.45) with respect to energy.

The leading behavior of the first term in equation (F.45) corresponding to scattering processes whose final states are the  $\psi_3\phi_3$  two-body state can be estimated as follows

$$\begin{aligned} & \int_0^\infty q_3''^2 dq_3'' T_c^* (Eq_3 q_3'') \left( 1 + G_\Sigma^{(2)*} (Eq_3'') \Sigma^* (Eq_3'') \right) (-2\pi i) \delta \left( E - \frac{q_3''^2}{2\nu_3} \right) \\ & \times \left( \Sigma (Eq_3'') G_\Sigma^{(2)} (Eq_3'') + 1 \right) T_c (Eq_3'' q_3') \end{aligned} \quad (\text{F.52})$$

The factors in the above equation become zero as the two-body state goes on-shell as shown below

$$\begin{aligned} \Sigma (Eq_3) G_\Sigma^{(2)} (Eq_3'') + 1 &= \left( G_0^{(2)} (Eq_3) \right)^{-1} G_\Sigma^{(2)} (Eq_3) \\ &= \frac{E - \frac{q_3^2}{2\nu_3}}{E - \frac{q_3^2}{2\nu_3} - ic_1 \sqrt{E - \frac{q_3^2}{2\nu_3}}} \rightarrow 0 \quad \text{as} \quad E \rightarrow \frac{q_3^2}{2\nu_3} \end{aligned} \quad (\text{F.53})$$

The first term in equation (F.45) therefore vanishes. In case of two-body and three-body thresholds are degenerate, the spectrum for  $\psi_3\phi_3$  two-body state vanishes.

The second term in equation (F.45) is

$$\int q_3''^2 dq_3'' T_c^* (Eq_3 q_3'') G_\Sigma^{(2)} (Eq_3'') \text{Im} \Sigma (Eq_3'') G_\Sigma^{(2)} (Eq_3'') T_c (Eq_3'' q_3') \quad (\text{F.54})$$

and can be estimated as follows leveraging the hyperspherical coordinates

$$\begin{aligned} & \int q_3'^2 dq_3' q_3''^2 dq_3'' p_3''^2 dp_3'' q_3'''^2 dq_3''' T_c^* (Eq_3 q_3') G_\Sigma^{(2)*} (Eq_3') \Gamma (q_3' q_3'' p_3'') \\ & \times (-2\pi i) \delta \left( E - \frac{q_3'^2}{2M_3} - \frac{p_3''^2}{2\mu_3} \right) \Gamma (q_3'' p_3'' q_3''') G_\Sigma^{(2)} (Eq_3''') T_c (Eq_3''' q_3''''') \\ & = \int q_3'^2 dq_3' p_3''^2 dp_3'' T_c^* (Eq_3 q_3') G_\Sigma^{(2)*} (Eq_3') \Gamma (q_3' p_3'') \\ & \times (-2\pi i) \delta \left( E - \frac{q_3'^2}{2M_3} - \frac{p_3''^2}{2\mu_3} \right) \Gamma (q_3' p_3'') G_\Sigma^{(2)} (Eq_3') T_c (Eq_3' q_3''''') \\ & \sim \int \rho^5 d\rho T_c^* (Eq_3 \rho) G_\Sigma^{(2)*} (E\rho) \Gamma (\rho) (-2\pi i) \delta (E - \rho^2/m) \Gamma (\rho) G_\Sigma^{(2)} (E\rho) T_c (E\rho q_3''''') \\ & \sim k^5 \frac{1}{k} \frac{1}{k} \frac{1}{k} \Theta(k) = k^2 \Theta(k) \sim E \Theta(E) \end{aligned} \quad (\text{F.55})$$

It can be shown that the third term in the generalized optical theorem which is induced by the interactions in the three-body state gives higher order in  $k$ . The leading behavior of  $\text{Im}T$  is therefore  $k^2$ .

$$\text{Im}T (Eqq') \sim k^2 \quad \text{as} \quad k \sim 0 \quad (\text{F.56})$$

Noting that  $k^2$  is proportional to total energy  $E$ , we can also express it as

$$\text{Im}T (Eqq') \sim E \quad \text{as} \quad E \sim 0 \quad (\text{F.57})$$

the leading behavior of  $\text{Im} (T (Eqq'))^{-1}$  is also  $E$

$$\text{Im} (T (Eqq'))^{-1} \sim c_1 E \quad (\text{F.58})$$

We now leverage the dispersion relation which  $(T(Eqq'))^{-1}$  satisfies. Its explicit expression is,

$$(T(Eqq'))^{-1} = \frac{1}{\pi} \int_0^\infty dE' \frac{\text{Im}(T(E'qq'))^{-1}}{E' - E - i\epsilon} \quad (\text{F.59})$$

What we want to know is how inverse of the  $T$ -matrix behaves near the threshold. We therefore perform one subtraction (see section F.2) and introduce a cut-off  $\Lambda$  to regularize the integral. The cut-off is taken to be an upper bound in which the expression (F.57) is valid. The leading behavior of  $T^{-1}(Eqq')$  is therefore evaluated to be

$$T^{-1}(E) = c_0 + \frac{1}{\pi} E \int_0^\Lambda dE' \frac{1}{E'} \frac{c_1 E'}{E' - E - i\epsilon} \sim c_0 - c_1 E \log(-E) \quad \text{as } E \sim 0 \quad (\text{F.60})$$

## F.5 Pole Behavior Near The Threshold

In this section, we perform a close analysis of the pole trajectories near the threshold which is governed by the equation (F.60)

$$c_0 - c_1 E \log(-E) = 0 \Rightarrow \frac{c_0}{c_1} - E \log(-E) = 0 \Rightarrow g - E \log(-E) = 0 \quad (\text{F.61})$$

where  $g$  is a dimensionless coupling constant. For notational simplicity, we let  $-E = re^{i\theta}$  and rewrite the above equation as below

$$g + r \{(\cos \theta \log r - \theta \sin \theta) + i(\sin \theta \log r + \theta \cos \theta)\} = 0 \quad (\text{F.62})$$

Since the coupling constant  $g$  is real, the imaginary part vanishes to give a following constraint between  $r$  and  $\theta$

$$r(\sin \theta \log r + \theta \cos \theta) = 0 \quad (\text{F.63})$$

The equation we must solve is therefore,

$$g + r(\cos \theta \log r - \theta \sin \theta) = 0 \quad (\text{F.64})$$

$$r(\sin \theta \log r + \theta \cos \theta) = 0 \quad (\text{F.65})$$

equation (F.65) has two obvious solutions

$$r = 0 \text{ and } \theta = \text{any} \quad (\text{F.66})$$

$$\theta = 0 \text{ and } r = \text{any} \quad (\text{F.67})$$

which correspond to zero energy and non-zero energy bound states respectively. For  $\theta = 0$ , that is, for bound states, the equation (F.64) becomes

$$g + r \log r = 0 \quad (\text{F.68})$$

This equation has real solution  $r$  for  $g > 0$  and  $r \simeq 0$  when  $g \simeq 0$ . This is most obviously understood in a graphical manner as shown in figure F.5. The intersection between a curve  $r \log r$  and the horizontal line  $g = \text{const.}$  gives the binding energy in the form  $E_b = r$ . Intersection which gives  $r \gg 0$  is meaningless one since it is a solution far from threshold.

Other possible solutions are, those satisfy the following equation which is equivalent to equation (F.65)

$$r(\sin \theta \log r + \theta \cos \theta) = 0 \Rightarrow \log r = -\frac{\theta}{\tan \theta} \Rightarrow r = \exp\left(-\frac{\theta}{\tan \theta}\right) \quad (r \neq 0, \theta \neq 0) \quad (\text{F.69})$$

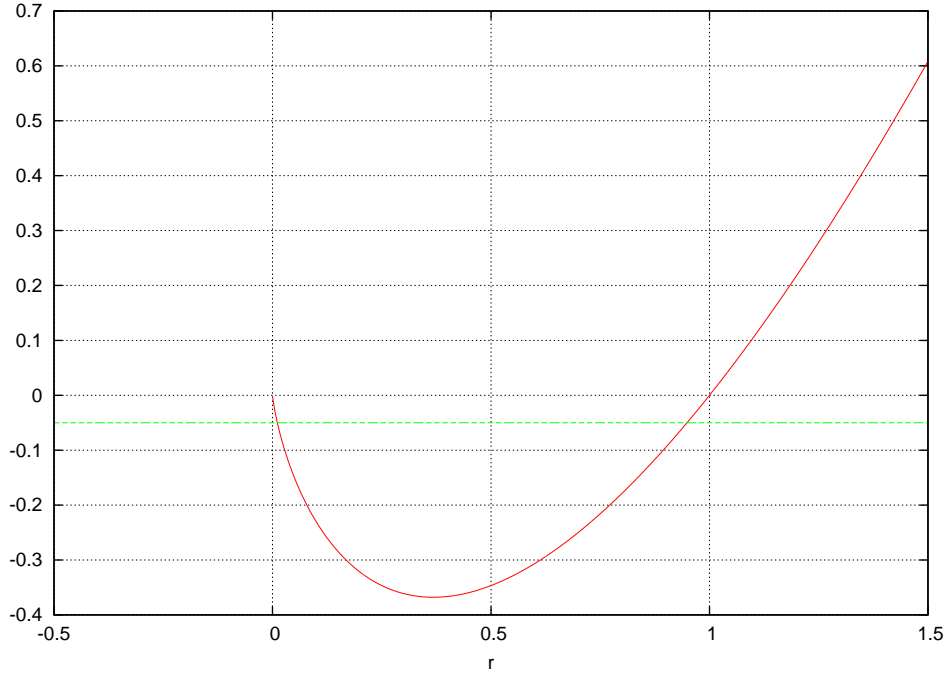


Figure F.5: A graphical expression of the equation (F.68). The  $x$  component of the intersection between the curve  $r \log r$  and horizontal line  $-g = \text{const.} < 0$  give the binding energy. The intersection on the right hand side is irrelevant since the equation (F.68) is valid for small  $r$ .

The third equation clearly determines the relation between  $r$  and  $\theta$  and therefore the shape of the trajectories. Since the equation (F.64), (F.65) is valid only for the energy regions close to the threshold  $E \ll 1$ , we require  $r \ll 1$  which restricts  $\theta$  to be

$$\theta \simeq n\pi \quad n = \pm 1, \pm 2, \dots \quad (\text{F.70})$$

Substituting the expression in equation (F.69) into (F.64) and with a bit of algebra, we obtain

$$g - \exp\left(-\frac{\theta}{\tan \theta}\right) \frac{\theta}{\sin \theta} = 0 \quad (\text{F.71})$$

This equation might also be the easiest to understand in a graphical manner (see figure F.5). The intersections between  $\exp(\theta/\tan \theta) \theta/\sin \theta$  and the horizontal line  $g = \text{const.}$  gives the argument  $\theta$ . When  $g$  approaches zero from a negative sign, infinite number of poles lying on each Riemann surfaces approach threshold and they eventually merge when  $g = 0$  then as  $g$  gradually become bigger  $g > 0$ , each poles goes away from threshold on each Riemann surfaces except the one which goes on through the negative real axis to become bound state.

As we mentioned earlier in this section, in case of single-channel two-body  $s$ -wave scattering, pole of the  $S$ -matrix approaches to threshold which we take to be the origin on the complex momentum plane, from the negative imaginary axis, going upward to become bound state. This can be clearly seen in the effective range expansion of the  $T$ -matrix [67]

$$T_s(Eqq') = \frac{1}{-\frac{1}{a} + \frac{r}{2}p^2 + \dots - ip} \simeq \frac{1}{-\frac{1}{a} - ip} \quad (\text{F.72})$$

The  $S$ -matrix pole trajectory close to threshold is therefore determined only by one parameter, namely the scattering length  $a$ . In  $\phi_1\phi_2\phi_3 - \psi_3\phi_3$  system, a same circumstances occur. The poles



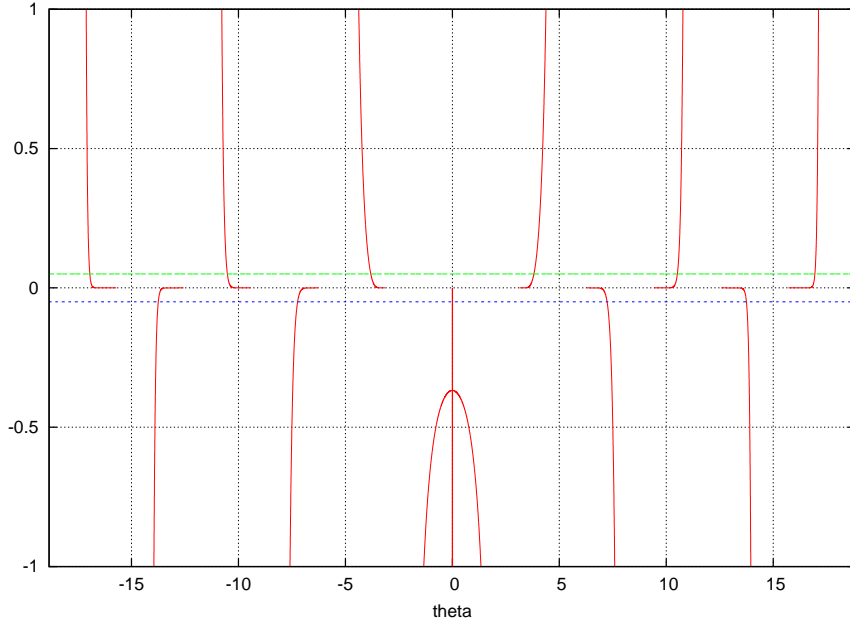


Figure F.6: The  $x$  component of the intersections between a curve  $-\exp\left(-\frac{\theta}{\tan\theta}\right)\frac{\theta}{\sin\theta}$  and horizontal line  $-g = \text{const.}$  give argument of the  $S$ -matrix poles. We can see that for  $g > 0$ , the equation has a solution  $\theta = 0$  which corresponds to a bound state. As  $g$  approaches zero from negative side, poles approach the threshold from the first and the fourth quadrant of the unphysical complex energy sheets and they eventually merge at threshold when  $g = 0$ . As we gradually increase  $g$  from zero, poles scatter away into the second and the third quadrant of the unphysical complex energy sheet except the one that becomes a bound state.

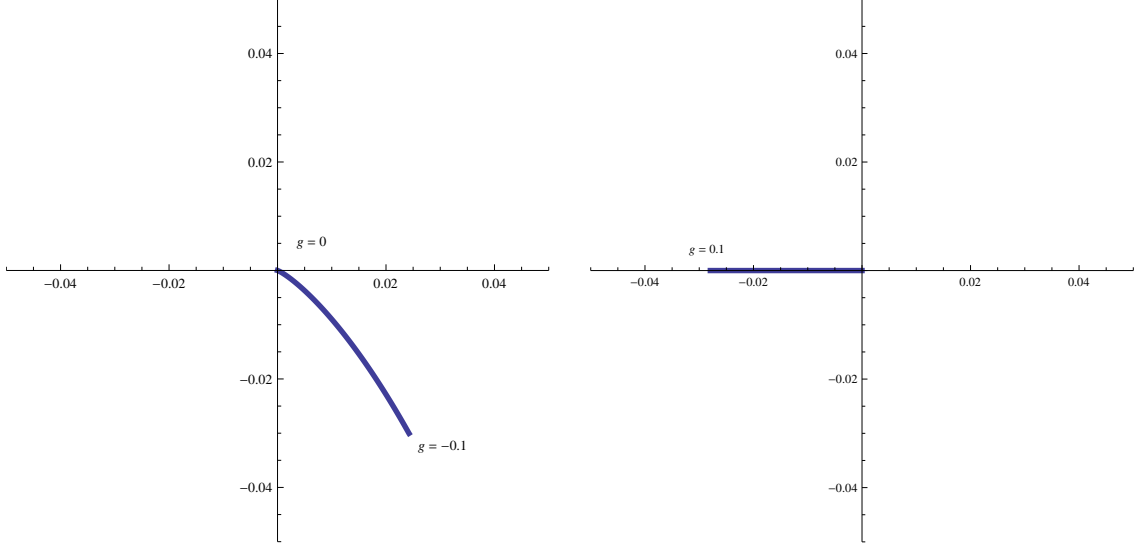


Figure F.7: The  $S$ -matrix pole trajectories characterized by (F.74) which lie on the relevant complex energy sheets are shown.

of the  $S$ -matrix in the two-body and three-body coupled-channels system satisfy the equation (F.61)

$$g - E \log(-E) = 0 \quad (\text{F.73})$$

We can see that for poles very close to threshold, trajectories of poles are determined by a single parameter  $g$ .  $E_p$  in the above equation can be expressed with the so-called Lambert  $W$  function  $W(E)$  as below

$$E_p = \frac{g}{W(-g)} \quad (\text{F.74})$$

The Lambert  $W$  function  $W(z)$  is a multi-valued function and whose definition is

$$z = W(z) e^{W(z)} \quad (\text{F.75})$$

The physical pole trajectory is given by one of branch often referred to  $W_{-1}(x)$  which satisfies

$$W_{-1}(xe^x) = x \quad \text{for} \quad x \leq -1 \quad (\text{F.76})$$

The  $S$ -matrix pole trajectories very close to threshold is determined by equation (F.74), and are given in figure F.7. This behavior is universal in a sense that any pole trajectories which are generated in a degenerated two-body and three-body coupled-channels system lie on the same curve (F.74) as we showed in the previous chapter (see figure 4.3.2).

## F.6 Relation Between The Present Work and The Efimov States

We briefly discuss the relation between our work and the Efimov physics which is a characteristic phenomenon in quantum mechanical three-body (and more-body) physics.

It was Efimov [77, 78, 79, 80] who showed that in quantum mechanical three-body system, infinite number of arbitrarily shallow bound states appear when at least two of three interaction are tuned so that they form zero-energy bound states. The binding energies form geometrical series

$$E_{N+1}/E_N = e^{-2\pi/s_0} \quad (\text{F.77})$$

where  $s_0$  is a constant which is a solution of the following equation

$$s_0 \cosh \frac{\pi s_0}{2} = \frac{8}{\sqrt{3}} \sinh \frac{\pi s_0}{6} \quad (\text{F.78})$$

It is however, in a decade or so that the relation between the Efimov effect and the renormalization group limit cycle was revealed (see [81, 82, 83, 84, 85, 86, 87, 88, 89] and [50, 90] for a recent review). In the following, we will see how the Efimov physics and the system we investigated in this thesis are related, specifically, why we did not encounter the Efimov spectrum.

We consider  $\phi_1\phi_2\phi_3 - \psi_1\phi_1 - \psi_2\phi_2 - \psi_3\phi_3$  coupled-channels system. It is always possible to formally take effects induced by the coupling to the three-body state  $\phi_1\phi_2\phi_3$  into account as effective interactions in the  $\psi_1\phi_1 - \psi_2\phi_2 - \psi_3\phi_3$  coupled-channels problem. The Lippmann-Schwinger equation which the  $T$ -matrix satisfies is,

$$T(E) = V + VG(E)T(E) \quad (\text{F.79})$$

where, all quantities are now  $3 \times 3$  matrix whose indices correspond to each  $\psi_i\phi_i$  two-body channels.

It is shown by authors [82, 83, 84, 85, 86, 87, 88, 89] that in case of three identical bosons, the scattering equation between a pair of two-particles (they call it “dimeron”) and another particle satisfies the formally equivalent equation to (F.79) except that the equation is one-dimensional instead of  $3 \times 3$  and the Efimov spectrum does appear. Therefore, if we set all corresponding parameters equal in the  $\phi_1\phi_2\phi_3 - \psi_1\phi_1 - \psi_2\phi_2 - \psi_3\phi_3$  coupled-channels system, we expect the solution contains symmetric solution, that is, a solution they derived which manifests the Efimov effect. The logic is almost trivial as we will demonstrate it in the following.

Since all the corresponding parameters are set to equal,  $T(E)$  and  $V$  then has only two independent components (one is diagonal and the other is off-diagonal element), the  $T(E)$  and  $V$  in the Lippmann-Schwinger equation (F.79) is explicitly written as follows

$$T(E) = \begin{pmatrix} T_1(E) & T_2(E) & T_2(E) \\ T_2(E) & T_1(E) & T_2(E) \\ T_2(E) & T_2(E) & T_1(E) \end{pmatrix} \quad V = \begin{pmatrix} V_1 & V_2 & V_2 \\ V_2 & V_1 & V_2 \\ V_2 & V_2 & V_1 \end{pmatrix} \quad (\text{F.80})$$

The  $T(E)$  and so is the Lippmann-Schwinger equation (F.79) is then diagonalized as

$$U^\dagger T(E) U = \begin{pmatrix} T_1(E) - T_2(E) & 0 & 0 \\ 0 & T_1(E) - T_2(E) & 0 \\ 0 & 0 & T_1(E) + 2T_2(E) \end{pmatrix} \quad (\text{F.81})$$

the third component is symmetric one and written explicitly, it becomes

$$t(E) = (V_1 + 2V_2) + (V_1 + 2V_2) G_0(E) t(E) \quad \text{where} \quad t(E) = T_1(E) + 2T_2(E) \quad (\text{F.82})$$

Though the off-diagonal components are doubled, it can be absorbed into the off-diagonal interaction strength. The fully-coupled system therefore does contain the Efimov phenomena.

We then consider the case that  $\psi_3$  is much heavier and  $\psi_3\phi_3$  decouples so that the equation reduces to  $2 \times 2$  matrices.  $T$  and  $V$  then has only two independent components.

$$T(E) = \begin{pmatrix} T_1(E) & T_2(E) \\ T_2(E) & T_1(E) \end{pmatrix} \quad V = \begin{pmatrix} V_1 & V_2 \\ V_2 & V_1 \end{pmatrix} \quad (\text{F.83})$$

The Lippmann-Schwinger equation (F.79) and so is the  $T$ -matrix then diagonalized to give

$$U^\dagger T(E) U = \begin{pmatrix} T_1(E) + T_2(E) & 0 \\ 0 & T_1(E) - T_2(E) \end{pmatrix} \quad (\text{F.84})$$

that is, the solution to the equation (F.79) still has symmetric part.

$$t(E) = (V_1 + V_2) + (V_1 + V_2) G_0(E) t(E) \quad \text{where} \quad t(E) = T_1(E) + T_2(E) \quad (\text{F.85})$$

Its meaning is that  $\phi_1\phi_2\phi_3 - \psi_1\phi_1 - \psi_2\phi_2$  coupled-channels system do exhibit the Efimov phenomena.

It is however, obvious that in case of  $\psi_2\phi_2$  is also decoupled, the structure of the Lippmann-Schwinger equation (F.79) is no longer the same as it were for previous two coupled-channels system. Written explicitly,

$$T_1(E) = V_1 + V_1 G_0(E) T_1(E) \quad (\text{F.86})$$

More specifically, it does not contain the off-diagonal element and therefore Efimov effect does not manifest itself in the  $\phi_1\phi_2\phi_3 - \psi_1\phi_1$  system, the very system we investigated in this thesis.

# Bibliography

- [1] A. Yokosawa. REVIEWS OF EXPERIMENTAL RESULTS FROM THE POLARIZED BEAM PROGRAM AT THE ARGONNE ZGS. *Phys. Rept.*, 64:47–86, 1980.
- [2] K. Kubodera, M. P. Locher, F. Myhrer, and Anthony William Thomas. Interference of Dibaryon Resonances With Faddeev Amplitudes for Elastic  $\pi d$  Scattering. *J. Phys.*, G6:171, 1980.
- [3] P. J. Mulders, A. T. M. Aerts, and J. J. De Swart. Multi - Quark States. 3.  $Q^{**6}$  Dibaryon Resonances. *Phys. Rev.*, D21:2653, 1980.
- [4] Kim Maltman. On the Possibility of Deeply Bound Dibaryon Resonances. *Nucl. Phys.*, A438:669, 1985.
- [5] M. M. Makarov. DIBARYON RESONANCE. (IN RUSSIAN). *Fiz. Elem. Chast. Atom. Yadra*, 15:941–981, 1984.
- [6] Fan Wang, Jia-lun Ping, and J. Terrance Goldman. An Extension of the fractional parentage expansion to nonrelativistic and relativistic SU-f(3) dibaryon calculations. *Phys. Rev.*, C51:1648–1665, 1995.
- [7] Chun Wa Wong. Production and decay of the  $d^*$  dibaryon. *Phys. Rev.*, C57:1962–1973, 1998.
- [8] A. J. Buchmann, Georg Wagner, and Amand Faessler. The d-prime dibaryon in a colored cluster model. *Phys. Rev.*, C57:3340–3355, 1998.
- [9] R. D. Mota, H. Garcilazo, A. Valcarce, and F. Fernandez. Bound state problem of the N Delta and N Delta Delta systems. *Phys. Rev.*, C59:46–52, 1999.
- [10] H. Garcilazo, A. Valcarce, and F. Fernandez. Bound state problem of the N N Delta, N N N, and N N systems. *Phys. Rev.*, C60:044002, 1999.
- [11] G. M. Huber et al. Probing the Delta N N component of He-3. *Phys. Rev.*, C62:044001, 2000.
- [12] M. Cvetič-Krivec, B. Golli, N. Mankoc-Borstnik, and M. Rosina. Dibaryon Resonances With Retarded Decay. *Phys. Lett.*, B99:486–488, 1981.
- [13] R. D. Mota, A. Valcarce, F. Fernandez, D. R. Entem, and H. Garcilazo. Nonlocal calculation for nonstrange dibaryons and tribaryons. *Phys. Rev.*, C65:034006, 2002.
- [14] S. K. Choi et al. Observation of a narrow charmonium - like state in exclusive  $B^\pm \rightarrow K^+ \pi^- \pi^+ \pi^- J/\psi$  decays. *Phys. Rev. Lett.*, 91:262001, 2003.

- [15] Bernard Aubert et al. A Study of  $B \rightarrow X(3872)K$ , with  $X_{3872} \rightarrow J/\Psi \pi^+ \pi^-$ . *Phys. Rev.*, D77:111101, 2008.
- [16] I. Adachi et al. Study of  $X(3872)$  in  $B$  meson decays. In *Proceedings, 34th International Conference on High Energy Physics (ICHEP 2008)*, 2008.
- [17] D. Acosta et al. Observation of the narrow state  $X(3872) \rightarrow J/\psi \pi^+ \pi^-$  in  $\bar{p}p$  collisions at  $\sqrt{s} = 1.96$  TeV. *Phys. Rev. Lett.*, 93:072001, 2004.
- [18] A. Abulencia et al. Analysis of the quantum numbers  $J^{PC}$  of the  $X(3872)$ . *Phys. Rev. Lett.*, 98:132002, 2007.
- [19] T. Aaltonen et al. Precision Measurement of the  $X(3872)$  Mass in  $J/\psi \pi^+ \pi^-$  Decays. *Phys. Rev. Lett.*, 103:152001, 2009.
- [20] V. M. Abazov et al. Observation and properties of the  $X(3872)$  decaying to  $J/\psi \pi^+ \pi^-$  in  $p\bar{p}$  collisions at  $\sqrt{s} = 1.96$  TeV. *Phys. Rev. Lett.*, 93:162002, 2004.
- [21] Kazuo Abe et al. Evidence for  $X(3872) \rightarrow \gamma J/\psi$  and the sub-threshold decay  $X(3872) \rightarrow \omega J/\psi$ . In *Lepton and photon interactions at high energies. Proceedings, 22nd International Symposium, LP 2005, Uppsala, Sweden, June 30-July 5, 2005*, 2005.
- [22] G. Gokhroo et al. Observation of a Near-threshold  $D^0$  anti- $D^0$   $\pi^0$  Enhancement in  $B \rightarrow \bar{D}^0 \pi^0 K$  Decay. *Phys. Rev. Lett.*, 97:162002, 2006.
- [23] T. Aushev et al. Study of the  $B \rightarrow \bar{D}^0 X(3872) (D^{*0} \text{ anti-} D^0) K$  decay. *Phys. Rev.*, D81:031103, 2010.
- [24] Bernard Aubert et al. Study of Resonances in Exclusive  $B$  Decays to anti- $D^{(*)} D^{(*)} K$ . *Phys. Rev.*, D77:011102, 2008.
- [25] Bernard Aubert et al. Evidence for  $X(3872) \rightarrow \psi_{2S} \gamma$  in  $B^\pm \rightarrow X_{3872} K^\pm$  decays, and a study of  $B \rightarrow c\bar{c} \gamma K$ . *Phys. Rev. Lett.*, 102:132001, 2009.
- [26] N. Brambilla et al. Heavy quarkonium: progress, puzzles, and opportunities. *Eur. Phys. J.*, C71:1534, 2011.
- [27] Stephan Lars Olsen. A New Hadron Spectroscopy. *PoS*, Bormio2015:050, 2015.
- [28] Geoffrey T. Bodwin, Eric Braaten, Estia Eichten, Stephen Lars Olsen, Todd K. Pedlar, and James Russ. Quarkonium at the Frontiers of High Energy Physics: A Snowmass White Paper. 2013.
- [29] Bernard Aubert et al. Search for the  $Z(4430)^-$  at BABAR. *Phys. Rev.*, D79:112001, 2009.
- [30] R. Mizuk et al. Dalitz analysis of  $B \rightarrow \bar{D}^0 K \pi^+ \psi'$  decays and the  $Z(4430)^+$ . *Phys. Rev.*, D80:031104, 2009.
- [31] K. Chilikin et al. Experimental constraints on the spin and parity of the  $Z(4430)^+$ . *Phys. Rev.*, D88(7):074026, 2013.
- [32] Roel Aaij et al. Observation of the resonant character of the  $Z(4430)^-$  state. *Phys. Rev. Lett.*, 112(22):222002, 2014.
- [33] P. Pakhlov and T. Uglov. Charged charmonium-like  $Z^+(4430)$  from rescattering in conventional  $B$  decays. *Phys. Lett.*, B748:183–186, 2015.

- [34] M. Agnello et al. Evidence for a kaon-bound state  $K^- p p$  produced in  $K^-$  absorption reactions at rest. *Phys. Rev. Lett.*, 94:212303, 2005.
- [35] T. Yamazaki and Y. Akaishi.  $(K^-, \pi^-)$  production of nuclear anti-K bound states in proton-rich systems via  $\Lambda^*$  doorways. *Phys. Lett.*, B535:70–76, 2002.
- [36] Toshimitsu Yamazaki and Yoshinori Akaishi. The Basic anti-K nuclear cluster  $K^- pp$  and its enhanced formation in the  $p + p \rightarrow K^+ + X$  reaction. *Phys. Rev.*, C76:045201, 2007.
- [37] Akinobu Dote, Tetsuo Hyodo, and Wolfram Weise.  $K^- pp$  system with chiral SU(3) effective interaction. *Nucl. Phys.*, A804:197–206, 2008.
- [38] Akinobu Dote, Tetsuo Hyodo, and Wolfram Weise. Variational calculation of the  $ppK^-$  system based on chiral SU(3) dynamics. *Phys. Rev.*, C79:014003, 2009.
- [39] S. Wycech and A. M. Green. Variational calculations for  $K^-$ -few-nucleon systems. *Phys. Rev.*, C79:014001, 2009.
- [40] N. Barnea, A. Gal, and E. Z. Liverts. Realistic calculations of  $\bar{K}NN$ ,  $\bar{K}NNN$ , and  $\bar{K}\bar{K}NN$  quasibound states. *Phys. Lett.*, B712:132–137, 2012.
- [41] N. V. Shevchenko, A. Gal, and J. Mares. Faddeev calculation of a  $K^- p p$  quasi-bound state. *Phys. Rev. Lett.*, 98:082301, 2007.
- [42] N. V. Shevchenko, A. Gal, J. Mares, and J. Revai. anti-K NN quasi-bound state and the anti-K N interaction: Coupled-channel Faddeev calculations of the anti-K NN -  $\pi$  Sigma N system. *Phys. Rev.*, C76:044004, 2007.
- [43] Y. Ikeda and T. Sato. Strange dibaryon resonance in the anti-K NN -  $\pi$  Sigma N system. *Phys. Rev.*, C76:035203, 2007.
- [44] Yoichi Ikeda and Toru Sato. On the resonance energy of the anti-K NN -  $\pi$  YN system. *Phys. Rev.*, C79:035201, 2009.
- [45] Yoichi Ikeda, Hiroyuki Kamano, and Toru Sato. On the resonance energy of the strange dibaryon. *Nucl. Phys.*, A835:386–389, 2010.
- [46] Yoichi Ikeda, Hiroyuki Kamano, and Toru Sato. Energy dependence of  $\bar{K}N$  interactions and resonance pole of strange dibaryons. *Prog. Theor. Phys.*, 124:533–539, 2010.
- [47] Shota Ohnishi, Yoichi Ikeda, Hiroyuki Kamano, and Toru Sato. Production Reaction of  $\bar{K}NN - \pi YN$  Resonance from Faddeev Equations. *Few Body Syst.*, 54:1119–1122, 2013.
- [48] D. Jido, J. A. Oller, E. Oset, A. Ramos, and U. G. Meissner. Chiral dynamics of the two  $\Lambda(1405)$  states. *Nucl. Phys.*, A725:181–200, 2003.
- [49] Tetsuo Hyodo and Wolfram Weise. Effective anti-K N interaction based on chiral SU(3) dynamics. *Phys. Rev.*, C77:035204, 2008.
- [50] Eric Braaten and H. W. Hammer. Universality in few-body systems with large scattering length. *Phys. Rept.*, 428:259–390, 2006.
- [51] Eric Braaten and Meng Lu. Operator Product Expansion in the Production and Decay of the  $X(3872)$ . *Phys. Rev.*, D74:054020, 2006.

- [52] S. Fleming, M. Kusunoki, T. Mehen, and U. van Kolck. Pion interactions in the  $X(3872)$ . *Phys. Rev.*, D76:034006, 2007.
- [53] Herman Feshbach. Unified theory of nuclear reactions. *Annals Phys.*, 5:357–390, 1958.
- [54] Herman Feshbach. A Unified theory of nuclear reactions. 2. *Annals Phys.*, 19:287–313, 1962. [Annals Phys.281,519(2000)].
- [55] L. D. Faddeev. Scattering theory for a three particle system. *Sov. Phys. JETP*, 12:1014–1019, 1961. [Zh. Eksp. Teor. Fiz.39,1459(1960)].
- [56] E. O. Alt, P. Grassberger, and W. Sandhas. Reduction of the three - particle collision problem to multichannel two - particle Lippmann-Schwinger equations. *Nucl. Phys.*, B2:167–180, 1967.
- [57] Michael E. Peskin and Daniel V. Schroeder. *An Introduction to quantum field theory*. 1995.
- [58] Tetsuo Hyodo. Structure and compositeness of hadron resonances. *Int. J. Mod. Phys.*, A28:1330045, 2013.
- [59] Tetsuo Hyodo. Compositeness of Hadron Resonances and Quasi-Bound States. In *12th International Conference on Hypernuclear and Strange Particle Physics (HYP 2015) Sendai, Japan, September 7-12, 2015*, 2015.
- [60] W. Glöckle. *The quantum mechanical few-body problem*. Texts and monographs in physics. Springer-Verlag, 1983.
- [61] F. Riesz and B. Székely-Nagy. *Functional Analysis*. Dover books on advanced mathematics. Dover Publications, 1990.
- [62] W. Glöckle and R. Brandenburg. Generalized three-body Alt-Grassberger-Sandhas equations including three-body forces. *Phys. Rev.*, C27:83–87, 1983.
- [63] I. R. Afnan. Resonances in few body systems. *Austral. J. Phys.*, 44:201–216, 1991.
- [64] B. C. Pearce and I. R. Afnan. Resonance Poles in Three-body Systems. *Phys. Rev.*, C30:2022–2025, 1984.
- [65] W. Glöckle. S-matrix pole trajectory in a three-neutron model. *Phys. Rev.*, C18:564–572, 1978.
- [66] A. Matsuyama and K. Yazaki. S matrix pole trajectory of the three-body system. *Nucl. Phys.*, A534:620–636, 1991.
- [67] H. A. Bethe. Theory of the Effective Range in Nuclear Scattering. *Phys. Rev.*, 76:38–50, 1949.
- [68] Steven Weinberg. Evidence That the Deuteron Is Not an Elementary Particle. *Phys. Rev.*, 137:B672–B678, 1965.
- [69] Steven Weinberg. Elementary particle theory of composite particles. *Phys. Rev.*, 130:776–783, 1963.
- [70] Thomas A. Osborn and K. L. Kowalski. Optimal Equations for Three Particle Scattering. *Annals Phys.*, 68:361, 1971.



- [71] T. S. H. Lee and A. Matsuyama. Theory of Mesonic and Dibarionic Excitations in the  $\pi NN$  System: Derivation of  $\pi NN$  Scattering Equations. *Phys. Rev.*, C32:516–530, 1985.
- [72] R. D. L. Kronig. On the theory of dispersion of x-rays. *Journal of the Optical Society of America (1917-1983)*, 12:547, nov 1926.
- [73] H.A. Kramers. *La diffusion de la lumière par les atomes*. Atti Cong. Int. Fisici Como 1927, 1927.
- [74] John F. Donoghue. Dispersion relations and effective field theory. In *Advanced School on Effective Theories Almunecar, Spain, June 25-July 1, 1995*, 1996.
- [75] Eugene Feenberg. The Scattering of Slow Electrons by Neutral Atoms. *Phys. Rev.*, 40:40–54, 1932.
- [76] R. E. Cutkosky. Singularities and discontinuities of Feynman amplitudes. *J. Math. Phys.*, 1:429–433, 1960.
- [77] V. Efimov. Energy levels arising from the resonant two-body forces in a three-body system. *Phys. Lett.*, B33:563–564, 1970.
- [78] V. N. Efimov. WEAKLY-BOUND STATES OF 3 RESONANTLY-INTERACTING PARTICLES. *Sov. J. Nucl. Phys.*, 12:589, 1971.
- [79] V. Efimov. Energy levels of three resonantly interacting particles. *Nuclear Physics A*, 210(1):157 – 188, 1973.
- [80] V. Efimov. Low-energy Properties of Three Resonantly Interacting Particles. *Sov. J. Nucl. Phys.*, 29:546, 1979. [*Yad. Fiz.*29,1058(1979)].
- [81] David B. Kaplan. More effective field theory for nonrelativistic scattering. *Nucl. Phys.*, B494:471–484, 1997.
- [82] Paulo F. Bedaque, H. W. Hammer, and U. van Kolck. Renormalization of the three-body system with short range interactions. *Phys. Rev. Lett.*, 82:463–467, 1999.
- [83] Paulo F. Bedaque, H. W. Hammer, and U. van Kolck. The Three boson system with short range interactions. *Nucl. Phys.*, A646:444–466, 1999.
- [84] Paulo F. Bedaque, H. W. Hammer, and U. van Kolck. Effective theory for neutron deuteron scattering: Energy dependence. *Phys. Rev.*, C58:641–644, 1998.
- [85] Paulo F. Bedaque and Ubirajara van Kolck. Effective field theory for few nucleon systems. *Ann. Rev. Nucl. Part. Sci.*, 52:339–396, 2002.
- [86] P. F. Bedaque, H. W. Hammer, and U. van Kolck. Narrow resonances in effective field theory. *Phys. Lett.*, B569:159–167, 2003.
- [87] Lucas Platter. Low-Energy Universality in Atomic and Nuclear Physics. *Few Body Syst.*, 46:139–171, 2009.
- [88] Lucas Platter. Few-Body Systems and the Pionless Effective Field Theory. *PoS*, CD09:104, 2009.
- [89] Hans-Werner Hammer and Lucas Platter. Efimov physics from a renormalization group perspective. *Phil. Trans. Roy. Soc. Lond.*, A369:2679, 2011.

- [90] Hans-Werner Hammer and Lucas Platter. Efimov States in Nuclear and Particle Physics. *Ann. Rev. Nucl. Part. Sci.*, 60:207–236, 2010.